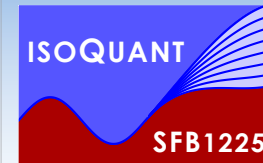


Spectral properties from the lattice: heavy $Q\bar{Q}$ and imaginary frequency simulations

Alexander Rothkopf
Institute for Theoretical Physics
Heidelberg University

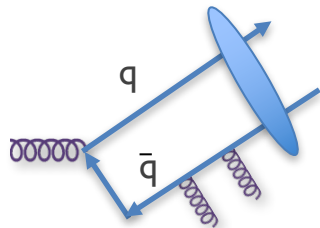
References:

- with S.Kim and P. Petreczky PRD91 (2015) 054511, NPA956 (2016) 713
in preparation
- with J. Pawlowski arXiv:1610.09531
- with J. Pawlowski, F. Ziegler in preparation



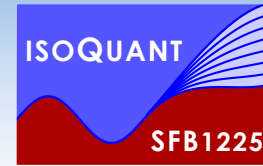
Physics motivation

- Hard probes: susceptible to medium but distinguishable from it $Q_{\text{probe}} > T_{\text{med}}$



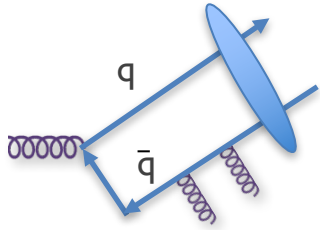
Bound states of $c\bar{c}$ or $b\bar{b}$: **Heavy quarkonium** $M_Q > T_{\text{med}}$

In vacuum: $m^\Upsilon = 9.460 \text{ GeV}$, $\Gamma^\Upsilon = 54(1) \text{ keV}$; $m^{J/\psi} = 3.096 \text{ GeV}$, $\Gamma^{J/\psi} = 93(3) \text{ keV}$



Physics motivation

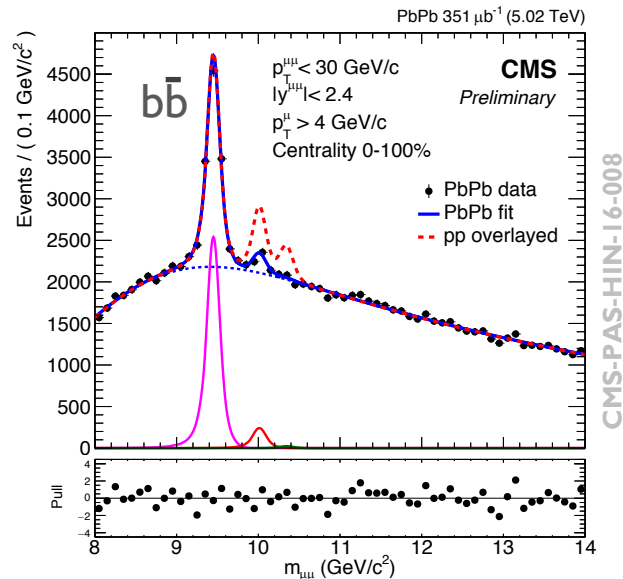
- Hard probes: susceptible to medium but distinguishable from it $Q_{\text{probe}} > T_{\text{med}}$



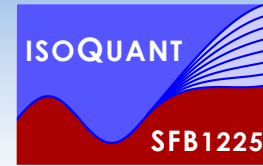
Bound states of $c\bar{c}$ or $b\bar{b}$: **Heavy quarkonium** $M_Q > T_{\text{med}}$

In vacuum: $m^\Upsilon = 9.460 \text{ GeV}$, $\Gamma^\Upsilon = 54(1) \text{ keV}$; $m^{J/\psi} = 3.096 \text{ GeV}$, $\Gamma^{J/\psi} = 93(3) \text{ keV}$

see QM2017 summary
by E. Scapparini arXiv:1705.05810

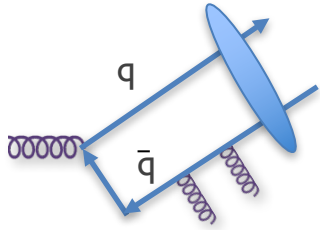


bb: sampling the full QGP evolution



Physics motivation

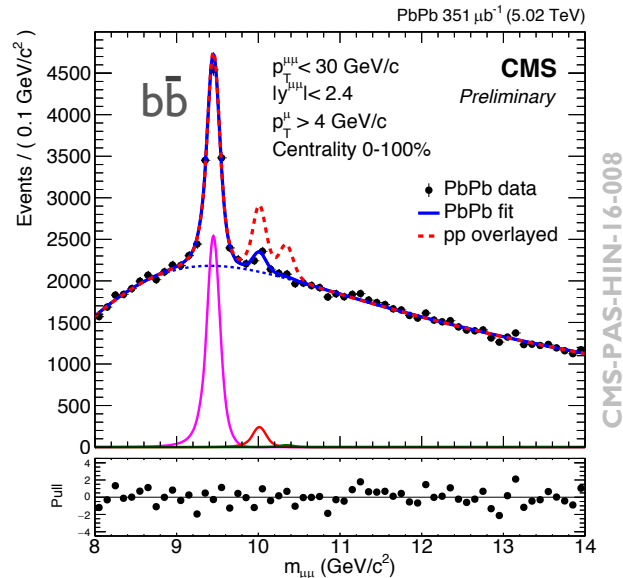
- Hard probes: susceptible to medium but distinguishable from it $Q_{\text{probe}} > T_{\text{med}}$



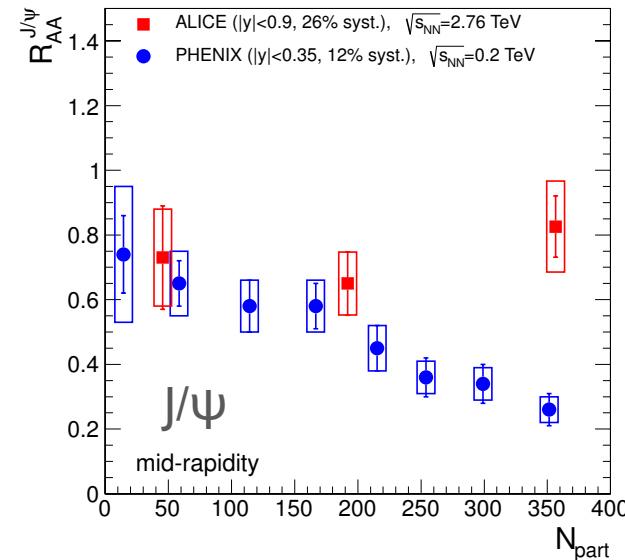
Bound states of $c\bar{c}$ or $b\bar{b}$: **Heavy quarkonium** $M_Q > T_{\text{med}}$

In vacuum: $m^\Upsilon = 9.460 \text{ GeV}$, $\Gamma^\Upsilon = 54(1) \text{ keV}$; $m^{J/\psi} = 3.096 \text{ GeV}$, $\Gamma^{J/\psi} = 93(3) \text{ keV}$

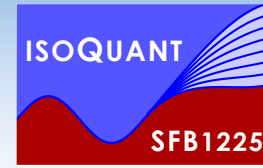
see QM2017 summary
by E. Scapparini arXiv:1705.05810



bb: sampling the full QGP evolution

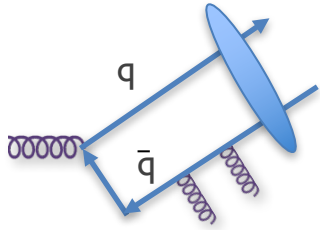


cc: a probe of the late stages



Physics motivation

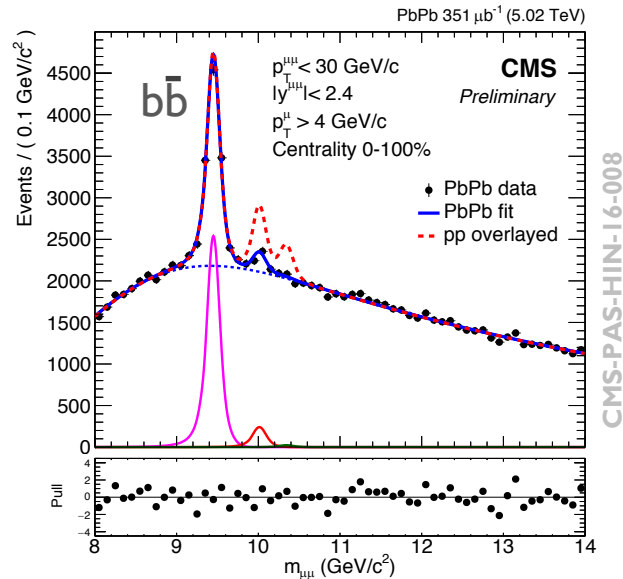
- Hard probes: susceptible to medium but distinguishable from it $Q_{\text{probe}} > T_{\text{med}}$



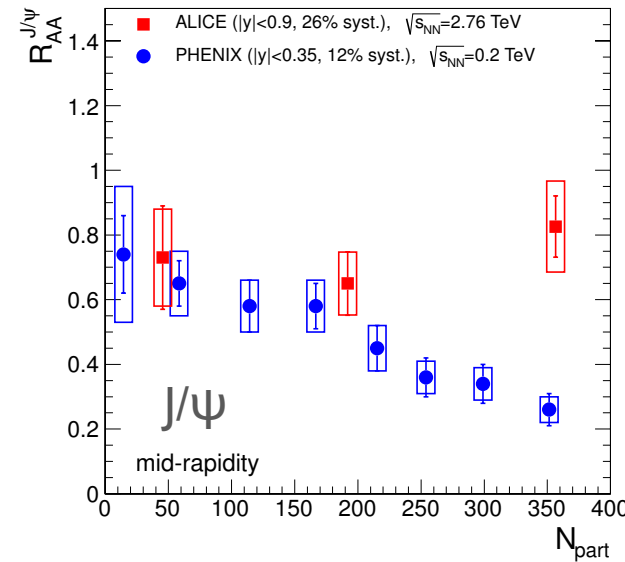
Bound states of $c\bar{c}$ or $b\bar{b}$: **Heavy quarkonium** $M_Q > T_{\text{med}}$

In vacuum: $m^\Upsilon = 9.460 \text{ GeV}$, $\Gamma^\Upsilon = 54(1) \text{ keV}$; $m^{J/\psi} = 3.096 \text{ GeV}$, $\Gamma^{J/\psi} = 93(3) \text{ keV}$

see QM2017 summary by E. Scapparini arXiv:1705.05810



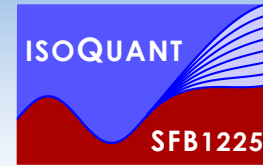
bb: sampling the full QGP evolution



cc: a probe of the late stages

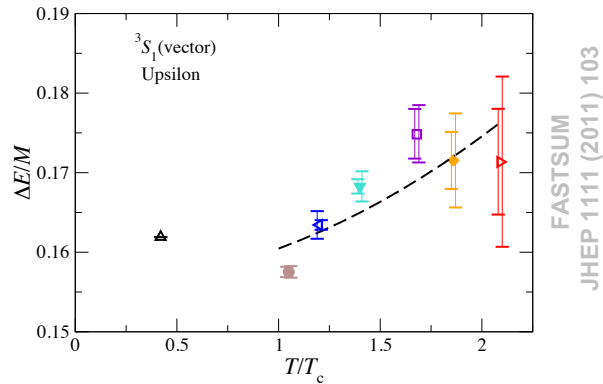
ALICE, PRL 109, 072301 (2012) adapted from Andronic, et. al. Nucl.Phys. A904 (2013) 535c

- Goal: first principles insight into heavy-quarkonium in heavy-ion collisions

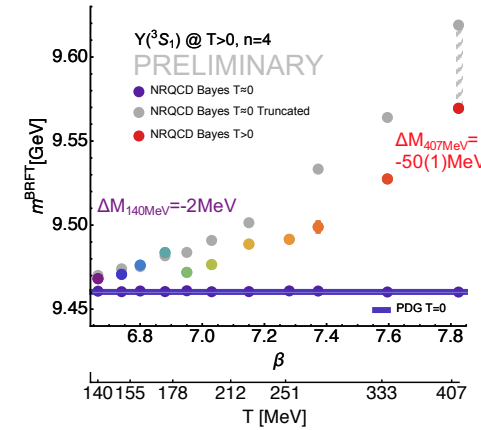


Theory answer to $T > 0$ S-wave?

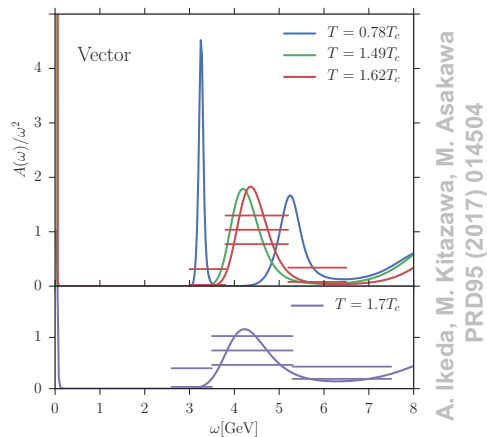
What is the theory status of in-medium Quarkonium ground state modification ?



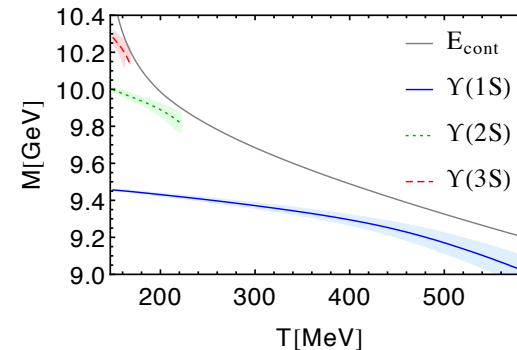
NRQCD MEM (Nf=2+1): bbar mass goes up



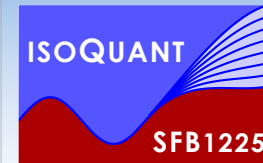
NRQCD BR (Nf=2+1): bbar/ccbar mass goes down



Relativistic MEM (Nf=0): ccbar mass goes up

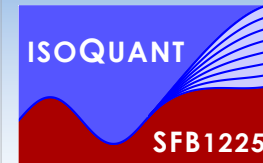


pNRQCD: bbar/ccbar mass goes down



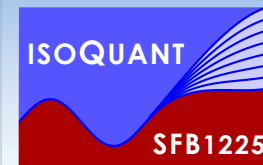
Outline

- Motivation
 - Coherent picture of in-medium heavy-quarkonium from the lattice
- In-medium quarkonium from a lattice EFT (NRQCD)
 - Numerical setup and spectral reconstruction
 - Current $T > 0$ results from realistic full QCD simulations
- Towards improved spectral information from thermal fields
 - Derivation of a novel simulation prescription
 - Current exploratory results from toy models to quenched QCD
- Conclusion



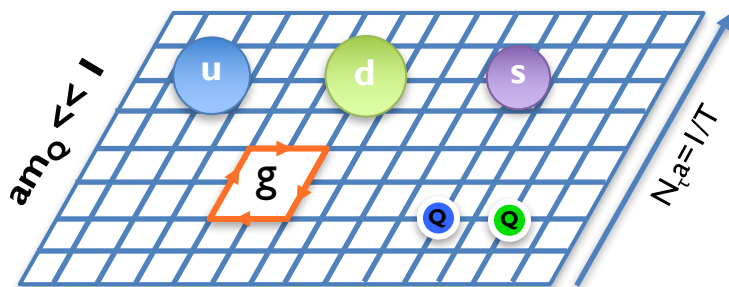
Outline

- Motivation
 - Coherent picture of in-medium heavy-quarkonium from the lattice
- In-medium quarkonium from a lattice EFT (NRQCD)
 - Numerical setup and spectral reconstruction
 - Current $T > 0$ results from realistic full QCD simulations
- Towards improved spectral information from thermal fields
 - Derivation of a novel simulation prescription
 - Current exploratory results from toy models to quenched QCD
- Conclusion

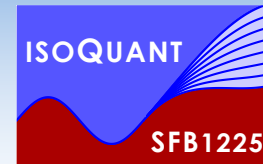


Heavy quarks on the lattice

Relativistic treatment of light
and heavy d.o.f.

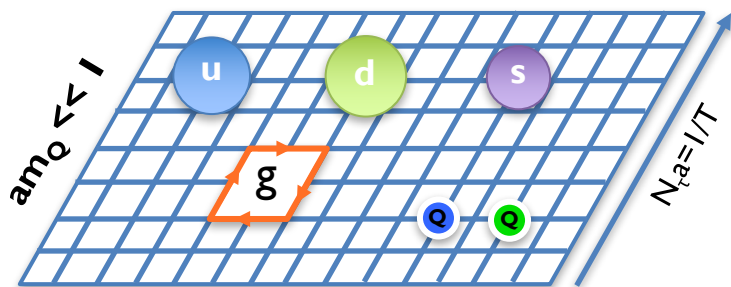


Full Lattice QCD simulation incl. QQ
(still too costly)



Heavy quarks on the lattice

Relativistic treatment of light
and heavy d.o.f.

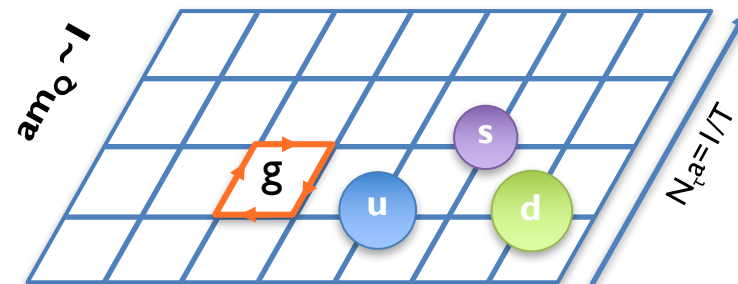


Full Lattice QCD simulation incl. QQ
(still too costly)

$$\frac{\Lambda_{\text{QCD}}}{m_Q} \ll 1$$

➔

$$\frac{T}{m_Q} \ll 1$$

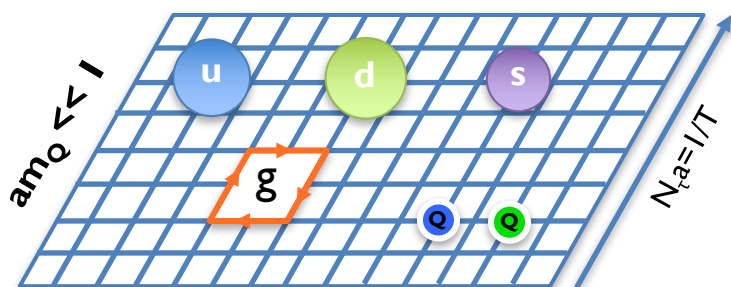


Lattice QCD simulation without QQ



Heavy quarks on the lattice

Relativistic treatment of light
and heavy d.o.f.

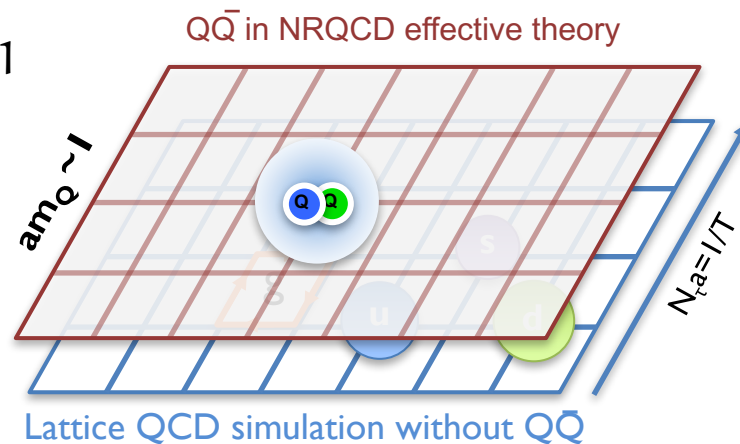


Full Lattice QCD simulation incl. $Q\bar{Q}$
(still too costly)

$$\frac{\Lambda_{\text{QCD}}}{m_Q} \ll 1$$

$$\frac{T}{m_Q} \ll 1$$

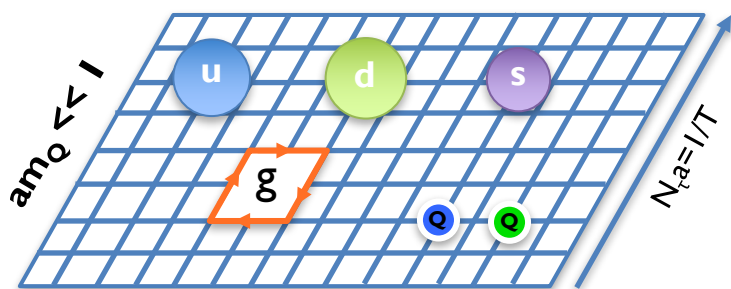
Kin. eq. non-relativistic $Q\bar{Q}$ in a
background of light medium d.o.f.





Heavy quarks on the lattice

Relativistic treatment of light
and heavy d.o.f.

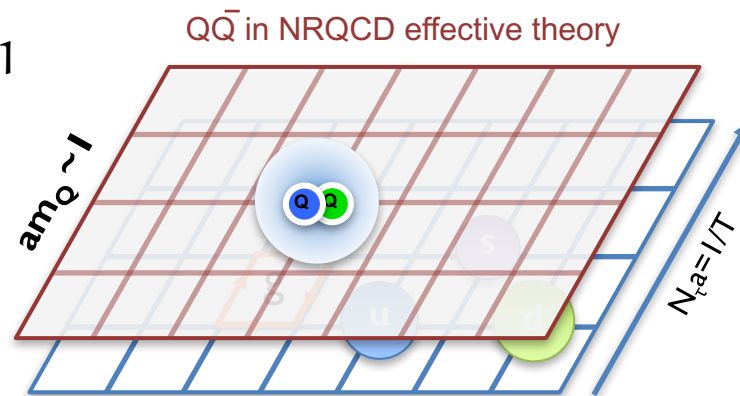


Full Lattice QCD simulation incl. $Q\bar{Q}$
(still too costly)

$$\frac{\Lambda_{\text{QCD}}}{m_Q} \ll 1$$

$$\frac{T}{m_Q} \ll 1$$

Kin. eq. non-relativistic $Q\bar{Q}$ in a
background of light medium d.o.f.



Lattice QCD simulation without $Q\bar{Q}$

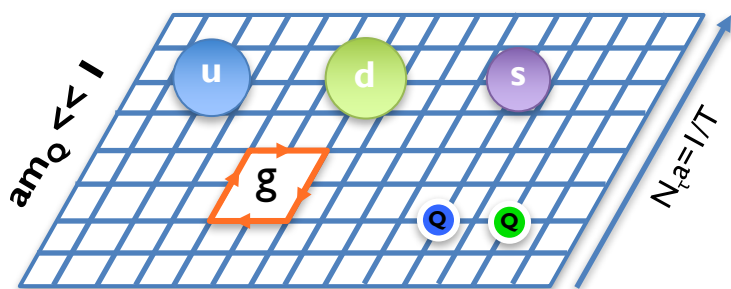
- Lattice Non-Relativistic QCD (NRQCD) well **established** at $T=0$, applicable at $T>0$
 - no modeling, systematic expansion of QCD action in $1/M_Q a n$, includes $v \neq 0$ contributions
 - adaptive discretization in temporal direction: Lepage parameter n ($b\bar{b}$ $n=4$, $c\bar{c}$ $n=8$)

Thacker, Lepage Phys.Rev. D43 (1991) 196-208



Heavy quarks on the lattice

Relativistic treatment of light and heavy d.o.f.

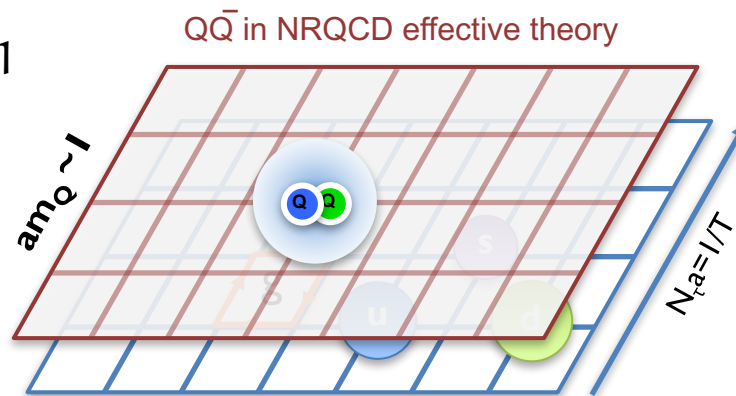


Full Lattice QCD simulation incl. QQ
(still too costly)

$$\frac{\Lambda_{\text{QCD}}}{m_Q} \ll 1$$

$$\frac{T}{m_Q} \ll 1$$

Kin. eq. non-relativistic QQ̄ in a background of light medium d.o.f.

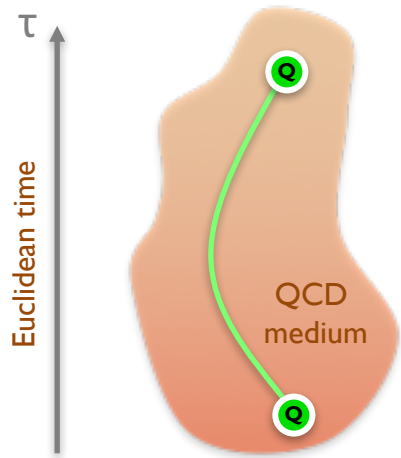
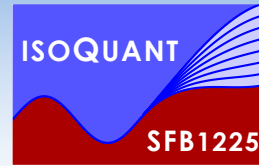


Lattice QCD simulation without QQ̄

- Lattice Non-Relativistic QCD (NRQCD) well **established** at $T=0$, applicable at $T>0$
 - no modeling, systematic expansion of QCD action in $1/M_Q a n$, includes $v \neq 0$ contributions
Thacker, Lepage Phys.Rev. D43 (1991) 196-208
 - adaptive discretization in temporal direction: Lepage parameter n ($b\bar{b}$ $n=4$, $c\bar{c}$ $n=8$)
- Realistic simulations of the QCD medium by HotQCD with extended T range
HotQCD PRD85 (2012) 054503, PRD90 (2014) 094503

■ $48^3 \times 12$ $m_\pi = 161 \text{ MeV}$ ($\beta = 6.664 - 7.825$)	$M_b a = [2.759 - 0.954]$ $T = [140 - 407] \text{ MeV}$	$M_c a = [0.757 - 0.42]$ $T = [140 - 251] \text{ MeV}$
---	--	---

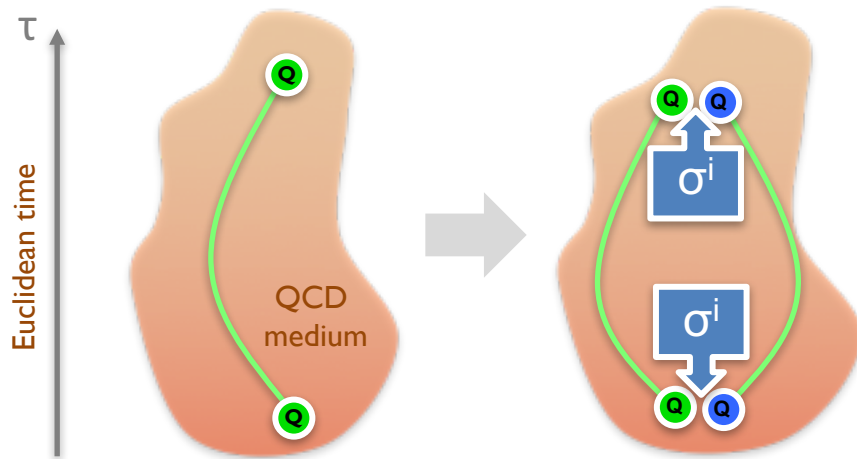
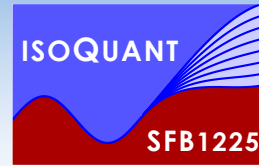
Correlation functions in NRQCD



Non-rel. propagator of
a single heavy quark G

Davies, Thacker Phys.Rev. D45 (1992)

Correlation functions in NRQCD



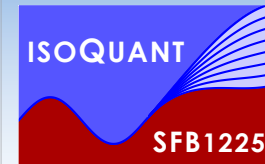
Non-rel. propagator of a single heavy quark G QQ propagator projected to a certain channel

Davies, Thacker Phys.Rev. D45 (1992)

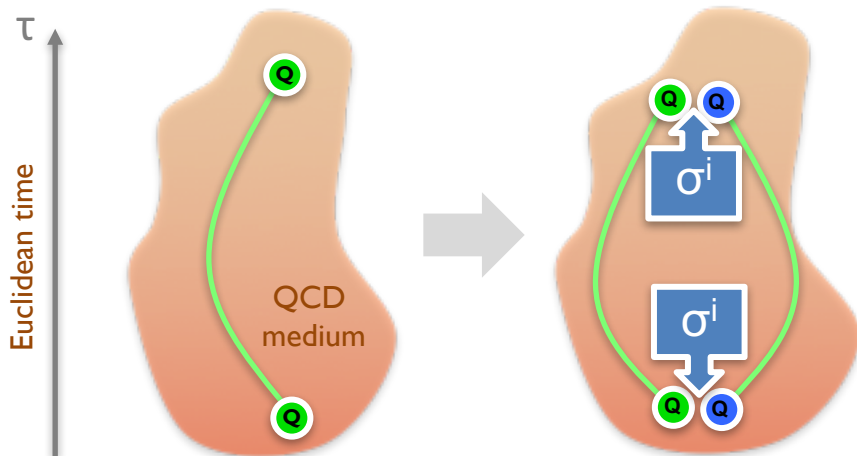
„correlator of QQ wavefct.

$$D_{J/\psi}(\tau) \hat{=} \langle \psi_{J/\psi}(\tau) \psi_{J/\psi}^\dagger(0) \rangle$$

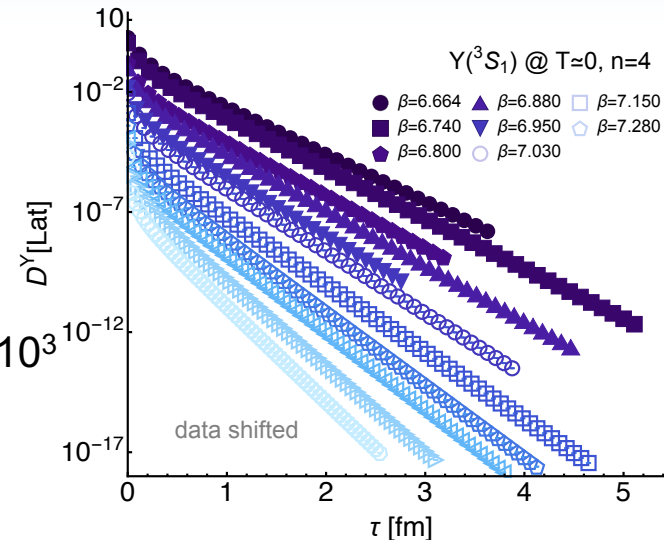
Brambilla et. al. Rev.Mod.Phys. 77 (2005) 1423



Correlation functions in NRQCD



$N_{bb}^{meas}(T=0)=400$
 $N_{bb}^{meas}(T>0)=1-4 \times 10^3$



S.Kim, P.Petreczky, A.R. in preparation

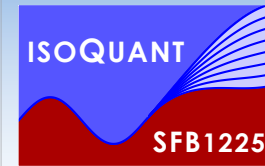
Non-rel. propagator of a single heavy quark G projected to a certain channel

Davies, Thacker Phys.Rev. D45 (1992)

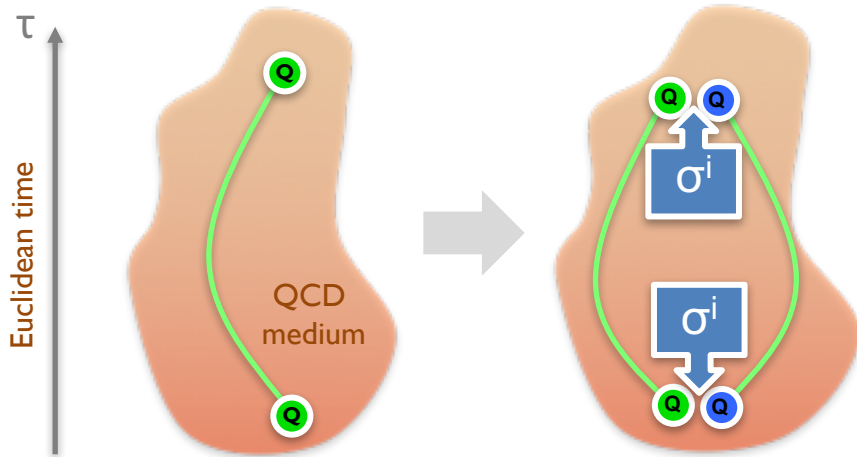
QQ propagator

„correlator of QQ wavefct.
 $D_{J/\psi}(\tau) \hat{=} \langle \psi_{J/\psi}(\tau) \psi_{J/\psi}^\dagger(0) \rangle$ “

Brambilla et. al. Rev.Mod.Phys. 77 (2005) 1423



Correlation functions in NRQCD



$N_{bb}^{meas}(T=0)=400$
 $N_{bb}^{meas}(T>0)=1-4 \times 10^3$

$N_{cc}^{meas}(T=0)=200$
 $N_{cc}^{meas}(T>0)=400$

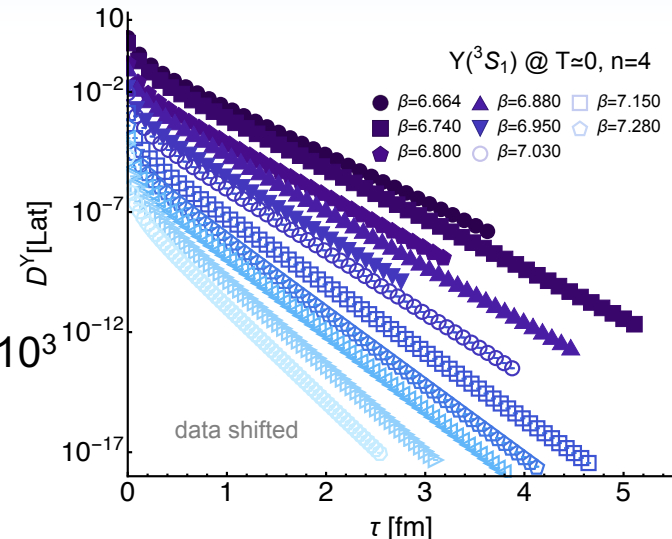
Non-rel. propagator of a single heavy quark G projected to a certain channel

Davies, Thacker Phys.Rev. D45 (1992)

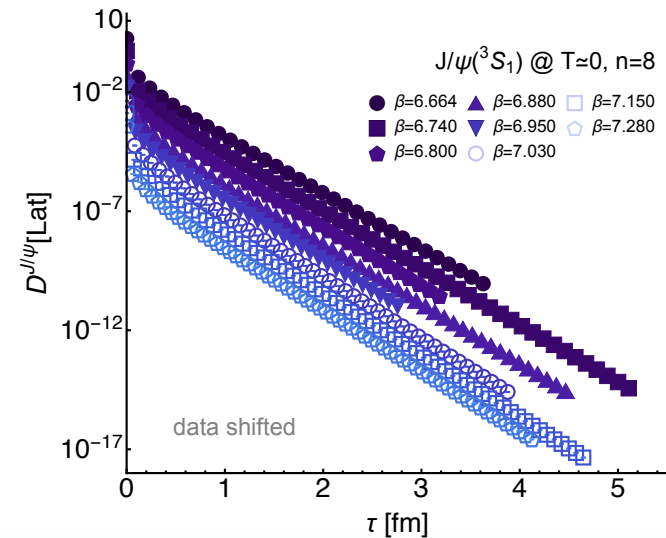
„correlator of QQ wavefct.

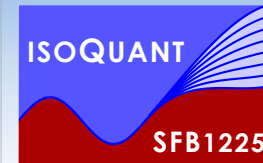
$$D_{J/\psi}(\tau) \hat{=} \langle \psi_{J/\psi}(\tau) \psi_{J/\psi}^\dagger(0) \rangle$$

Brambilla et. al. Rev.Mod.Phys. 77 (2005) 1423



S.Kim, P.Petreczky, A.R. in preparation

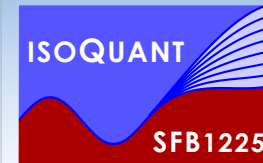




Accessing spectral functions

- Inversion of Laplace transform required to obtain spectra from correlators

$$D(\tau) = \int_{-2M_Q}^{\infty} d\omega e^{-\tau\omega} \rho(\omega)$$

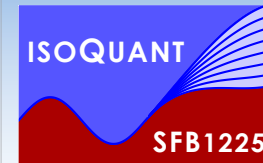


Accessing spectral functions

- Inversion of Laplace transform required to obtain spectra from correlators

$$D_i = \sum_{l=1}^{N_\omega} \exp[-\omega_l \tau_i] \rho_l \Delta\omega_l$$

1. N_ω parameters $\rho_l \gg N_T$ datapoints
2. data D_i has finite precision



Accessing spectral functions

- Inversion of Laplace transform required to obtain spectra from correlators

$$D_i = \sum_{l=1}^{N_\omega} \exp[-\omega_l \tau_i] \rho_l \Delta\omega_l$$

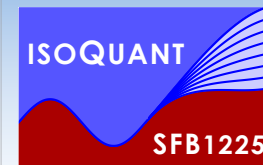
1. N_ω parameters $\rho_l \gg N_T$ datapoints
2. data D_i has finite precision

- Give meaning to problem by incorporating prior knowledge: Bayesian approach

M. Jarrell, J. Gubernatis, Physics Reports 269 (3) (1996)

- Bayes theorem: Regularize the naïve χ^2 functional $P[D|\rho]$ through a prior $P[\rho|I]$

$$P[\rho|D, I] \propto P[D|\rho] P[\rho|I]$$



Accessing spectral functions

- Inversion of Laplace transform required to obtain spectra from correlators

$$D_i = \sum_{l=1}^{N_\omega} \exp[-\omega_l \tau_i] \rho_l \Delta\omega_l$$

1. N_ω parameters $\rho_l \gg N_T$ datapoints
2. data D_i has finite precision

- Give meaning to problem by incorporating prior knowledge: Bayesian approach

M. Jarrell, J. Gubernatis, Physics Reports 269 (3) (1996)

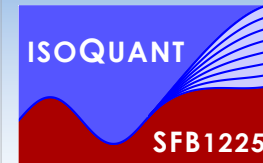
- Bayes theorem: Regularize the naïve χ^2 functional $P[D|\rho]$ through a prior $P[\rho|I]$

$$P[\rho|D, I] \propto P[D|\rho] P[\rho|I]$$

- Our prior enforces: ρ positive definite, smoothness of ρ , result independent of units

$$P[\rho|I] \propto e^S \quad S = \alpha \sum_{l=1}^{N_\omega} \Delta\omega_l \left(1 - \frac{\rho_l}{m_l} + \log \left[\frac{\rho_l}{m_l} \right] \right)$$

Y.Burnier, A.R.
PRL 111 (2013) 18, 182003



Accessing spectral functions

- Inversion of Laplace transform required to obtain spectra from correlators

$$D_i = \sum_{l=1}^{N_\omega} \exp[-\omega_l \tau_i] \rho_l \Delta\omega_l$$

1. N_ω parameters $\rho_l \gg N_T$ datapoints
2. data D_i has finite precision

- Give meaning to problem by incorporating prior knowledge: Bayesian approach

M. Jarrell, J. Gubernatis, Physics Reports 269 (3) (1996)

- Bayes theorem: Regularize the naïve χ^2 functional $P[D|\rho]$ through a prior $P[\rho|I]$

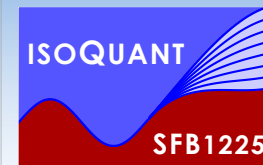
$$P[\rho|D, I] \propto P[D|\rho] P[\rho|I]$$

- Our prior enforces: ρ positive definite, smoothness of ρ , result independent of units

$$P[\rho|I] \propto e^S \quad S = \alpha \sum_{l=1}^{N_\omega} \Delta\omega_l \left(1 - \frac{\rho_l}{m_l} + \log \left[\frac{\rho_l}{m_l} \right] \right)$$

Y. Burnier, A.R.
PRL 111 (2013) 18, 182003

- **Different from Maximum Entropy Method:** S not entropy, no more flat directions



Accessing spectral functions

- Inversion of Laplace transform required to obtain spectra from correlators

$$D_i = \sum_{l=1}^{N_\omega} \exp[-\omega_l \tau_i] \rho_l \Delta\omega_l$$

1. N_ω parameters $\rho_l \gg N_T$ datapoints
2. data D_i has finite precision

- Give meaning to problem by incorporating prior knowledge: Bayesian approach

M. Jarrell, J. Gubernatis, Physics Reports 269 (3) (1996)

- Bayes theorem: Regularize the naïve χ^2 functional $P[D|\rho]$ through a prior $P[\rho|I]$

$$P[\rho|D, I] \propto P[D|\rho] P[\rho|I]$$

- Our prior enforces: ρ positive definite, smoothness of ρ , result independent of units

$$P[\rho|I] \propto e^S \quad S = \alpha \sum_{l=1}^{N_\omega} \Delta\omega_l \left(1 - \frac{\rho_l}{m_l} + \log \left[\frac{\rho_l}{m_l} \right] \right)$$

Y. Burnier, A.R.
PRL 111 (2013) 18, 182003

- **Different from Maximum Entropy Method:** S not entropy, no more flat directions

$$\left. \frac{\delta}{\delta\rho} P[\rho|D, I] \right|_{\rho=\rho^{BR}} = 0$$

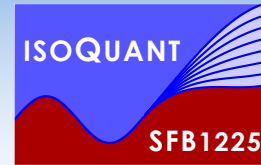
An improved Bayesian strategy



- **Improvement I:** incorporate both Euclidean and imaginary frequency data in unfolding

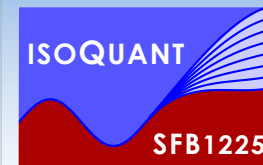
$$D(\tau) = \int_{-2M_Q}^{\infty} d\omega e^{-\tau\omega} \rho(\omega)$$

An improved Bayesian strategy



- Improvement I: incorporate both Euclidean and imaginary frequency data in unfolding

$$D(\tau) = \int_{-2M_Q}^{\infty} d\omega e^{-\tau\omega} \rho(\omega) \quad \longleftrightarrow \text{Fourier} \quad D(\mu) = \int_{-2M_Q}^{\infty} d\omega \frac{\rho(\omega)}{\omega - i\mu}$$

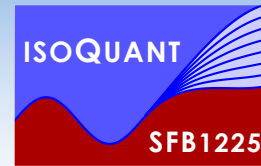


An improved Bayesian strategy

- Improvement I: incorporate both Euclidean and imaginary frequency data in unfolding

$$D(\tau) = \int_{-2M_Q}^{\infty} d\omega e^{-\tau\omega} \rho(\omega) \quad \longleftrightarrow \text{Fourier} \quad D(\mu) = \int_{-2M_Q}^{\infty} d\omega \frac{\rho(\omega)}{\omega - i\mu}$$

- Improvement II: Use different regulators to crosscheck the systematics



An improved Bayesian strategy

- Improvement I: incorporate both Euclidean and imaginary frequency data in unfolding

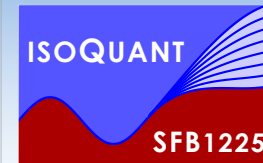
$$D(\tau) = \int_{-2M_Q}^{\infty} d\omega e^{-\tau\omega} \rho(\omega) \quad \longleftrightarrow \quad \text{Fourier} \quad D(\mu) = \int_{-2M_Q}^{\infty} d\omega \frac{\rho(\omega)}{\omega - i\mu}$$

- Improvement II: Use different regulators to crosscheck the systematics

Standard BR method (BRFT)

$$S_{BR} = \alpha \int d\omega \left(1 - \frac{\rho}{m} + \log \left[\frac{\rho}{m} \right] \right)$$

- Resolves narrow peaked structures with high accuracy
- Ringings in broad structures if reconstructed from small # of datapoints



An improved Bayesian strategy

- Improvement I: incorporate both Euclidean and imaginary frequency data in unfolding

$$D(\tau) = \int_{-2M_Q}^{\infty} d\omega e^{-\tau\omega} \rho(\omega) \quad \longleftrightarrow \text{Fourier} \quad D(\mu) = \int_{-2M_Q}^{\infty} d\omega \frac{\rho(\omega)}{\omega - i\mu}$$

- Improvement II: Use different regulators to crosscheck the systematics

Standard BR method (BRFT)

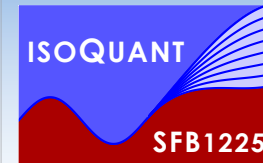
$$S_{BR} = \alpha \int d\omega \left(1 - \frac{\rho}{m} + \log \left[\frac{\rho}{m} \right] \right)$$

- Resolves narrow peaked structures with high accuracy
- Ringing in broad structures if reconstructed from small # of datapoints

New low ringing BR method

$$S_{BR}^{lr} = \alpha \int d\omega \left(\left(\frac{\partial \rho}{\partial \omega} \right)^2 + 1 - \frac{\rho}{m} + \log \left[\frac{\rho}{m} \right] \right)$$

- Introduces penalty on arc length of reconstruction $(dL/d\omega)^2 = 1 + (d\rho/d\omega)^2$
- Efficiently removes ringing but may lead to overestimated peak widths



An improved Bayesian strategy

- Improvement I: incorporate both Euclidean and imaginary frequency data in unfolding

$$D(\tau) = \int_{-2M_Q}^{\infty} d\omega e^{-\tau\omega} \rho(\omega) \quad \longleftrightarrow \text{Fourier} \quad D(\mu) = \int_{-2M_Q}^{\infty} d\omega \frac{\rho(\omega)}{\omega - i\mu}$$

- Improvement II: Use different regulators to crosscheck the systematics

Standard BR method (BRFT)

$$S_{BR} = \alpha \int d\omega \left(1 - \frac{\rho}{m} + \log \left[\frac{\rho}{m} \right] \right)$$

- Resolves narrow peaked structures with high accuracy
- Ringing in broad structures if reconstructed from small # of datapoints

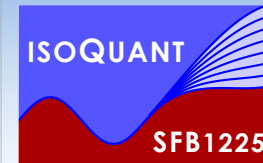
„high gain – high noise“

New low ringing BR method

$$S_{BR}^{lr} = \alpha \int d\omega \left(\left(\frac{\partial \rho}{\partial \omega} \right)^2 + 1 - \frac{\rho}{m} + \log \left[\frac{\rho}{m} \right] \right)$$

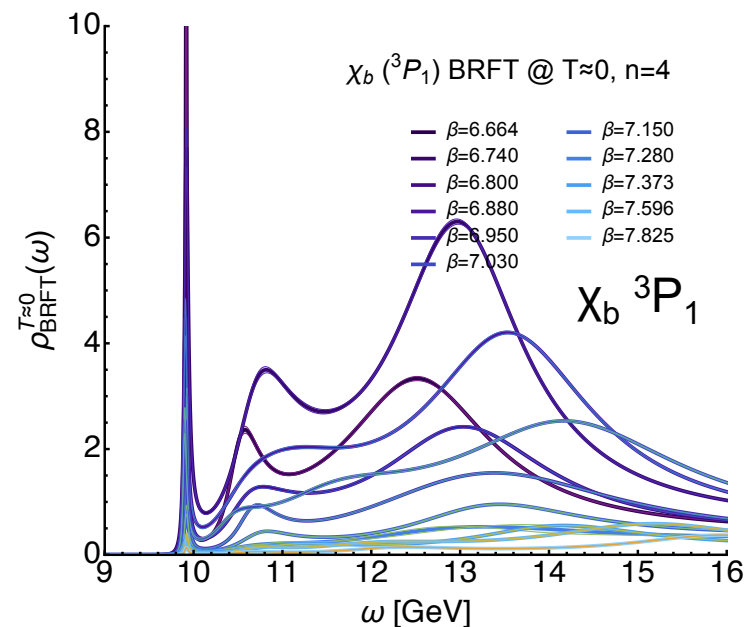
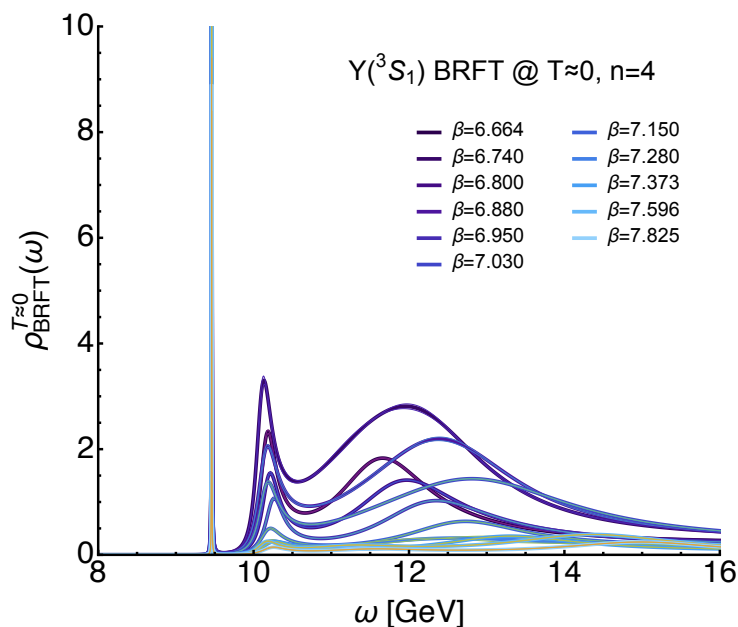
- Introduces penalty on arc length of reconstruction $(dL/d\omega)^2 = 1 + (d\rho/d\omega)^2$
- Efficiently removes ringing but may lead to overestimated peak widths

„low gain – low noise“



Bayesian spectra at $T=0$

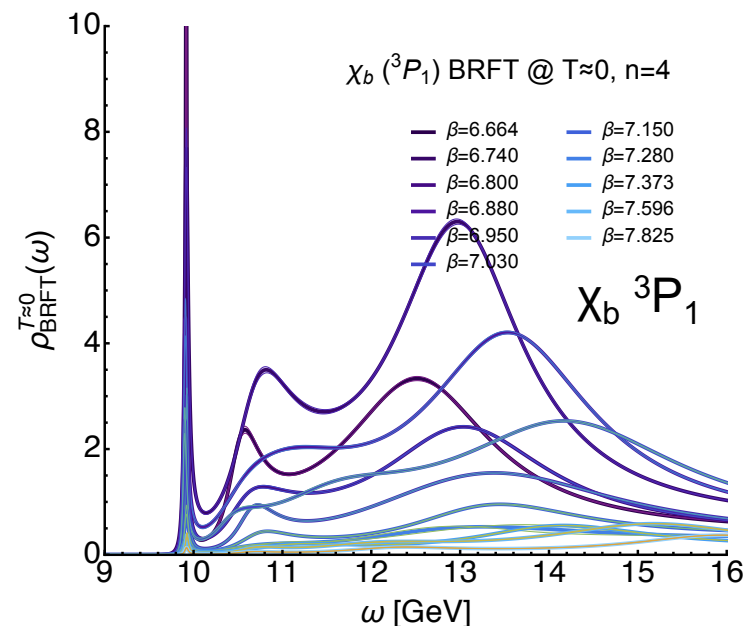
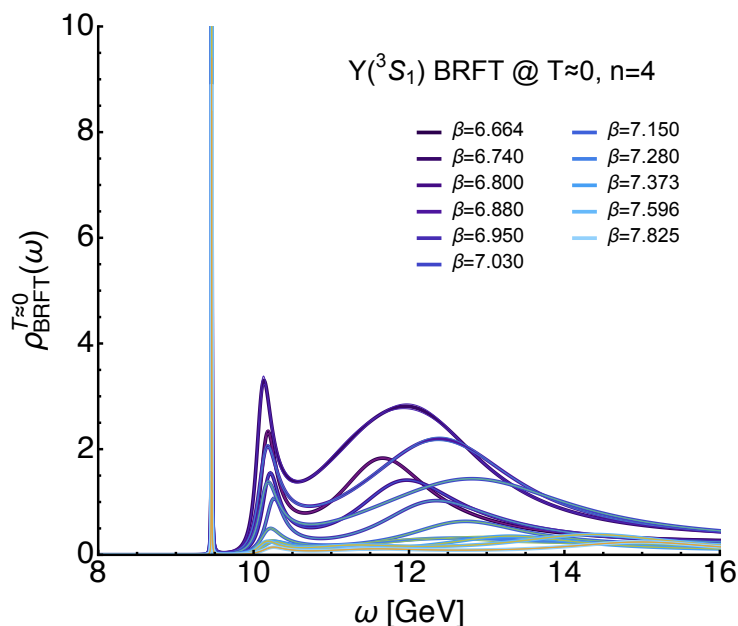
- BR reconstruction exhibits strong ground state signal, shows signs of excited state





Bayesian spectra at $T=0$

- BR reconstruction exhibits strong ground state signal, shows signs of excited state

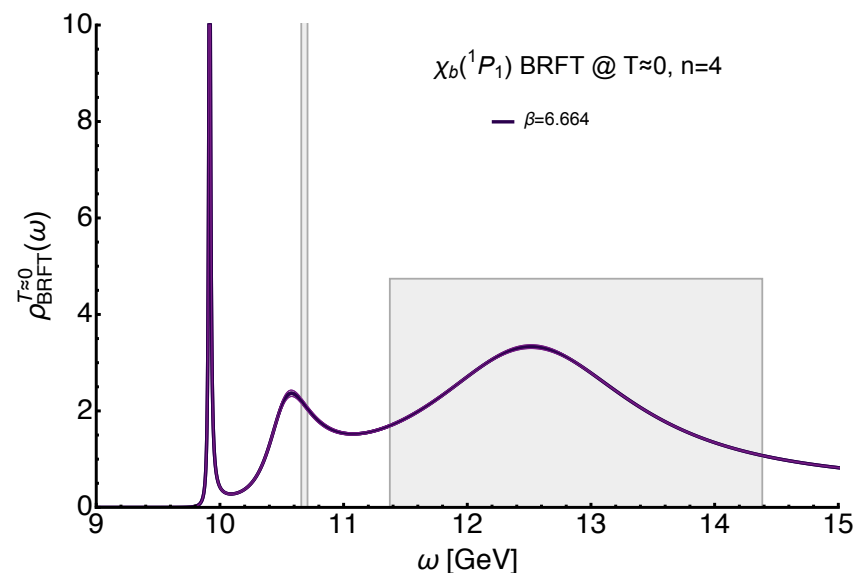
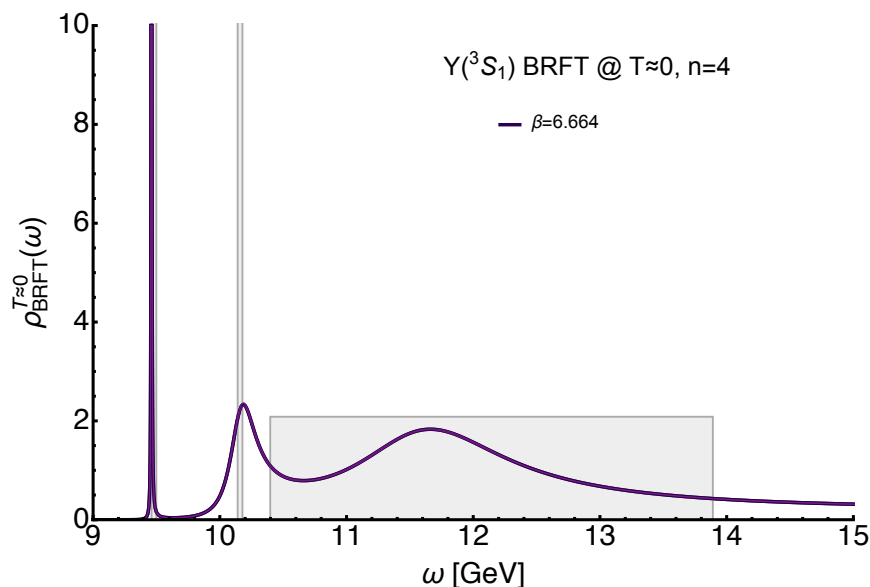


- How to interpret the Bayesian $T=0$ spectral reconstructions: simple fit model
two peaks and a continuum reproduce correlators within statistical errors

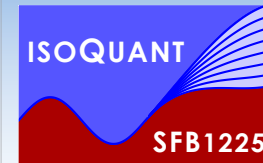


Bayesian spectra at T=0

- BR reconstruction exhibits strong ground state signal, shows signs of excited state

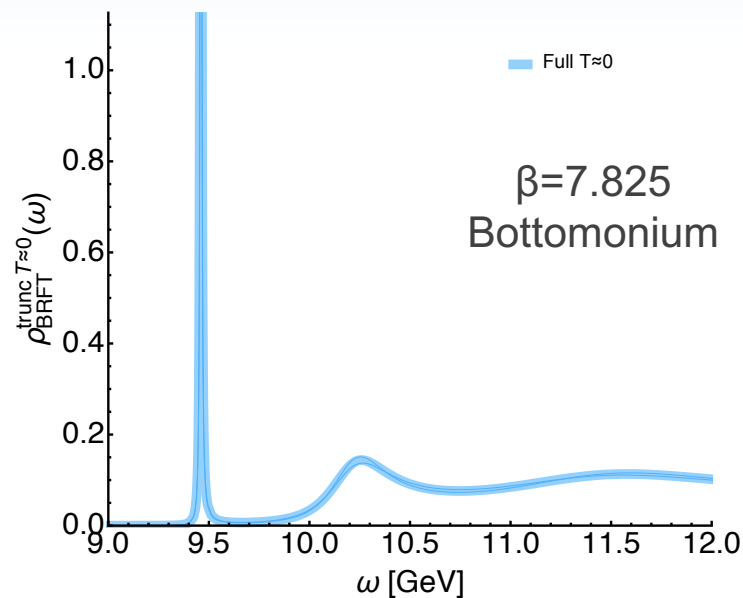
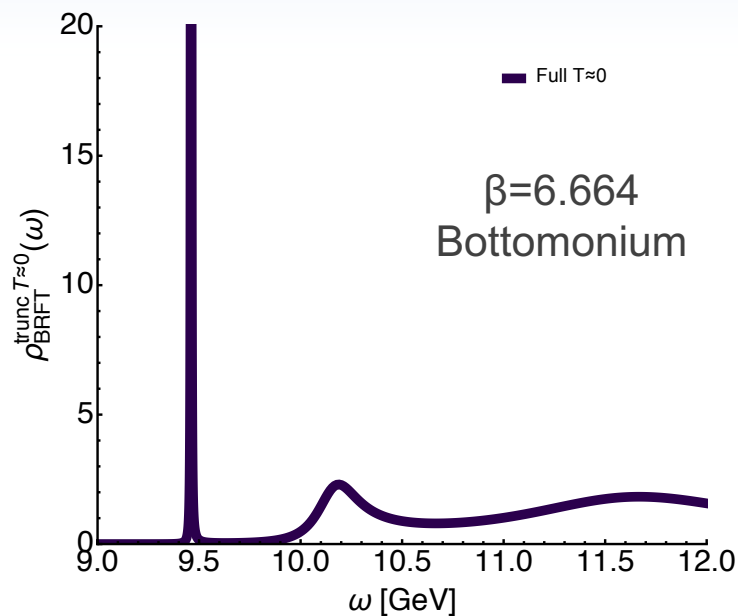


- How to interpret the Bayesian T=0 spectral reconstructions: simple fit model
two peaks and a continuum reproduce correlators within statistical errors



Taking control of systematics I

S.Kim, P.Petreczky, A.R. in preparation

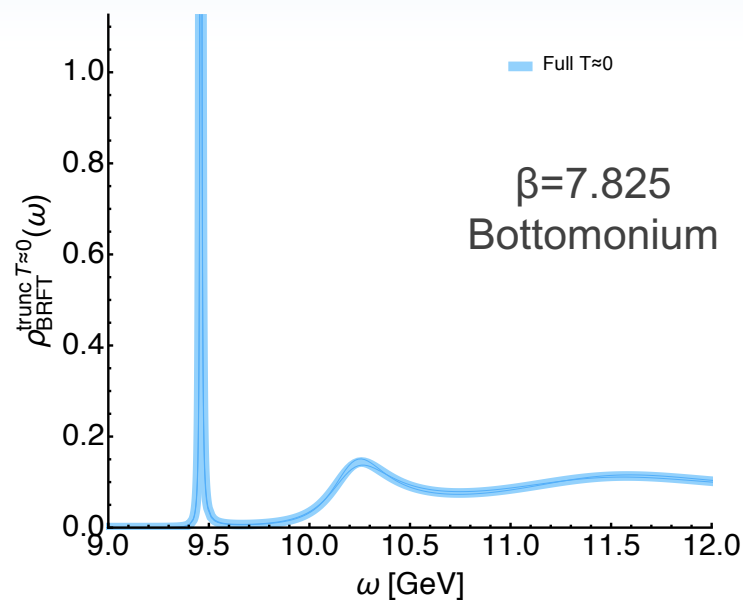
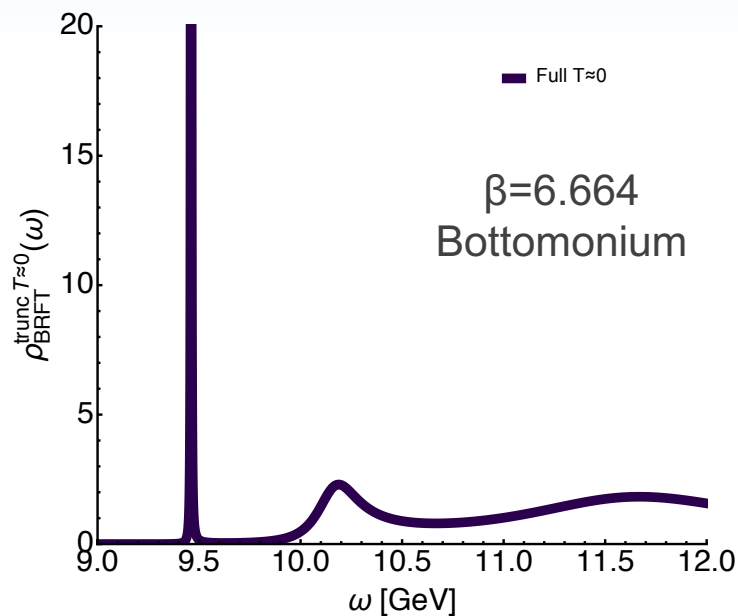


- The “high-gain” BR method resolves $T=0$ ground state very well from $N_T=48-64$ points

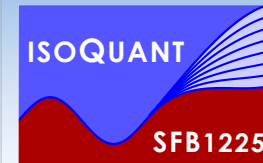


Taking control of systematics I

S.Kim, P.Petreczky, A.R. in preparation

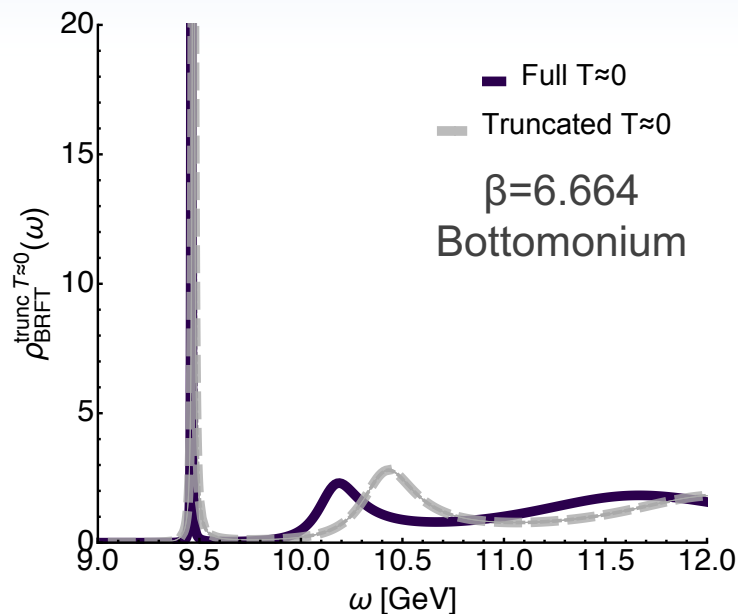


- The “high-gain” BR method resolves $T=0$ ground state very well from $N_T=48-64$ points
- How does accuracy suffer from limited available information at $T>0$ ($N_T=12$) ?

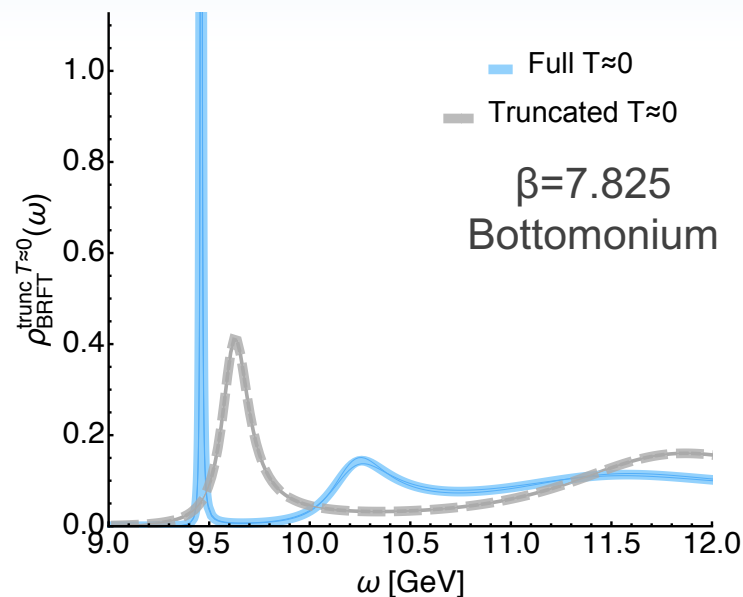


Taking control of systematics I

S.Kim, P.Petreczky, A.R. in preparation



$$\Delta M_{6.664} = 9.3(2) \text{ MeV}$$



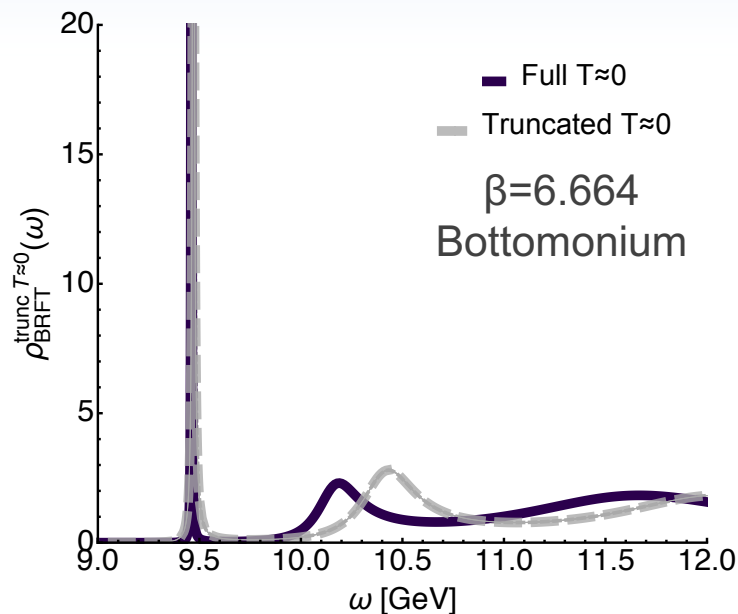
$$\Delta M_{7.825} = 159(1) \text{ MeV}$$

- The “high-gain” BR method resolves $T=0$ ground state very well from $N_T=48-64$ points
- How does accuracy suffer from limited available information at $T>0$ ($N_T=12$) ?

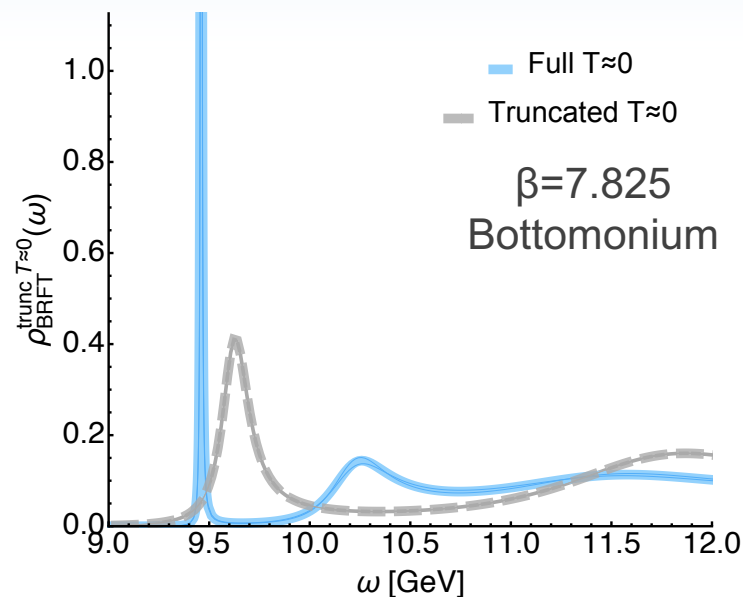


Taking control of systematics I

S.Kim, P.Petreczky, A.R. in preparation



$$\Delta M_{6.664} = 9.3(2) \text{ MeV}$$

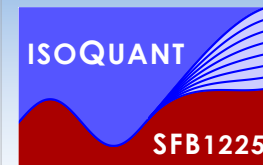


$$\Delta M_{7.825} = 159(1) \text{ MeV}$$

- The “high-gain” BR method resolves $T=0$ ground state very well from $N_T=48-64$ points
- How does accuracy suffer from limited available information at $T>0$ ($N_T=12$) ?

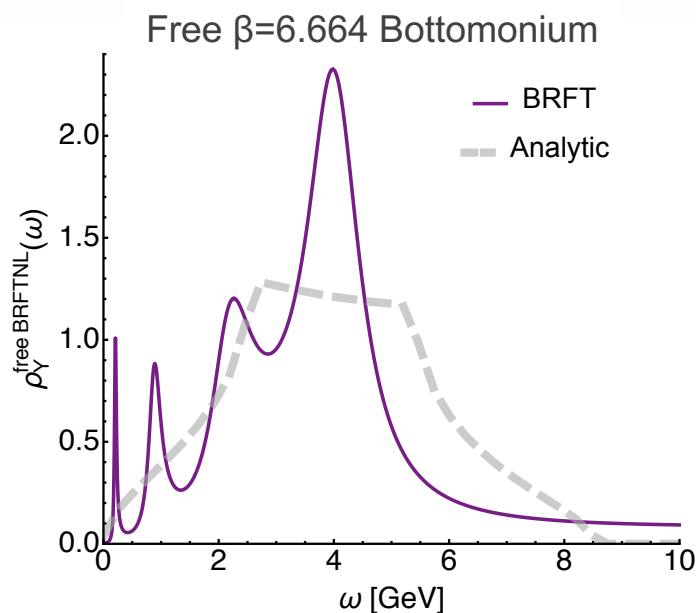


Systematic shift of peaks to higher frequencies, as well as broadening. needs to be accounted for when analyzing $T>0$ spectra

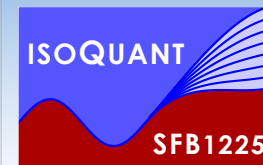


Taking control of systematics II

S.Kim, P.Petreczky, A.R. in preparation

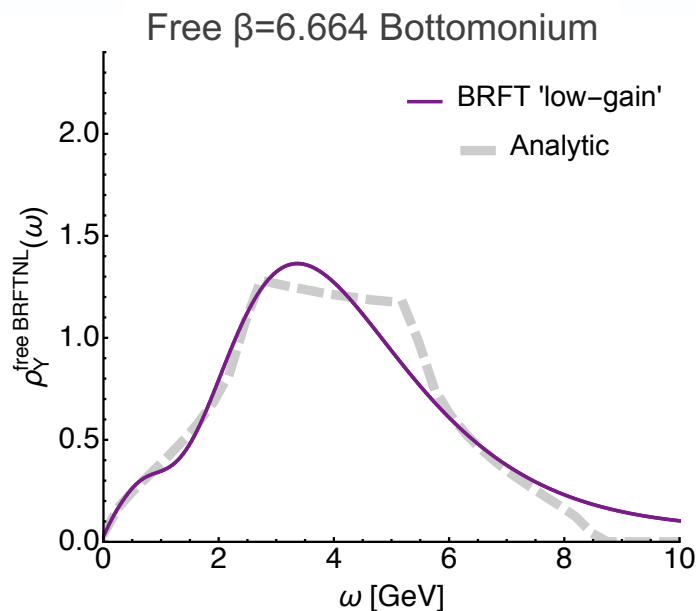


- Standard “high-gain” BR on small ($N_T=12$) simulation datasets suffers from ringing



Taking control of systematics II

S.Kim, P.Petreczky, A.R. in preparation

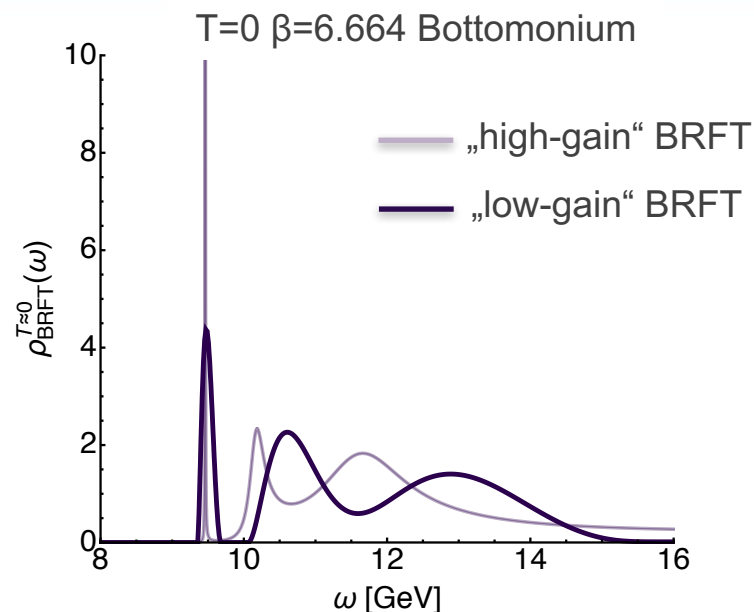
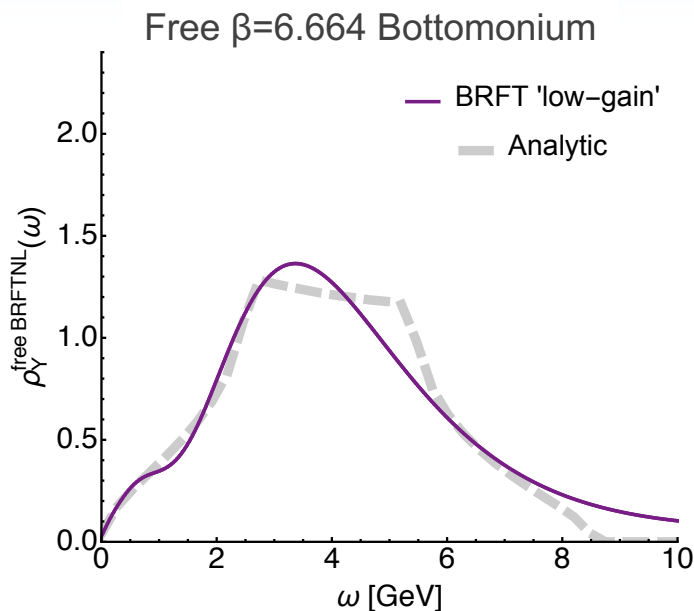


- Standard “high-gain” BR on small ($N_T=12$) simulation datasets suffers from ringing
- New “low-gain” BR removes ringing from reconstructed analytic free spectra at low ω



Taking control of systematics II

S.Kim, P.Petreczky, A.R. in preparation

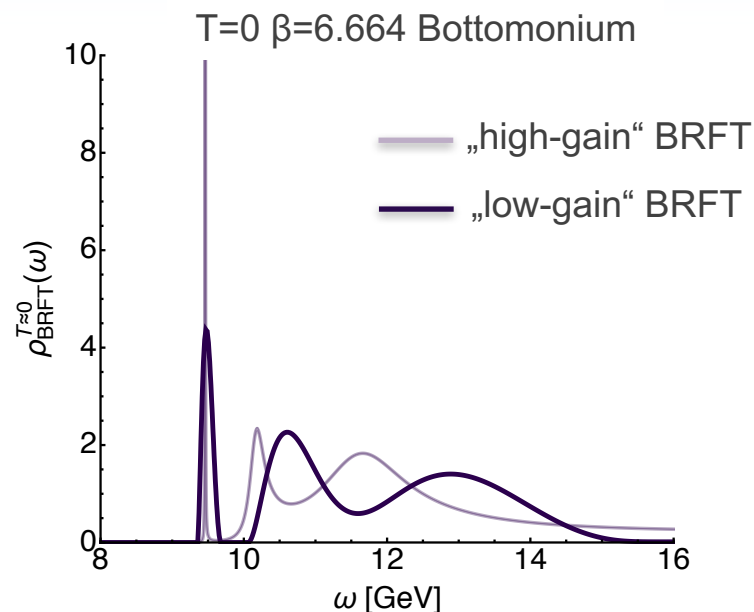
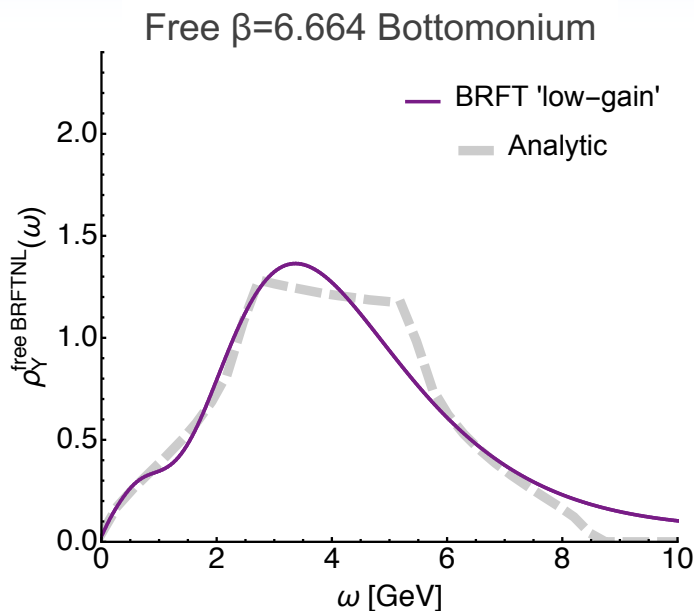


- Standard “high-gain” BR on small ($N_T=12$) simulation datasets suffers from ringing
- New “low-gain” BR removes ringing from reconstructed analytic free spectra at low ω
- New “low-gain” BR method still identifies presence of peaks encoded in data

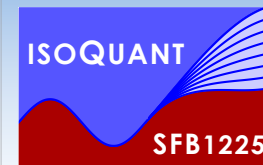


Taking control of systematics II

S.Kim, P.Petreczky, A.R. in preparation

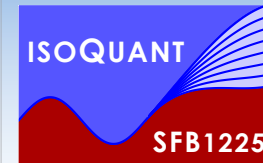


- Standard “high-gain” BR on small ($N_T=12$) simulation datasets suffers from ringing
- New “low-gain” BR removes ringing from reconstructed analytic free spectra at low ω
- New “low-gain” BR method still identifies presence of peaks encoded in data
- Strategy: - Test with “low-gain” reconstruction whether peaks are genuine
- Use “high-gain” reconstruction to extract peak features, e.g. position



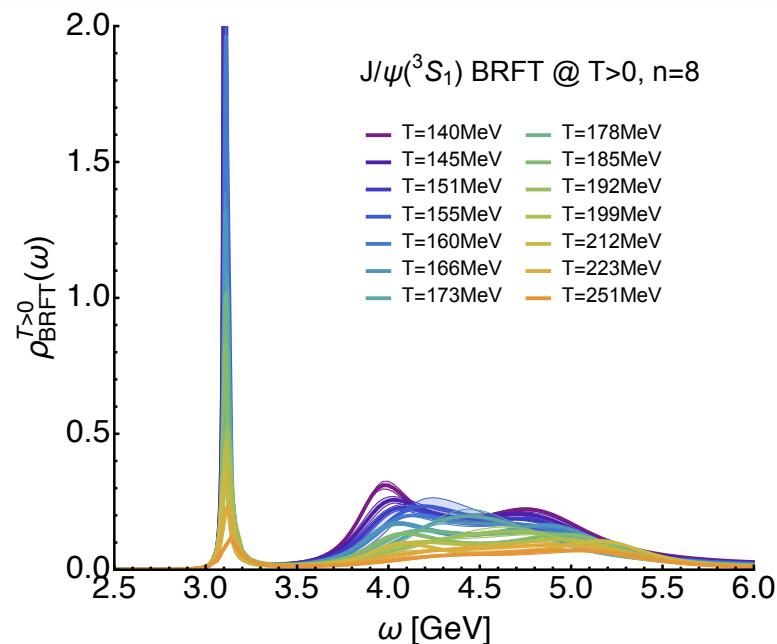
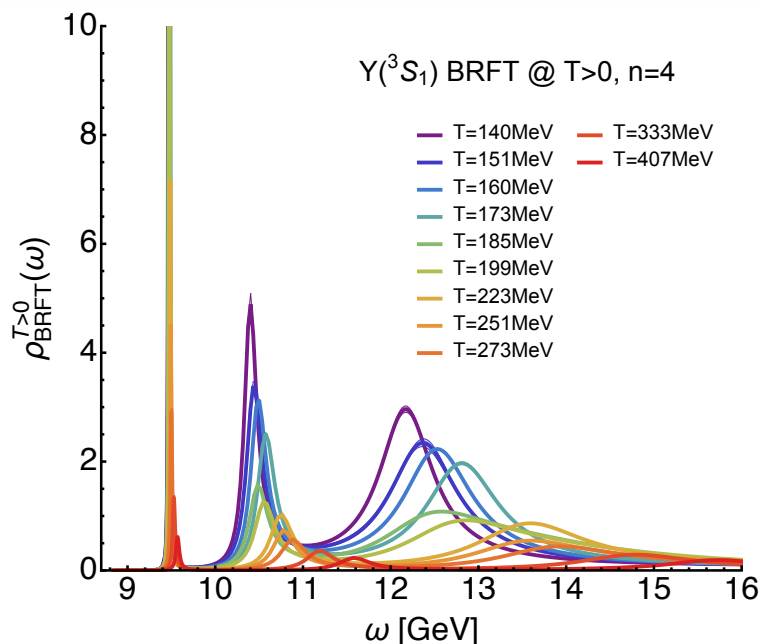
Outline

- Motivation
 - Coherent picture of in-medium heavy-quarkonium from the lattice
- In-medium quarkonium from a lattice EFT (NRQCD)
 - Numerical setup and spectral reconstruction
 - Current $T > 0$ results from realistic full QCD simulations
- Towards improved spectral information from thermal fields
 - Derivation of a novel simulation prescription
 - Current exploratory results from toy models to quenched QCD
- Conclusion

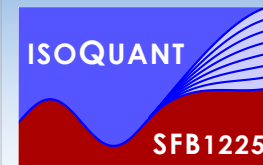


NRQCD S-wave spectra at $T > 0$

S.Kim, P.Petreczky, A.R. in preparation

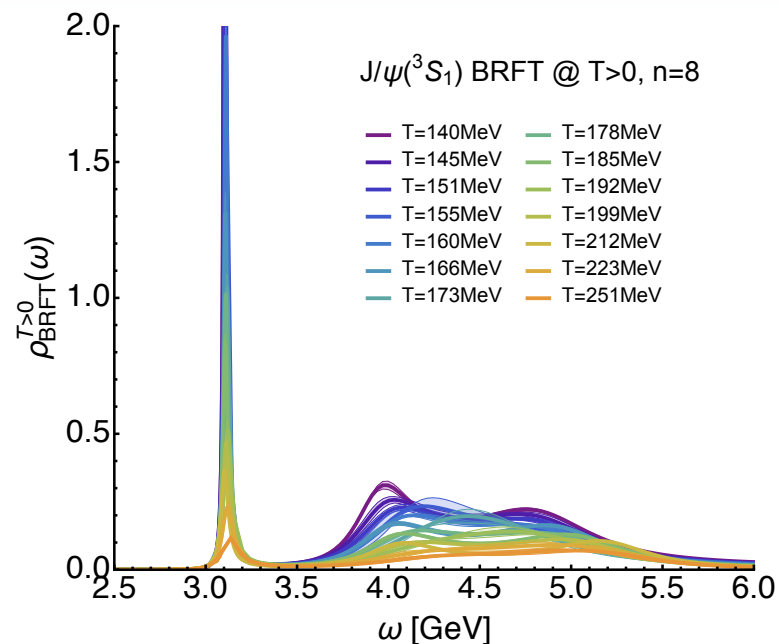
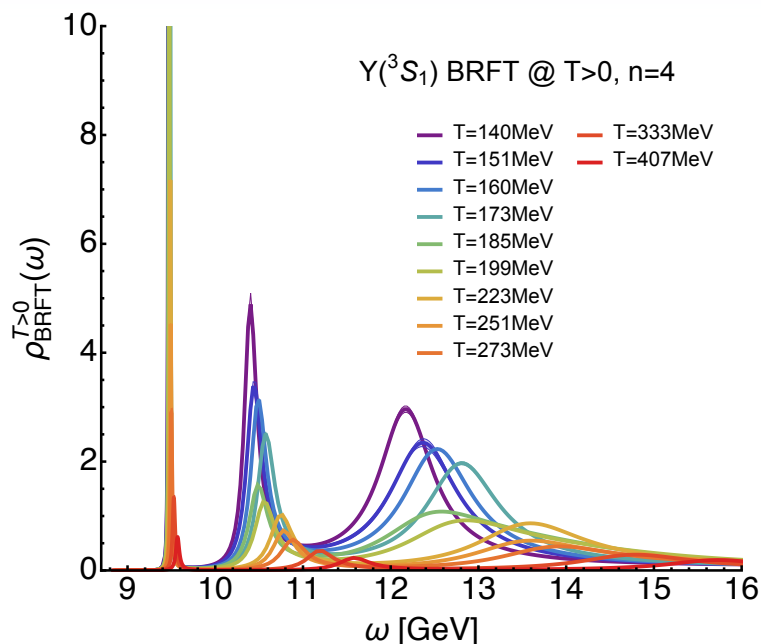


- Ground state well resolved and well separated from higher lying structures

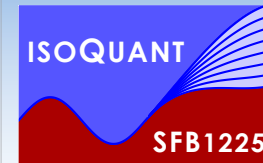


NRQCD S-wave spectra at $T > 0$

S.Kim, P.Petreczky, A.R. in preparation

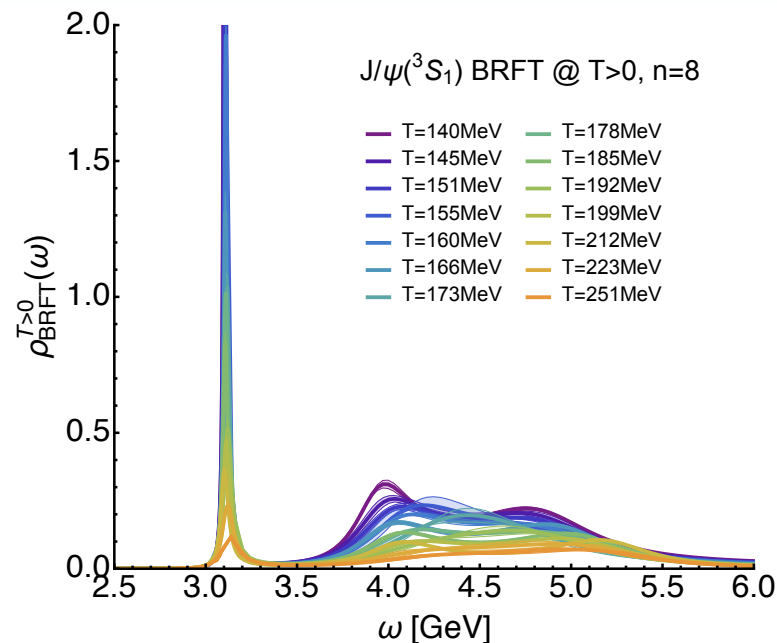
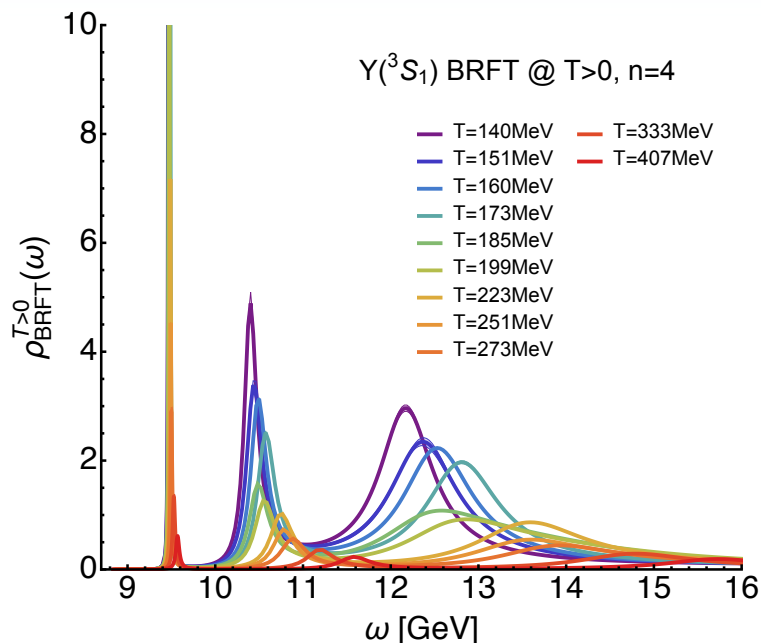


- Ground state well resolved and well separated from higher lying structures
- Combining Euclidean and imaginary frequency data reduces ringing at large ω

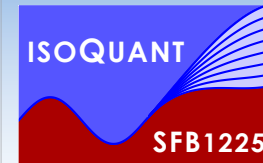


NRQCD S-wave spectra at $T > 0$

S. Kim, P. Petreczky, A.R. in preparation

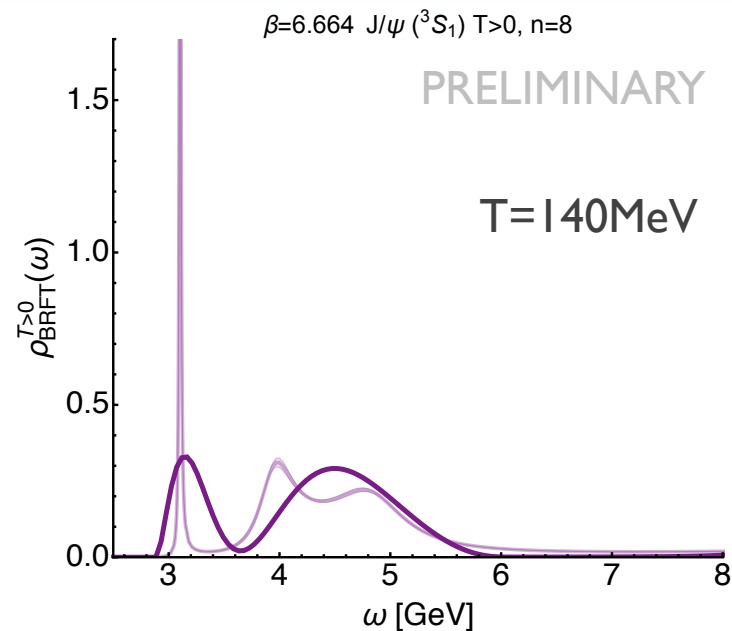
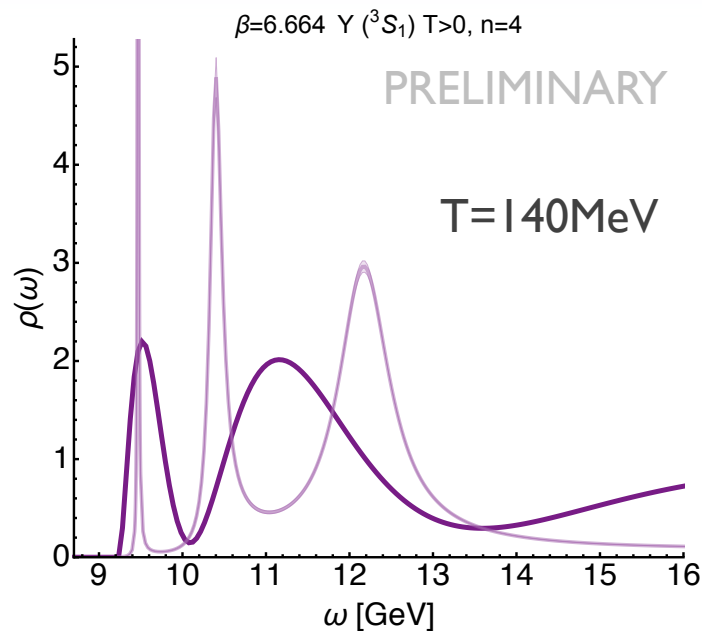


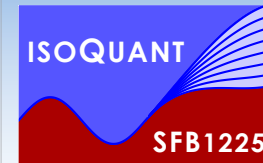
- Ground state well resolved and well separated from higher lying structures
- Combining Euclidean and imaginary frequency data reduces ringing at large ω
- Gradual broadening and shifting of lowest lying peak visible



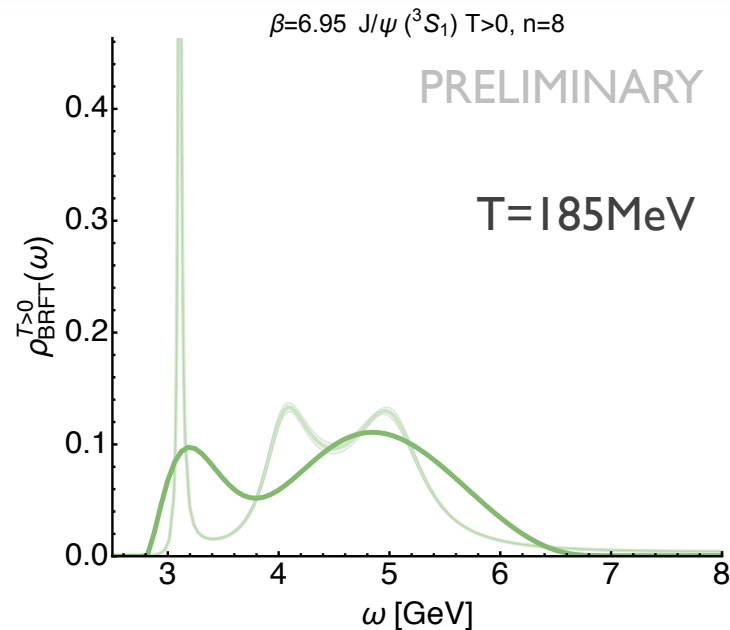
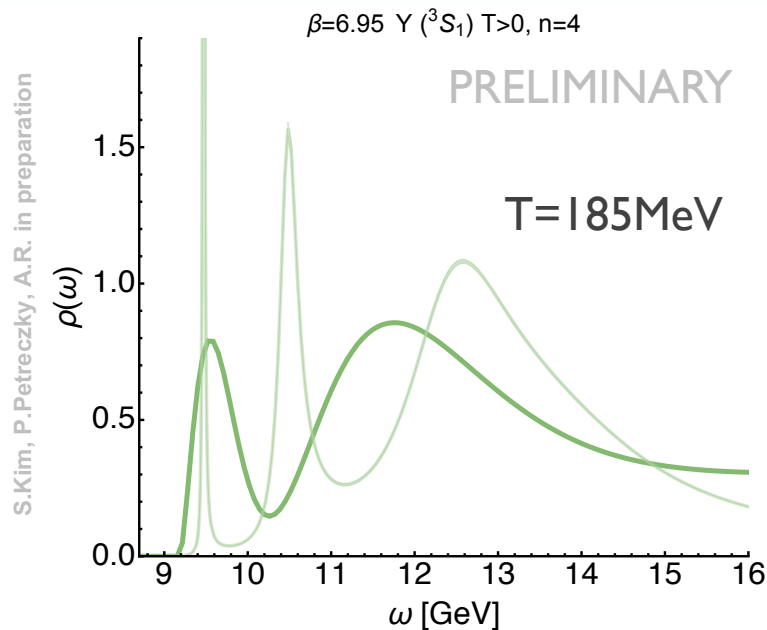
Presence of ground state signals?

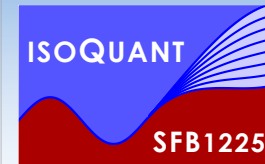
S.Kim, P.Petreczky, A.R. in preparation



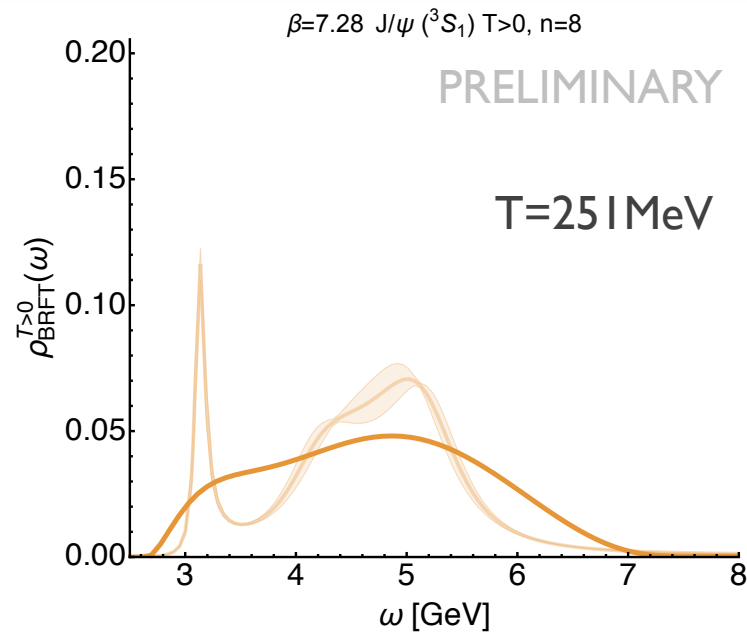
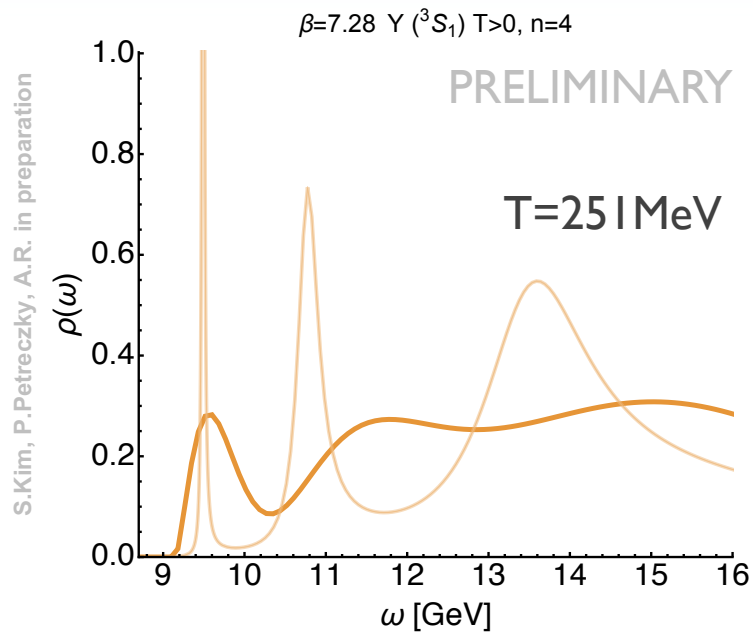


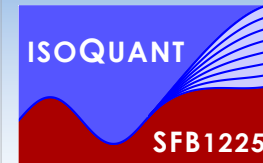
Presence of ground state signals?



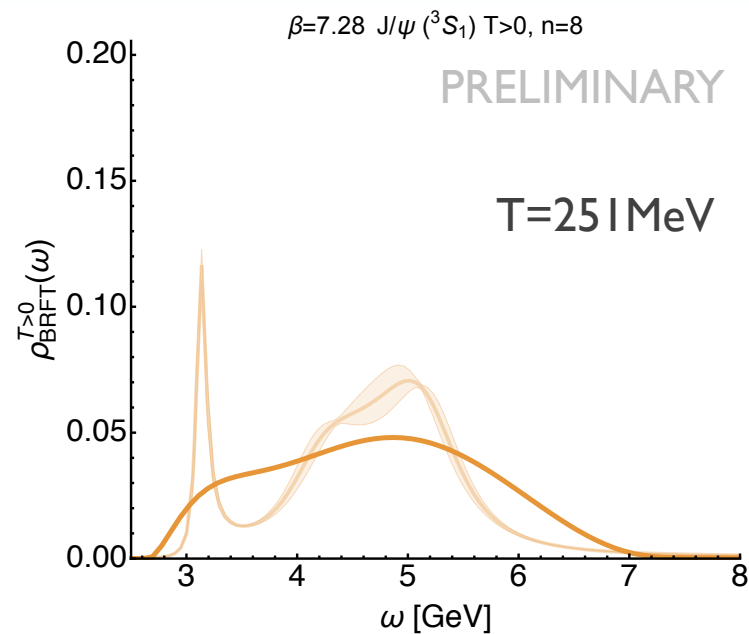
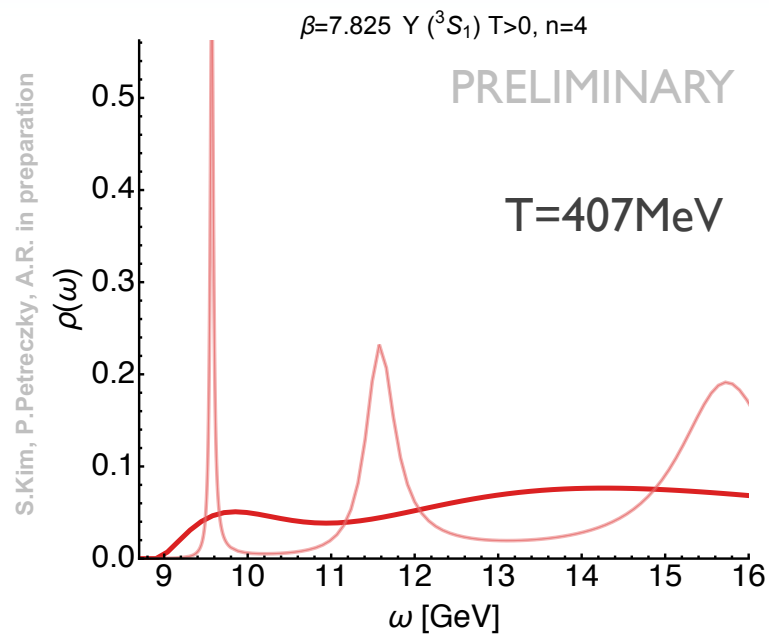


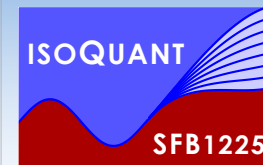
Presence of ground state signals?



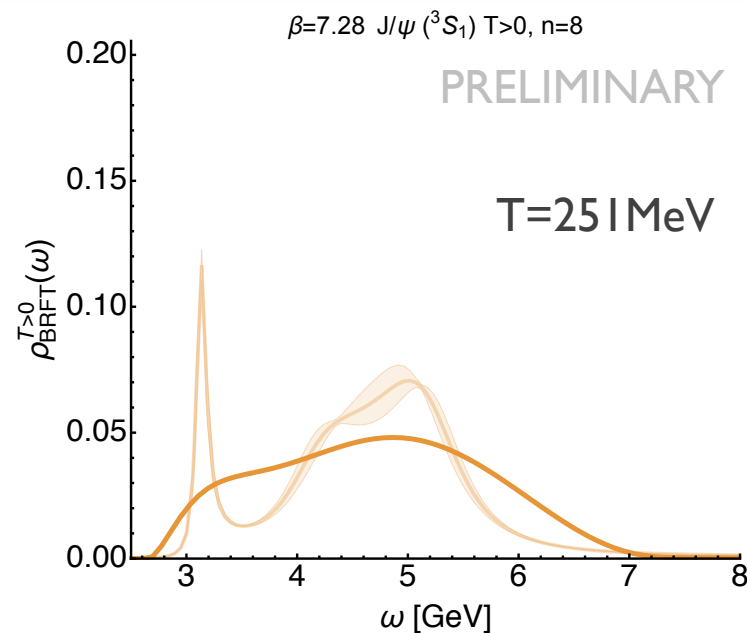
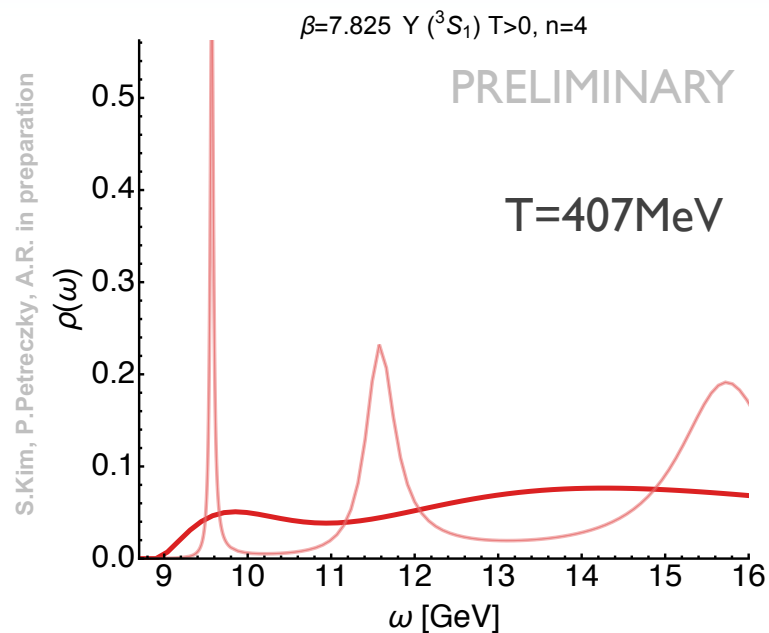


Presence of ground state signals?

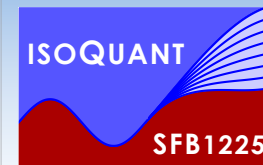




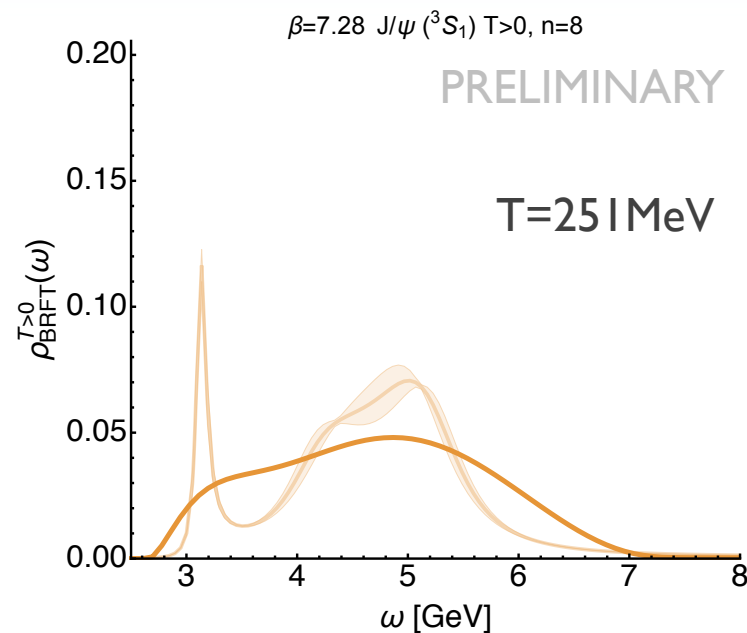
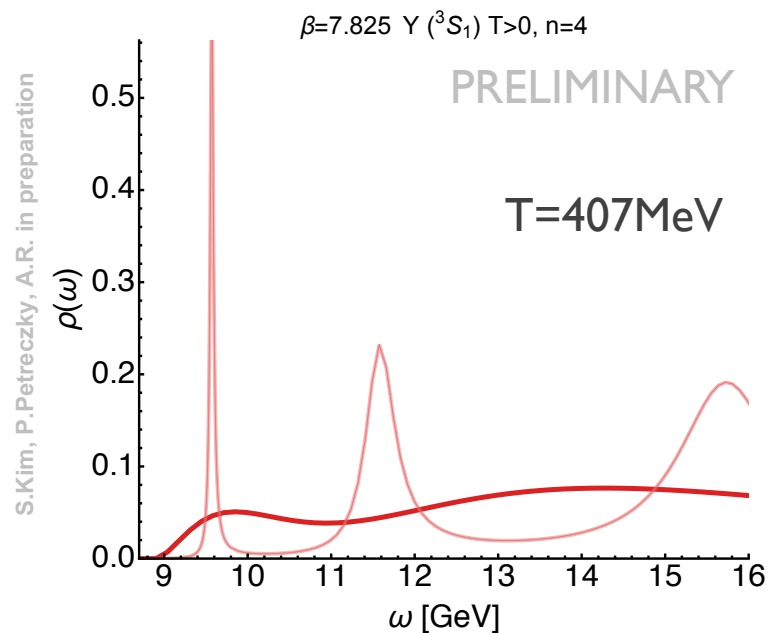
Presence of ground state signals?



- New “low-gain” BR method shows gradual weakening of ground state signal



Presence of ground state signals?



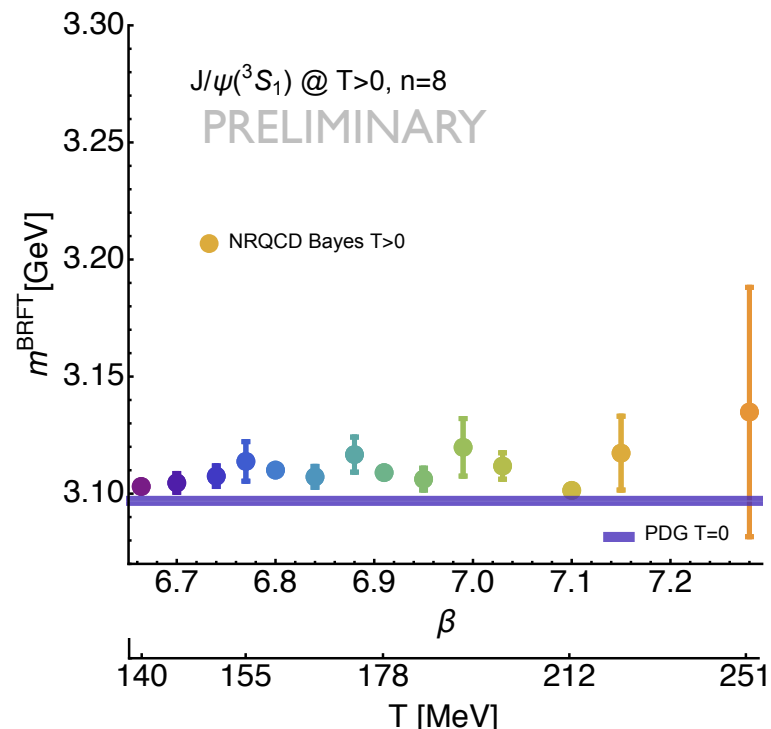
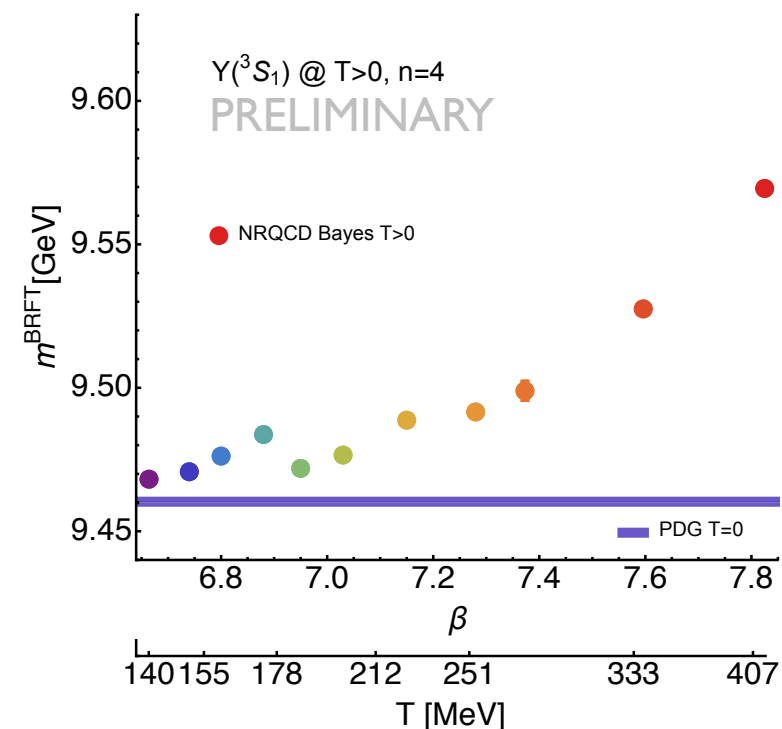
- New “low-gain” BR method shows gradual weakening of ground state signal
- At highest T in individual channels: weak ground state remnants remain visible

Upsilon signal up to $T=407\text{MeV}$

Faint J/ψ signal up to $T=251\text{MeV}$



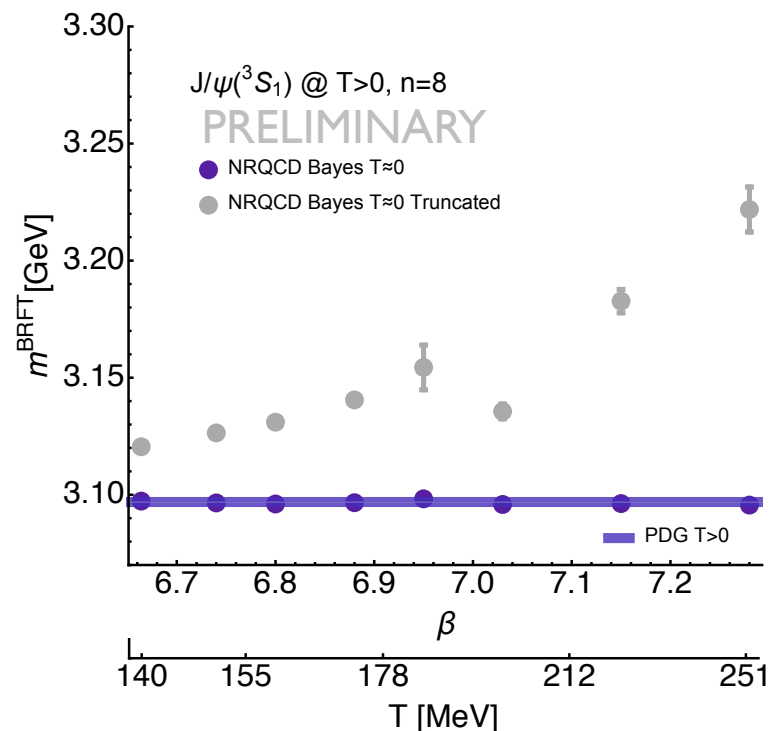
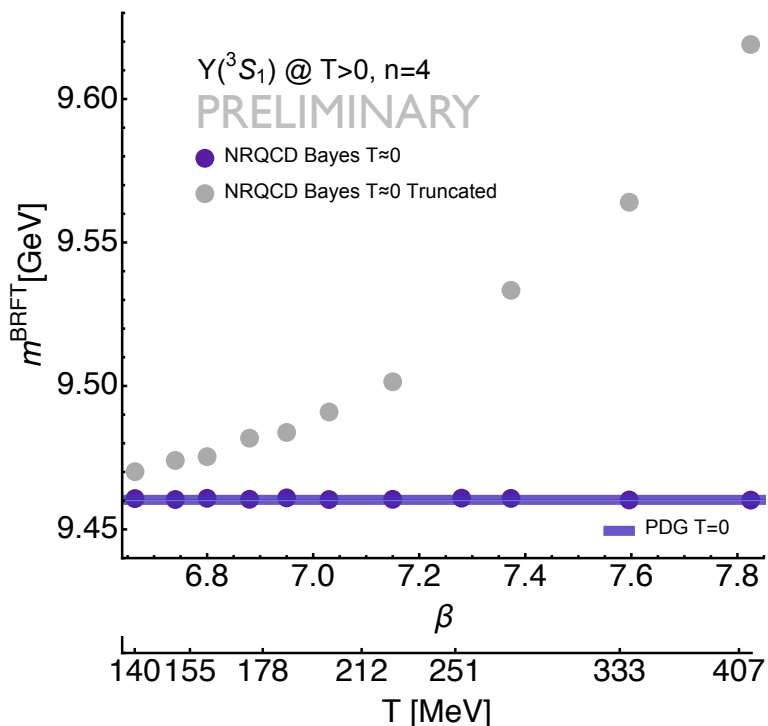
In-medium S -wave mass shifts



Naïve inspection of in-medium modification appears to show increasing masses



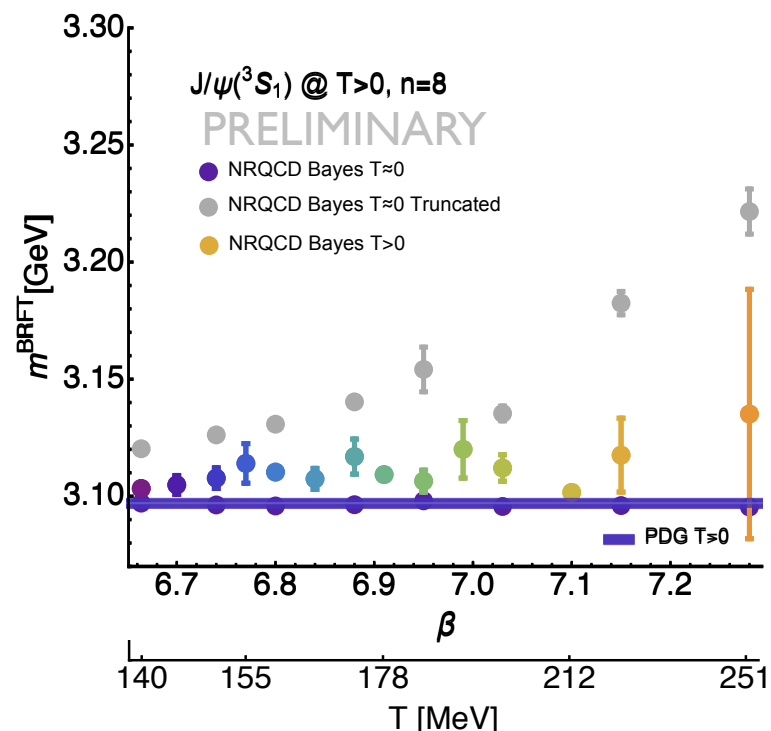
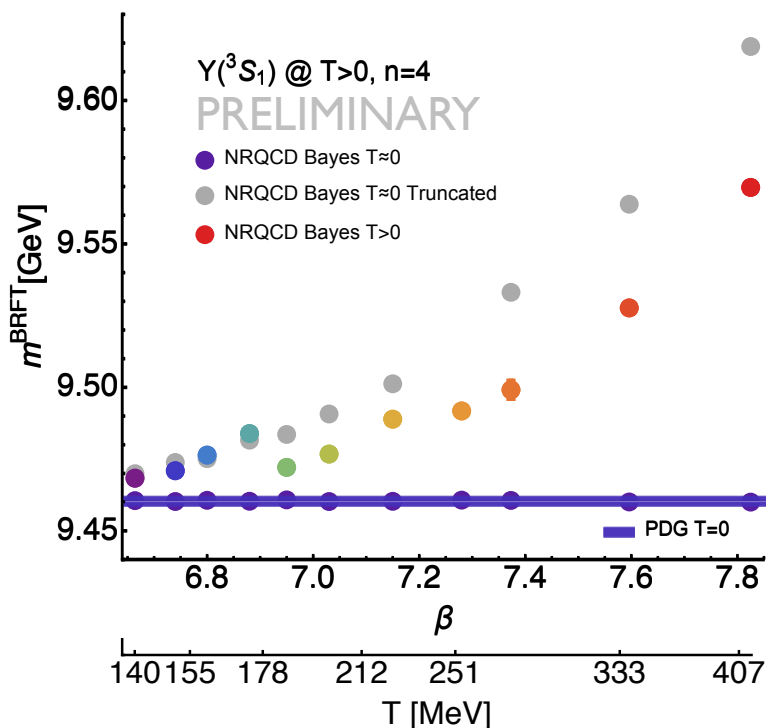
In-medium S -wave mass shifts



- Naïve inspection of in-medium modification appears to show increasing masses
- BR method systematics: Low number of datapoints introduces shifts to larger masses



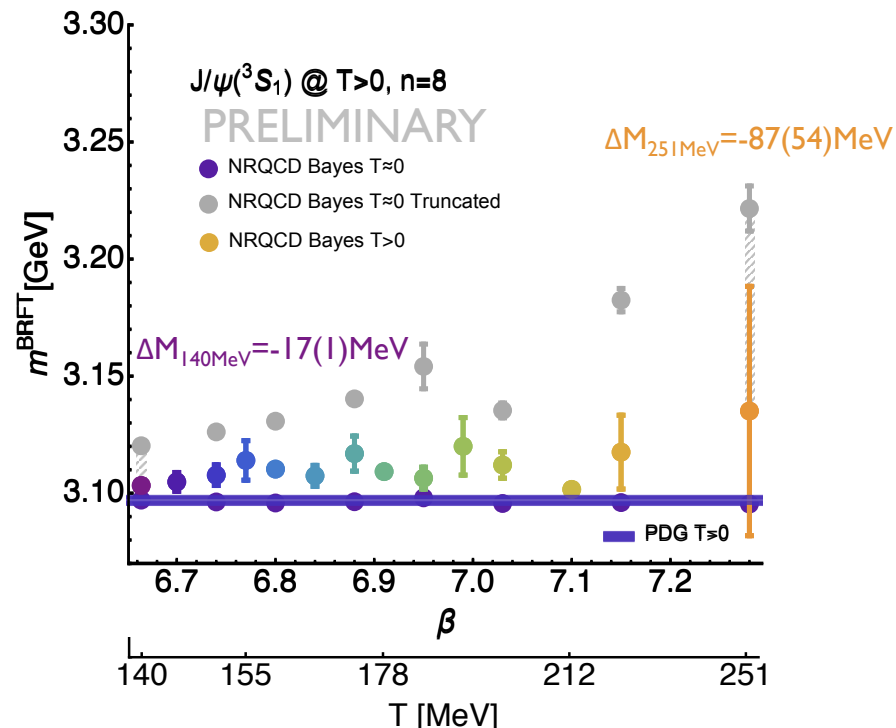
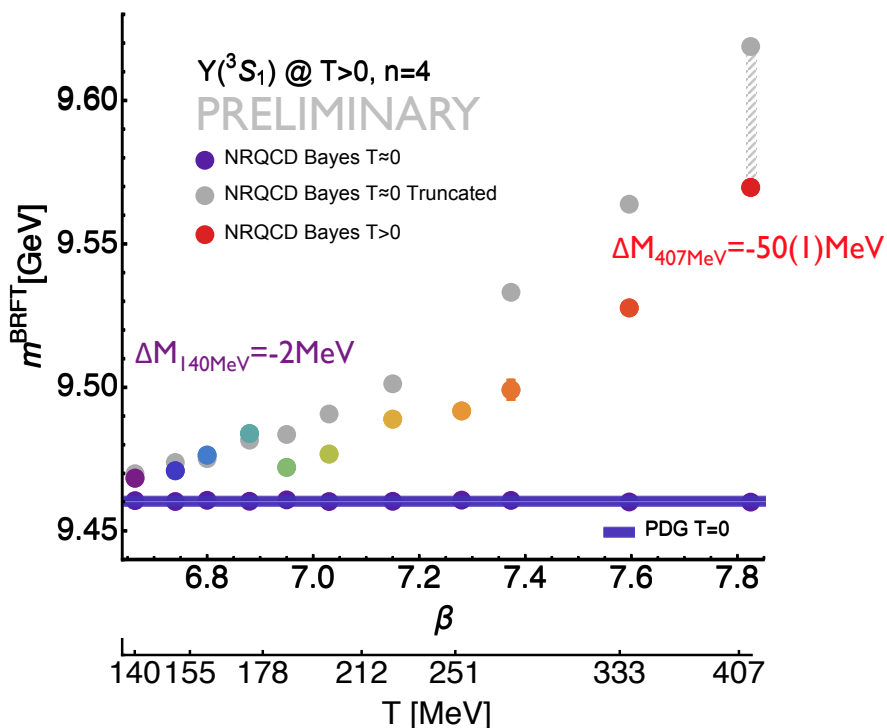
In-medium S -wave mass shifts



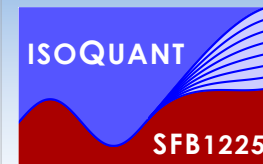
- Naïve inspection of in-medium modification appears to show increasing masses
- BR method systematics: Low number of datapoints introduces shifts to larger masses



In-medium S -wave mass shifts

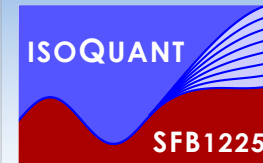


- Naïve inspection of in-medium modification appears to show increasing masses
- BR method systematics: Low number of datapoints introduces shifts to larger masses
- Actual in-medium effect: lowering of bound state mass, consistent with potential studies



Outline

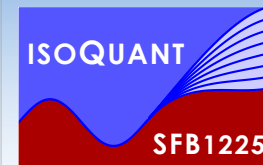
- Motivation
 - Coherent picture of in-medium heavy-quarkonium from the lattice
- In-medium quarkonium from a lattice EFT (NRQCD)
 - Numerical setup and spectral reconstruction
 - Current $T>0$ results from realistic full QCD simulations
- Towards improved spectral information from thermal fields
 - Derivation of a novel simulation prescription
 - Current exploratory results from toy models to quenched QCD
- Conclusion



The underlying difficulty

- Intrinsic problem of standard spectral reconstruction: exponential information loss

$$D(\tau) = \int_0^{\infty} d\omega \frac{\cosh[\omega(\tau - \beta/2)]}{\sinh[\omega\beta/2]} \rho(\omega)$$

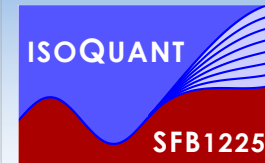


The underlying difficulty

- Intrinsic problem of standard spectral reconstruction: exponential information loss

$$D(\tau) = \int_0^{\infty} d\omega \frac{\cosh[\omega(\tau - \beta/2)]}{\sinh[\omega\beta/2]} \rho(\omega) \quad \longrightarrow \quad D(\omega_n) = \int_0^{\infty} d\omega \frac{2\omega}{\omega_n^2 + \omega^2} \rho(\omega)$$

- 1st part of the remedy: go over to imaginary frequencies (hint of possible exp. improvement)

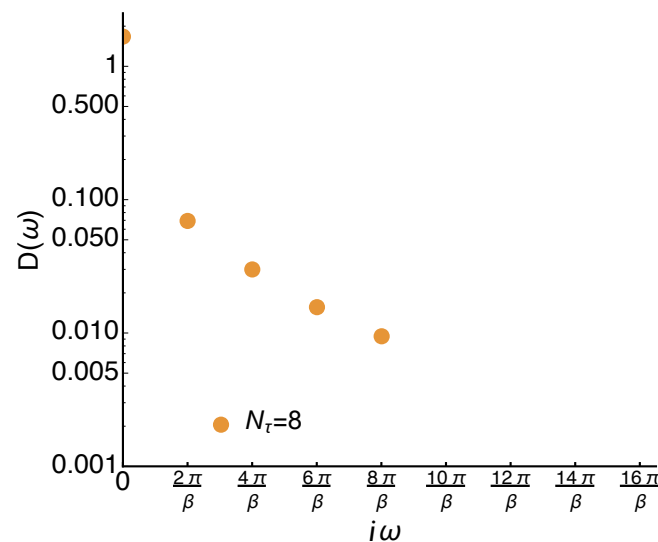
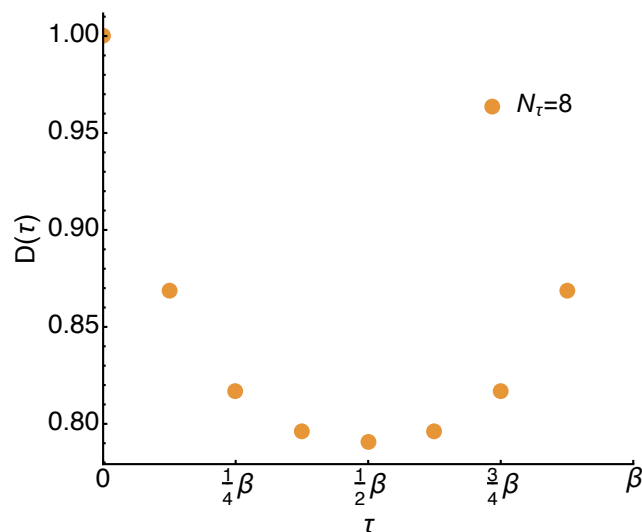


The underlying difficulty

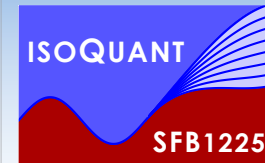
- Intrinsic problem of standard spectral reconstruction: exponential information loss

$$D(\tau) = \int_0^\infty d\omega \frac{\cosh[\omega(\tau - \beta/2)]}{\sinh[\omega\beta/2]} \rho(\omega) \quad \longrightarrow \quad D(\omega_n) = \int_0^\infty d\omega \frac{2\omega}{\omega_n^2 + \omega^2} \rho(\omega)$$

- 1st part of the remedy: go over to imaginary frequencies (hint of possible exp. improvement)



- Standard lattice simulation access only Matsubara frequencies: $\omega_n = 2\pi nT$, $n \in \mathbb{Z}$

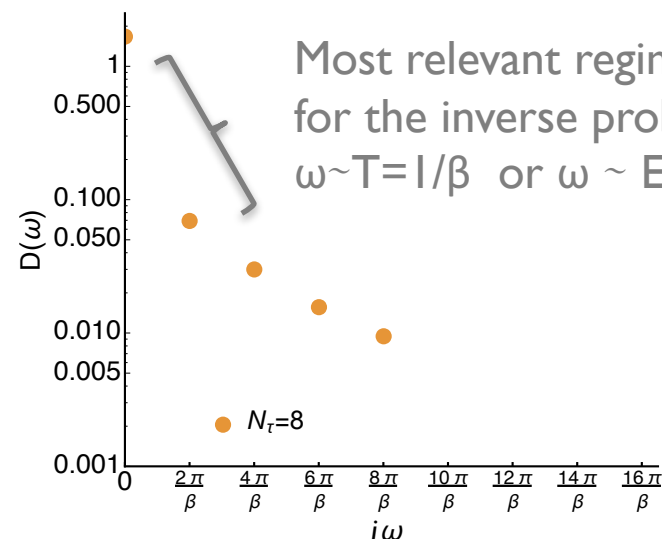
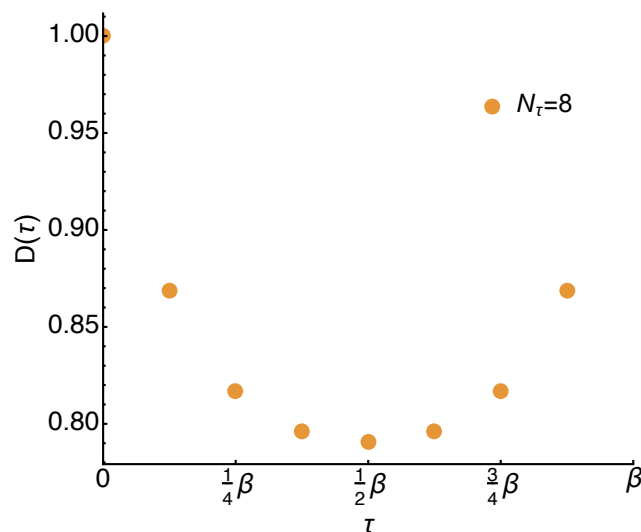


The underlying difficulty

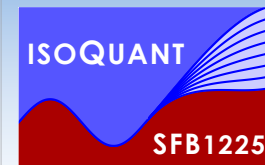
- Intrinsic problem of standard spectral reconstruction: exponential information loss

$$D(\tau) = \int_0^\infty d\omega \frac{\cosh[\omega(\tau - \beta/2)]}{\sinh[\omega\beta/2]} \rho(\omega) \quad \longrightarrow \quad D(\omega_n) = \int_0^\infty d\omega \frac{2\omega}{\omega_n^2 + \omega^2} \rho(\omega)$$

- 1st part of the remedy: go over to imaginary frequencies (hint of possible exp. improvement)



- Standard lattice simulation access only Matsubara frequencies: $\omega_n = 2\pi nT$, $n \in \mathbb{Z}$

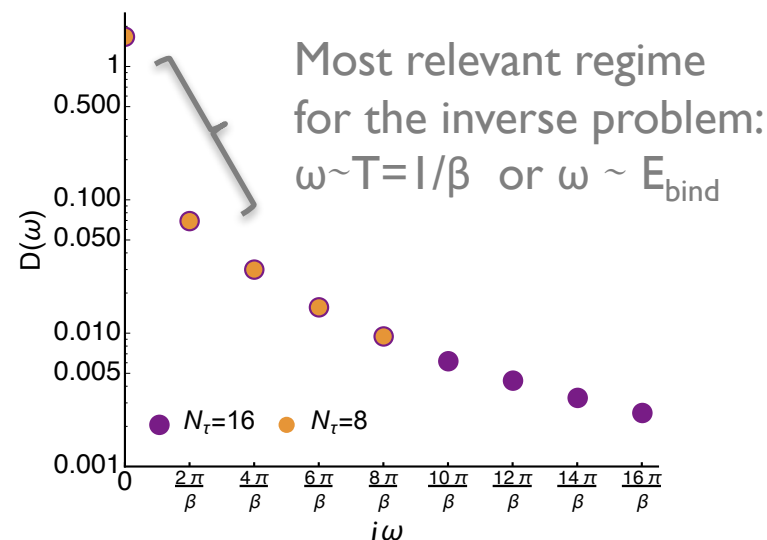
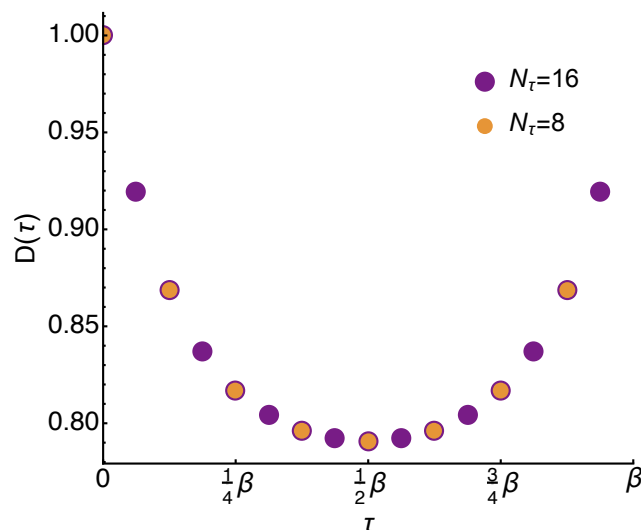


The underlying difficulty

- Intrinsic problem of standard spectral reconstruction: exponential information loss

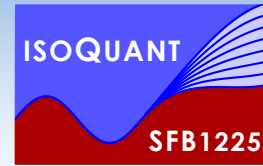
$$D(\tau) = \int_0^\infty d\omega \frac{\cosh[\omega(\tau - \beta/2)]}{\sinh[\omega\beta/2]} \rho(\omega) \quad \longrightarrow \quad D(\omega_n) = \int_0^\infty d\omega \frac{2\omega}{\omega_n^2 + \omega^2} \rho(\omega)$$

- 1st part of the remedy: go over to imaginary frequencies (hint of possible exp. improvement)

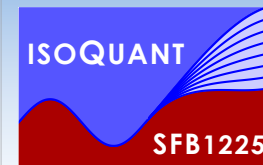


- Standard lattice simulation access only Matsubara frequencies: $\omega_n = 2\pi nT$, $n \in \mathbb{Z}$

The Schwinger-Keldysh contour



- The thermal scalar field as real-time initial value problem $Z = \text{Tr}[\rho(0) = e^{-\beta H}]$



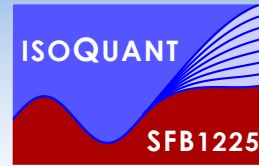
The Schwinger-Keldysh contour

- The thermal scalar field as real-time initial value problem $Z = \text{Tr}[\rho(0) = e^{-\beta H}]$

$$Z = \int [d\varphi_0^+] [d\varphi_0^-] \langle \varphi_0^+ | \rho(0) | \varphi_0^- \rangle \langle \varphi_0^- | \varphi_0^+ \rangle$$

— initial conditions





The Schwinger-Keldysh contour

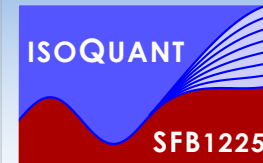
- The thermal scalar field as real-time initial value problem $Z = \text{Tr}[\rho(0) = e^{-\beta H}]$

$$Z = \int [d\varphi_0^+] [d\varphi_0^-] \langle \varphi_0^+ | \rho(0) | \varphi_0^- \rangle \int [d\varphi_t] \langle \varphi_0^- | e^{iHt} | \varphi_t \rangle \langle \varphi_t | e^{-iHt} | \varphi_0^+ \rangle$$

— initial conditions

— — quantum dynamics





The Schwinger-Keldysh contour

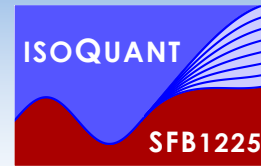
- The thermal scalar field as real-time initial value problem $Z = \text{Tr}[\rho(0) = e^{-\beta H}]$

$$Z = \int [d\varphi_0^+] [d\varphi_0^-] \langle \varphi_0^+ | e^{-\beta \hat{H}} | \varphi_0^- \rangle \int_{\varphi_0^+}^{\varphi_0^-} \mathcal{D}\varphi e^{iS_M[\varphi^+] - iS_M[\varphi^-]}$$

— initial conditions

— — quantum dynamics

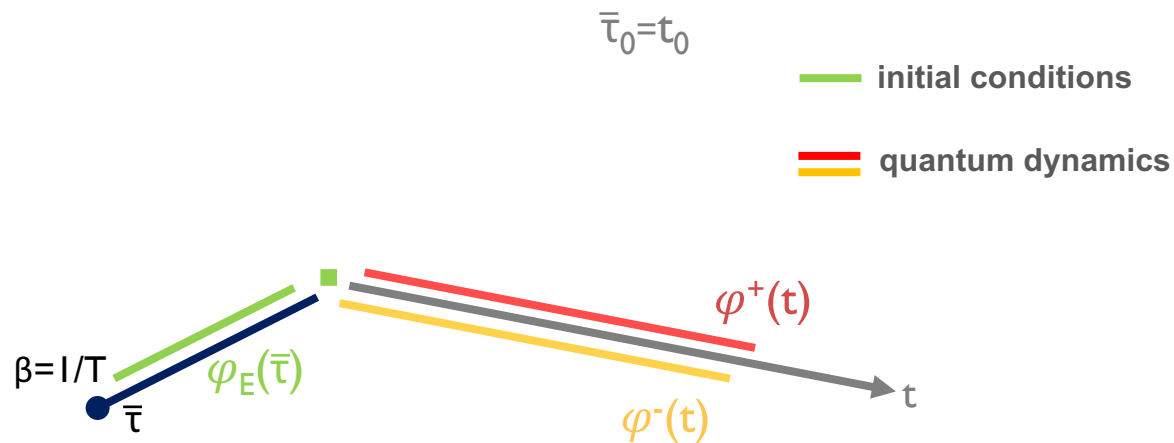


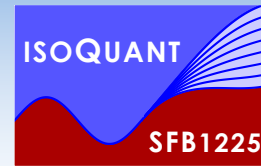


The Schwinger-Keldysh contour

- The thermal scalar field as real-time initial value problem $Z = \text{Tr}[\rho(0) = e^{-\beta H}]$

$$Z = \int_{\varphi_E(0) = \varphi_E(\beta)} \mathcal{D}\varphi_E e^{-S_E[\varphi_E]} \int_{\varphi^+(t_0, \mathbf{x}) = \varphi_E(0)}^{\varphi^-(t_0, \mathbf{x}) = \varphi_E(\beta)} \mathcal{D}\varphi e^{iS_M[\varphi^+] - iS_M[\varphi^-]}$$

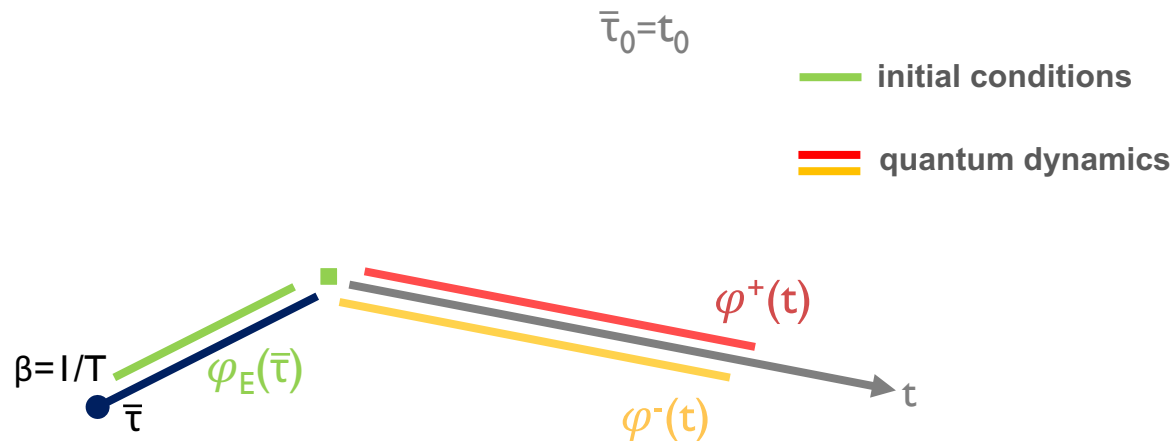




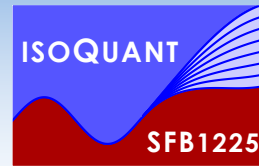
The Schwinger-Keldysh contour

- The thermal scalar field as real-time initial value problem $Z = \text{Tr}[\rho(0) = e^{-\beta H}]$

$$Z = \int_{\varphi_E(0) = \varphi_E(\beta)} \mathcal{D}\varphi_E e^{-S_E[\varphi_E]} \int_{\varphi^+(t_0, \mathbf{x}) = \varphi_E(0)}^{\varphi^-(t_0, \mathbf{x}) = \varphi_E(\beta)} \mathcal{D}\varphi e^{iS_M[\varphi^+] - iS_M[\varphi^-]}$$



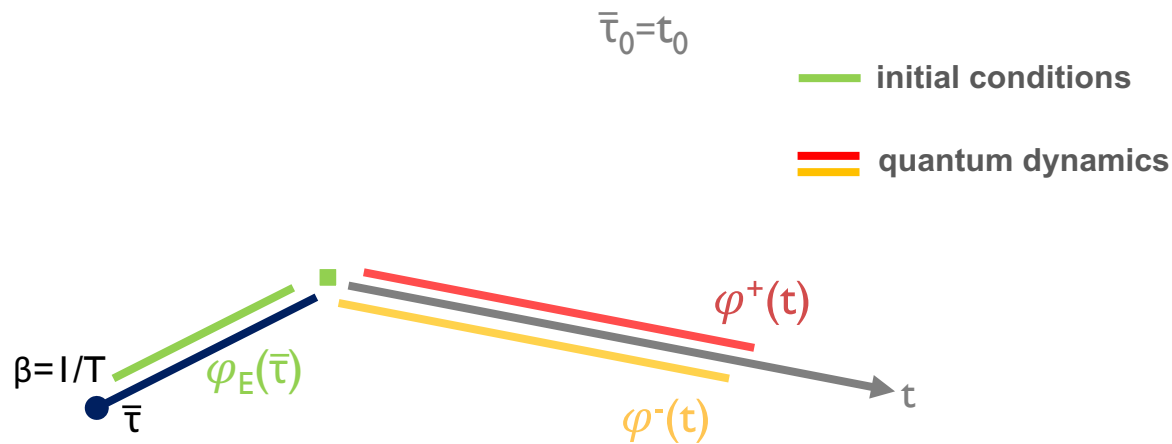
- At this stage: Euclidean time as a mathematical tool to sample $\varphi^+(t_0)$ and $\varphi^-(t_0)$

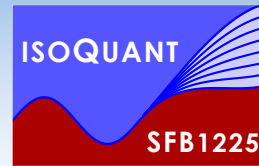


How do the two paths contribute?

- Thermal equilibrium is special: $G^{++} = \langle \varphi^+ \varphi^+ \rangle$ correlator alone suffices to compute ρ

$$G^{++}(p^0, \mathbf{p}) = \int \frac{dq^0}{2\pi i} \frac{\rho(q^0, \mathbf{p})}{p^0 - q^0 + i\epsilon} - n(p^0) \rho(p^0, \mathbf{p})$$



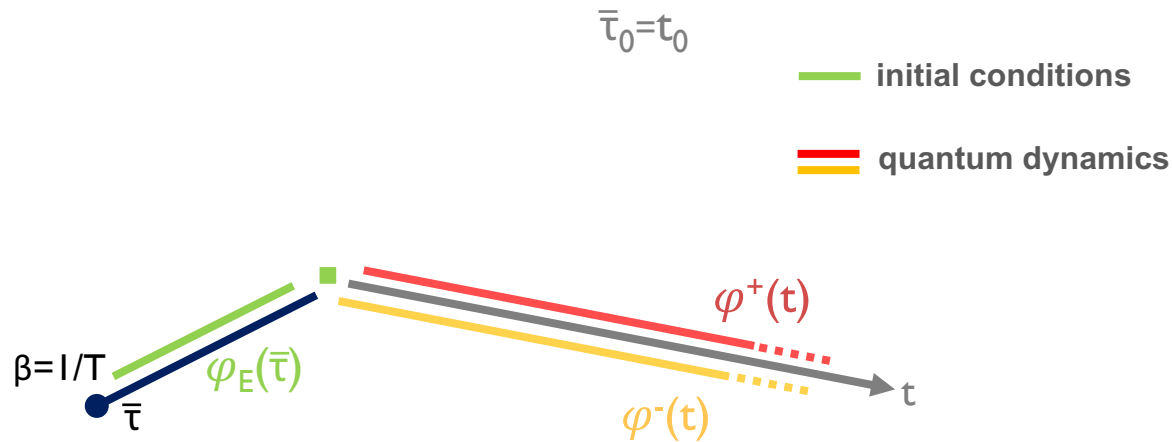


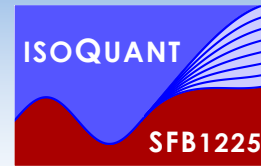
How do the two paths contribute?

- Thermal equilibrium is special: $G^{++} = \langle \varphi^+ \varphi^+ \rangle$ correlator alone suffices to compute ρ

$$G^{++}(p^0, \mathbf{p}) = \int \frac{dq^0}{2\pi i} \frac{\rho(q^0, \mathbf{p})}{p^0 - q^0 + i\epsilon} - n(p^0) \rho(p^0, \mathbf{p})$$

- In thermal equilibrium: time translational invariance $t_0 \rightarrow -\infty$



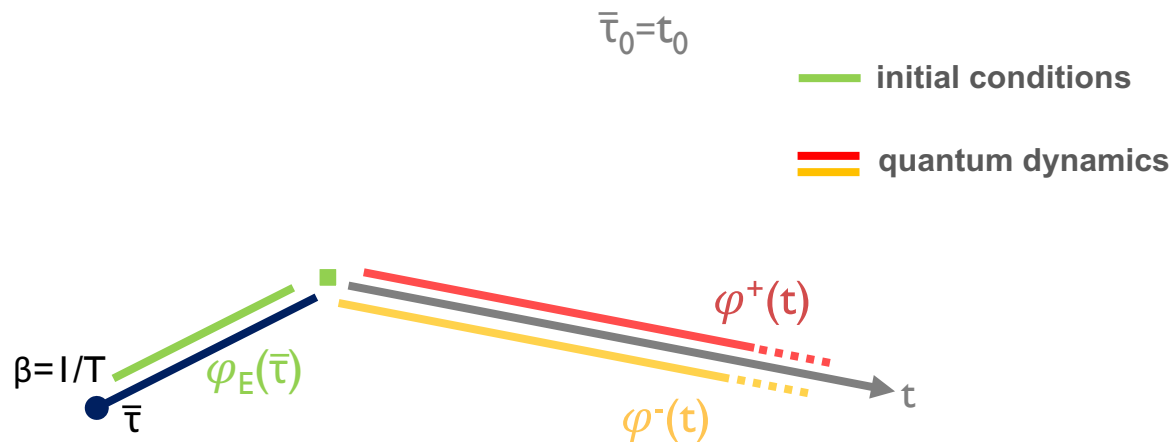


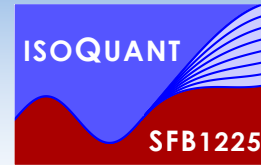
How do the two paths contribute?

- Thermal equilibrium is special: $G^{++} = \langle \varphi^+ \varphi^+ \rangle$ correlator alone suffices to compute ρ

$$G^{++}(p^0, \mathbf{p}) = \int \frac{dq^0}{2\pi i} \frac{\rho(q^0, \mathbf{p})}{p^0 - q^0 + i\epsilon} - n(p^0) \rho(p^0, \mathbf{p})$$

- In thermal equilibrium: time translational invariance $t_0 \rightarrow -\infty$
- Correlations between any finite time t on forward branch and endpoint are damped



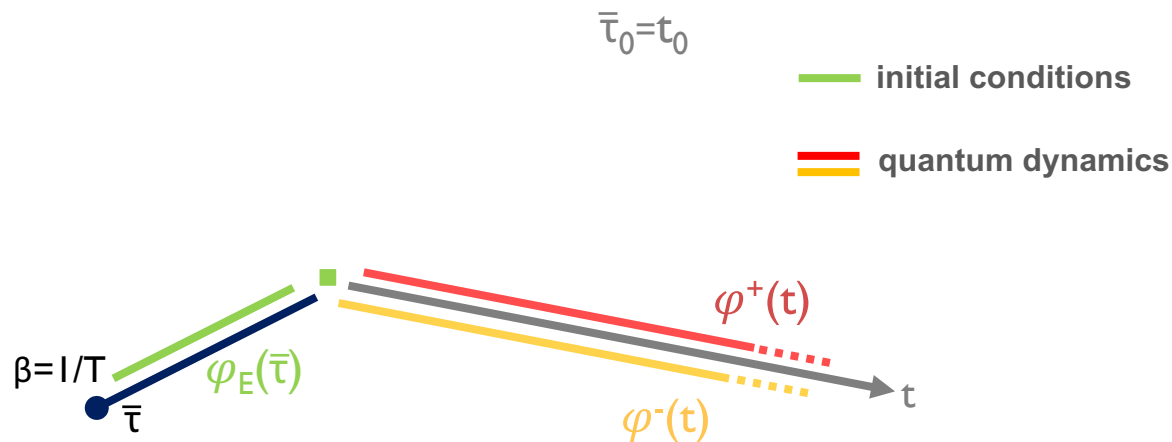


How do the two paths contribute?

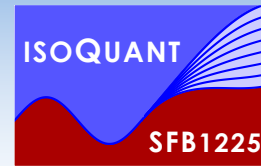
- Thermal equilibrium is special: $G^{++} = \langle \varphi^+ \varphi^+ \rangle$ correlator alone suffices to compute ρ

$$G^{++}(p^0, \mathbf{p}) = \int \frac{dq^0}{2\pi i} \frac{\rho(q^0, \mathbf{p})}{p^0 - q^0 + i\epsilon} - n(p^0) \rho(p^0, \mathbf{p})$$

- In thermal equilibrium: time translational invariance $t_0 \rightarrow -\infty$
- Correlations between any finite time t on forward branch and endpoint are damped



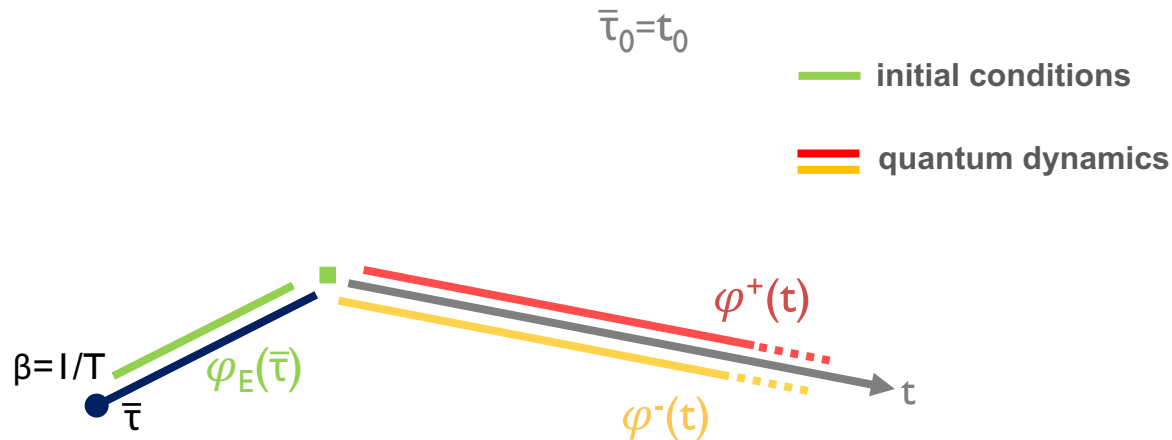
- Focus on treating the forward branch with φ^+ in the following

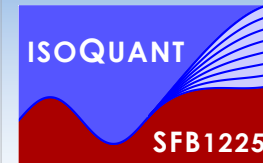


Analytic continuation

- Our idea: rotate branches of the real-time contour into noncompact imaginary time

$$\mathcal{Z} = \int_{\varphi_E(0)=\varphi_E(\beta)} \mathcal{D}\varphi_E e^{-S_E[\varphi_E]} \int_{\varphi^+(t_0, \mathbf{x})=\varphi_E(0)}^{\varphi^-(t_0, \mathbf{x})=\varphi_E(\beta)} \mathcal{D}\varphi e^{iS_M[\varphi^+] - iS_M[\varphi^-]}$$

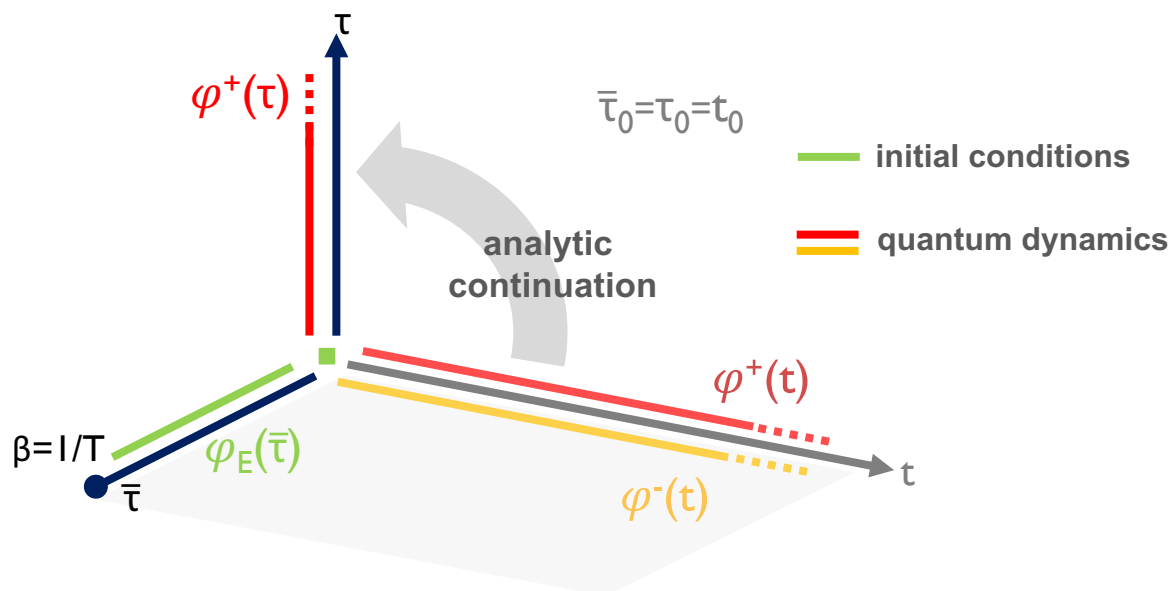


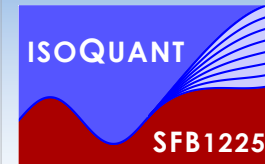


Analytic continuation

- Our idea: rotate branches of the real-time contour into noncompact imaginary time

$$\mathcal{Z} = \int \mathcal{D}\varphi_E e^{-S_E[\varphi_E]} \int_{\varphi^+(\tau_0)=\varphi_E(0)}^{\varphi^+(\infty)} \mathcal{D}\varphi^+ e^{-S_E[\varphi^+]} \int_{\varphi^-(\infty)}^{\varphi^-(\tau_0)=\varphi_E(\beta)} \mathcal{D}\varphi^- e^{-S_E[\varphi^-]}$$

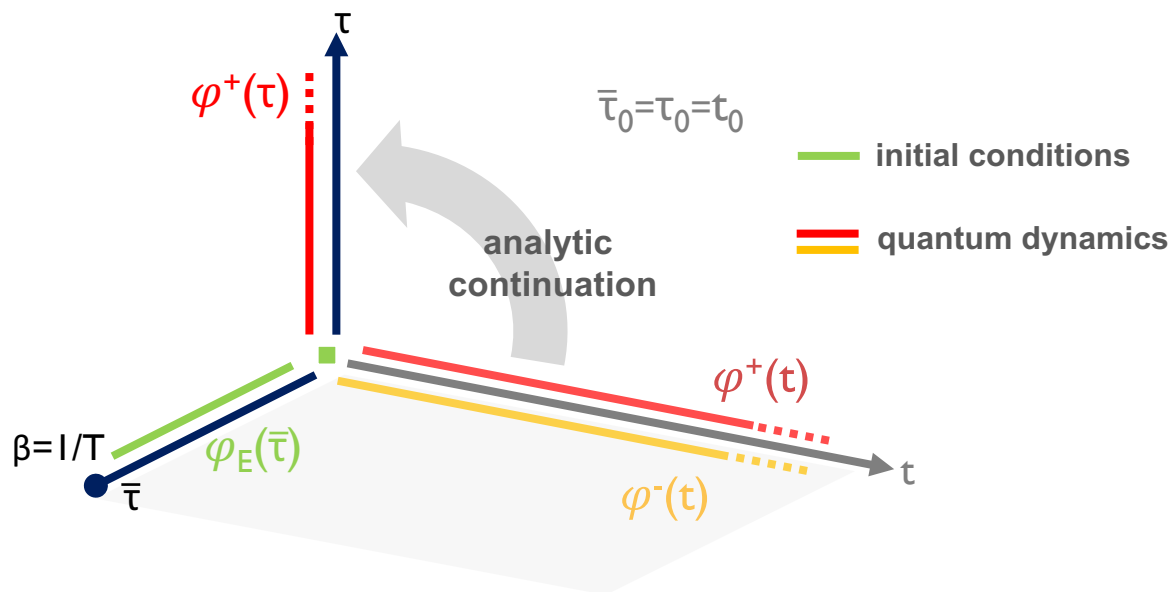




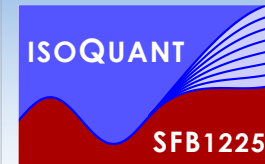
Analytic continuation

- Our idea: rotate branches of the real-time contour into noncompact imaginary time

$$\mathcal{Z} = \int \mathcal{D}\varphi_E e^{-S_E[\varphi_E]} \int_{\varphi^+(\tau_0)=\varphi_E(0)}^{\varphi^+(\infty)} \mathcal{D}\varphi^+ e^{-S_E[\varphi^+]} \int_{\varphi^-(\infty)}^{\varphi^-(\tau_0)=\varphi_E(\beta)} \mathcal{D}\varphi^- e^{-S_E[\varphi^-]}$$



- After analytic continuation ρ from G^{++} : $G^{++}(ip^0, \mathbf{p}) = \int \frac{dq^0}{2\pi} \frac{\rho(q^0, \mathbf{p})}{ip^0 - q^0} - n(p^0) \underbrace{\rho(ip^0, \mathbf{p})}_{=0}$



Simulating φ^+ in $(0+1)$ dimensions

- Combine standard simulation of $\varphi_E(\bar{\tau})$ with additional simulation of $\varphi^+(\tau)$

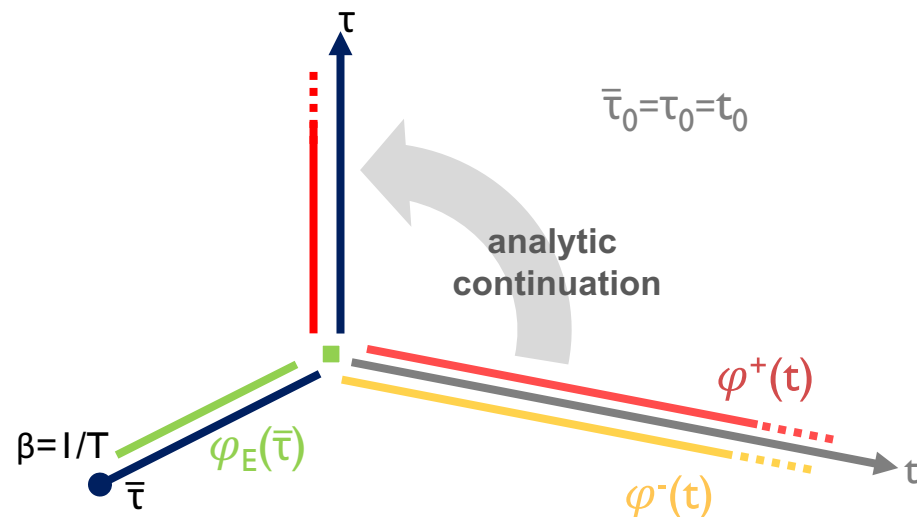
$$S_E = \int d\tau \left(\underbrace{\frac{1}{2}(\partial_\tau \varphi_E)^2 + \frac{1}{2}m^2 \varphi_E^2}_{S_E^0} + \underbrace{\frac{\lambda}{4!} \varphi_E^4}_{S_E^{\text{int}}} \right)$$

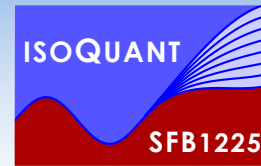
$$\partial_{t_5} \varphi_E(\bar{\tau}) = - \frac{\delta S_E[\varphi_E]}{\delta \varphi_E(\bar{\tau})} + \eta(\bar{\tau}) \quad \bar{\tau} \in [0, \beta = 1/T]$$

$$\langle \eta(\tau)\eta(\tau') \rangle = 2\delta(\tau - \tau')$$

$$\partial_{t_5} \varphi^+(\tau) = - \frac{\delta S_E[\varphi^+]}{\delta \varphi^+(\tau)} + \eta(\tau) \quad \tau \in [0, \infty]$$

- We use standard stochastic quantization in an artificial *Langevin* time t_5





Simulating φ^+ in $(0+1)$ dimensions

- Combine standard simulation of $\varphi_E(\bar{\tau})$ with additional simulation of $\varphi^+(\tau)$

$$S_E = \int d\tau \left(\underbrace{\frac{1}{2}(\partial_\tau \varphi_E)^2 + \frac{1}{2}m^2 \varphi_E^2}_{S_E^0} + \underbrace{\frac{\lambda}{4!} \varphi_E^4}_{S_E^{\text{int}}} \right)$$

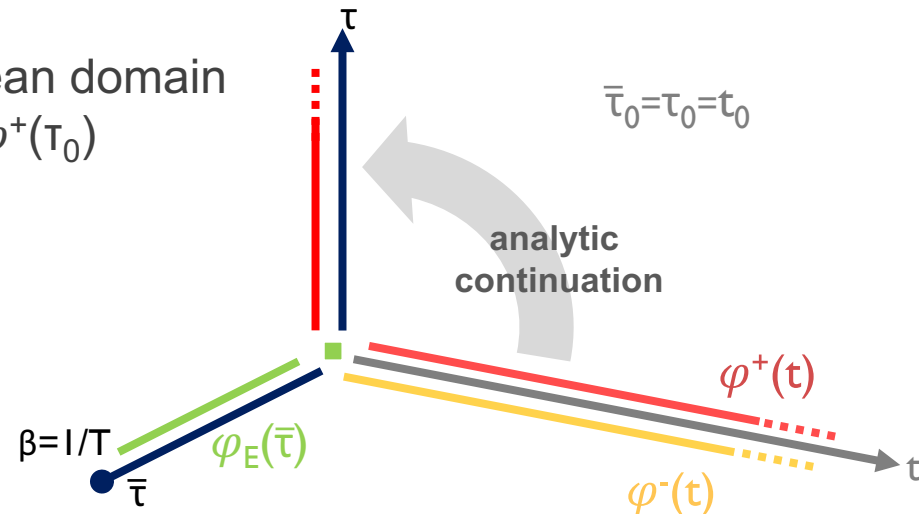
$$\partial_{t_5} \varphi_E(\bar{\tau}) = - \frac{\delta S_E[\varphi_E]}{\delta \varphi_E(\bar{\tau})} + \eta(\bar{\tau}) \quad \bar{\tau} \in [0, \beta = 1/T]$$

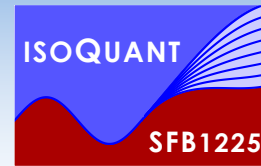
$$\langle \eta(\tau)\eta(\tau') \rangle = 2\delta(\tau - \tau')$$

$$\partial_{t_5} \varphi^+(\tau) = - \frac{\delta S_E[\varphi^+]}{\delta \varphi^+(\tau)} + \eta(\tau) \quad \tau \in [0, \infty]$$

- We use standard stochastic quantization in an artificial *Langevin* time t_5

- Temperature in φ_E via compact Euclidean domain
Temperature in φ^+ via initial condition $\varphi^+(\tau_0)$





Simulating φ^+ in $(0+1)$ dimensions

- Combine standard simulation of $\varphi_E(\bar{\tau})$ with additional simulation of $\varphi^+(\tau)$

$$S_E = \int d\tau \left(\underbrace{\frac{1}{2}(\partial_\tau \varphi_E)^2 + \frac{1}{2}m^2 \varphi_E^2}_{S_E^0} + \underbrace{\frac{\lambda}{4!} \varphi_E^4}_{S_E^{\text{int}}} \right)$$

$$\partial_{t_5} \varphi_E(\bar{\tau}) = - \frac{\delta S_E[\varphi_E]}{\delta \varphi_E(\bar{\tau})} + \eta(\bar{\tau}) \quad \bar{\tau} \in [0, \beta = 1/T]$$

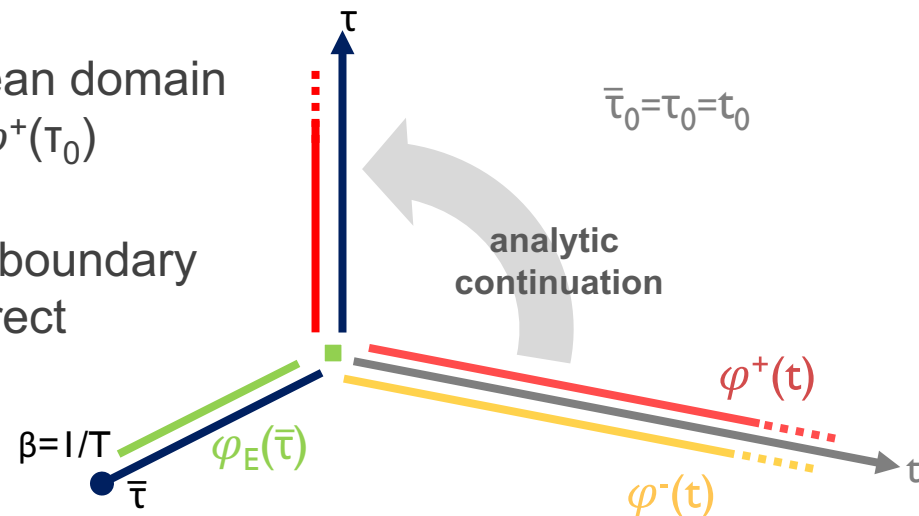
$$\langle \eta(\tau)\eta(\tau') \rangle = 2\delta(\tau - \tau')$$

$$\partial_{t_5} \varphi^+(\tau) = - \frac{\delta S_E[\varphi^+]}{\delta \varphi^+(\tau)} + \eta(\tau) \quad \tau \in [0, \infty]$$

- We use standard stochastic quantization in an artificial *Langevin* time t_5

- Temperature in φ_E via compact Euclidean domain
Temperature in φ^+ via initial condition $\varphi^+(\tau_0)$

- Finite τ extent in simulation introduces boundary artefacts: G^{++} converges slowly to correct infinite temporal extent result





Simulating φ^+ in $(0+1)$ dimensions

- Combine standard simulation of $\varphi_E(\bar{\tau})$ with additional simulation of $\varphi^+(\tau)$

$$S_E = \int d\tau \left(\underbrace{\frac{1}{2}(\partial_\tau \varphi_E)^2 + \frac{1}{2}m^2 \varphi_E^2}_{S_E^0} + \underbrace{\frac{\lambda}{4!} \varphi_E^4}_{S_E^{\text{int}}} \right)$$

$$\partial_{t_5} \varphi_E(\bar{\tau}) = - \frac{\delta S_E[\varphi_E]}{\delta \varphi_E(\bar{\tau})} + \eta(\bar{\tau}) \quad \bar{\tau} \in [0, \beta = 1/T]$$

$$\langle \eta(\tau)\eta(\tau') \rangle = 2\delta(\tau - \tau')$$

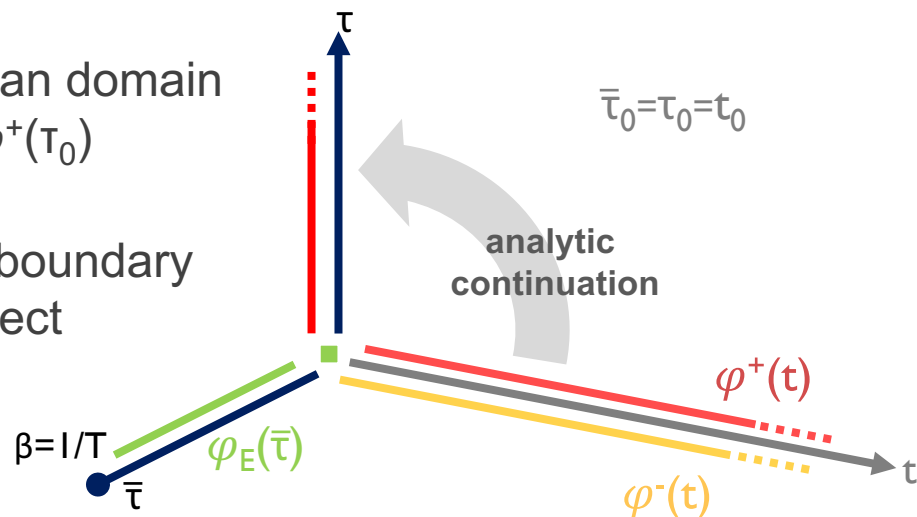
$$\partial_{t_5} \varphi^+(\tau) = - \frac{\delta S_E[\varphi^+]}{\delta \varphi^+(\tau)} + \eta(\tau) \quad \tau \in [0, \infty]$$

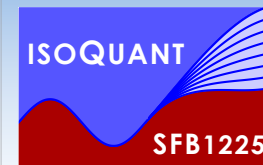
- We use standard stochastic quantization in an artificial *Langevin* time t_5

- Temperature in φ_E via compact Euclidean domain
Temperature in φ^+ via initial condition $\varphi^+(\tau_0)$

- Finite τ extent in simulation introduces boundary artefacts: G^{++} converges slowly to correct infinite temporal extent result

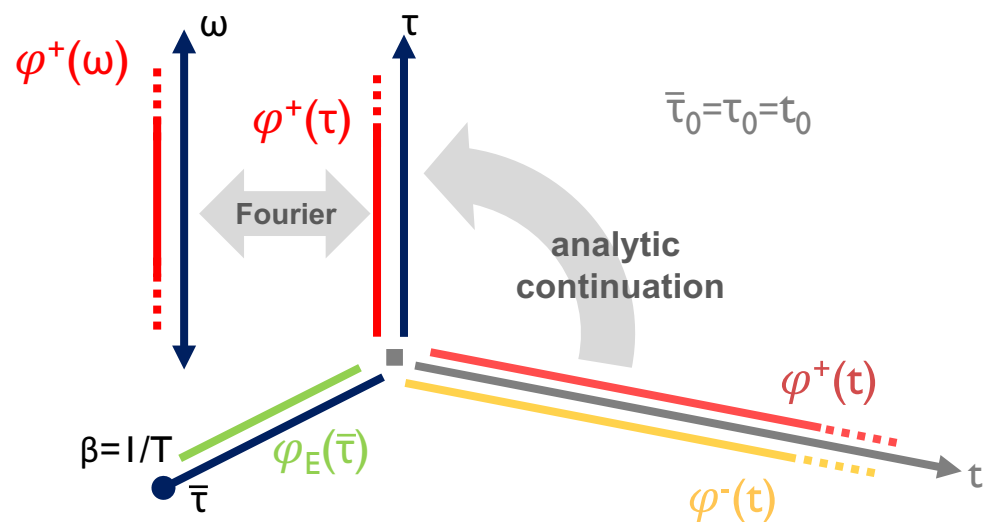
- Can this convergence be improved?

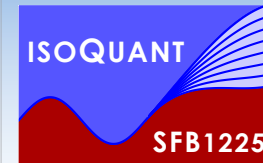




Fourier space implementation

- The kinetic term becomes diagonal after Fourier transform
 - It does not receive contributions from initial conditions (in the free theory T indep. G^{++})



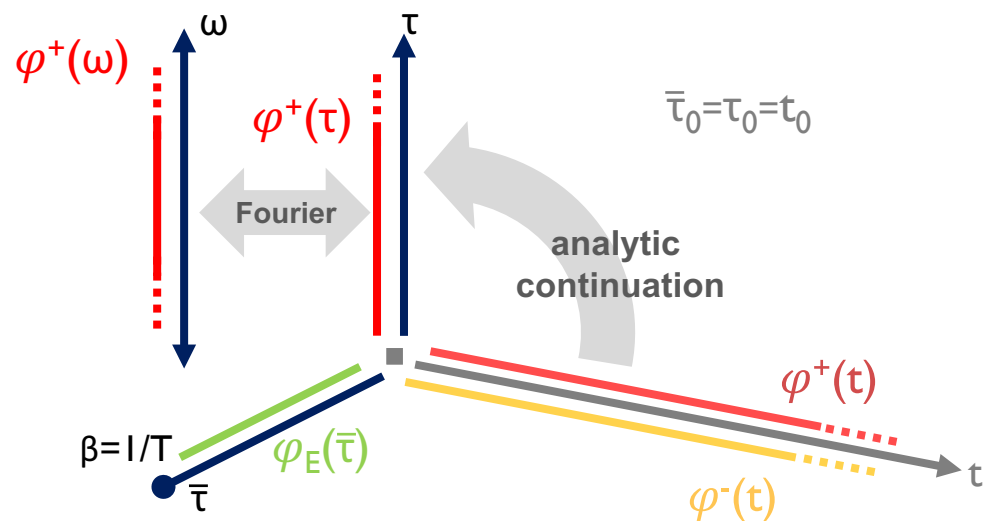


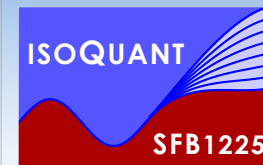
Fourier space implementation

- The kinetic term becomes diagonal after Fourier transform
 - It does not receive contributions from initial conditions (in the free theory T indep. G^{++})
- Mixed representation: T enters only via interaction term, which is diagonal in τ

$$\partial_{t_5} \varphi^+(\omega_l) = -\frac{\delta S_0}{\delta \varphi^+(\omega_l)} - \frac{\delta S_E^{\text{int}}}{\delta \varphi^+(\tau_j)} \frac{\delta \varphi^+(\tau_j)}{\delta \varphi^+(\omega_l)} + \eta(\omega_l)$$

- Strategy: when evaluating $\delta S_E^{\text{int}}/\delta \varphi^+(\tau)$ replace $\varphi^+(\tau=0) = \varphi_E(0)$





Fourier space implementation

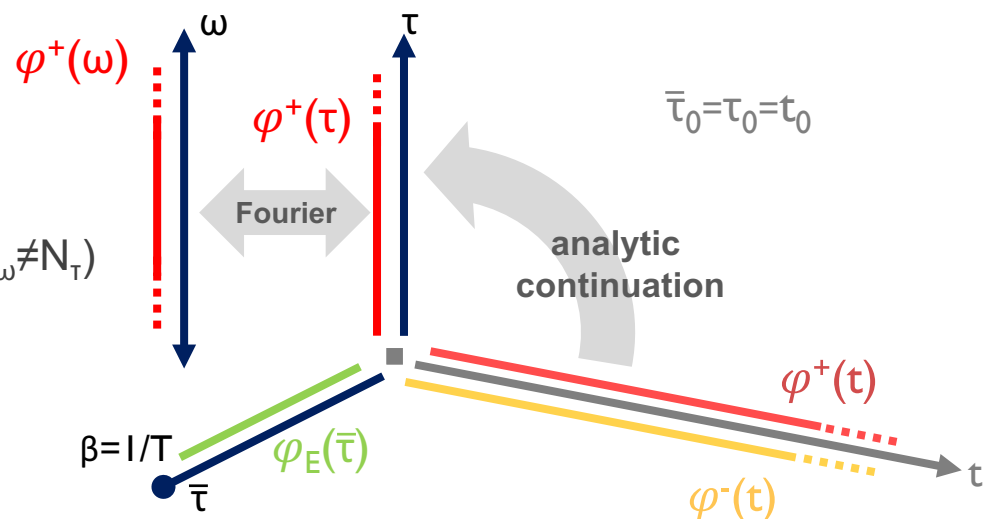
- The kinetic term becomes diagonal after Fourier transform
 - It does not receive contributions from initial conditions (in the free theory T indep. G^{++})
- Mixed representation: T enters only via interaction term, which is diagonal in τ

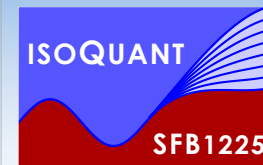
$$\partial_{t_5} \varphi^+(\omega_l) = -\frac{\delta S_0}{\delta \varphi^+(\omega_l)} - \frac{\delta S_E^{\text{int}}}{\delta \varphi^+(\tau_j)} \frac{\delta \varphi^+(\tau_j)}{\delta \varphi^+(\omega_l)} + \eta(\omega_l)$$

- Strategy: when evaluating $\delta S_E^{\text{int}}/\delta \varphi^+(\tau)$ replace $\varphi^+(\tau=0) = \varphi_E(0)$

Actual numerical setup:

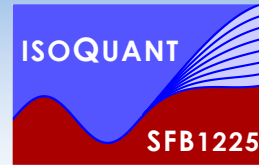
- Standard update of φ_E along N_τ steps
- Compute $\delta S_E/\delta \varphi^+(\omega)$ in Fourier space ($N_\omega \neq N_\tau$)
- Evaluate $\delta S_E^{\text{int}}/\delta \varphi^+$ using current $\varphi_E(\tau=0)$
- Update $\varphi^+(\omega)$





Outline

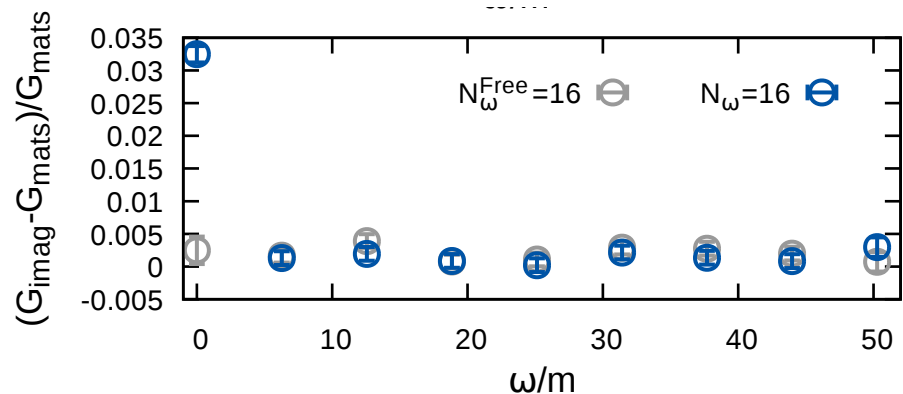
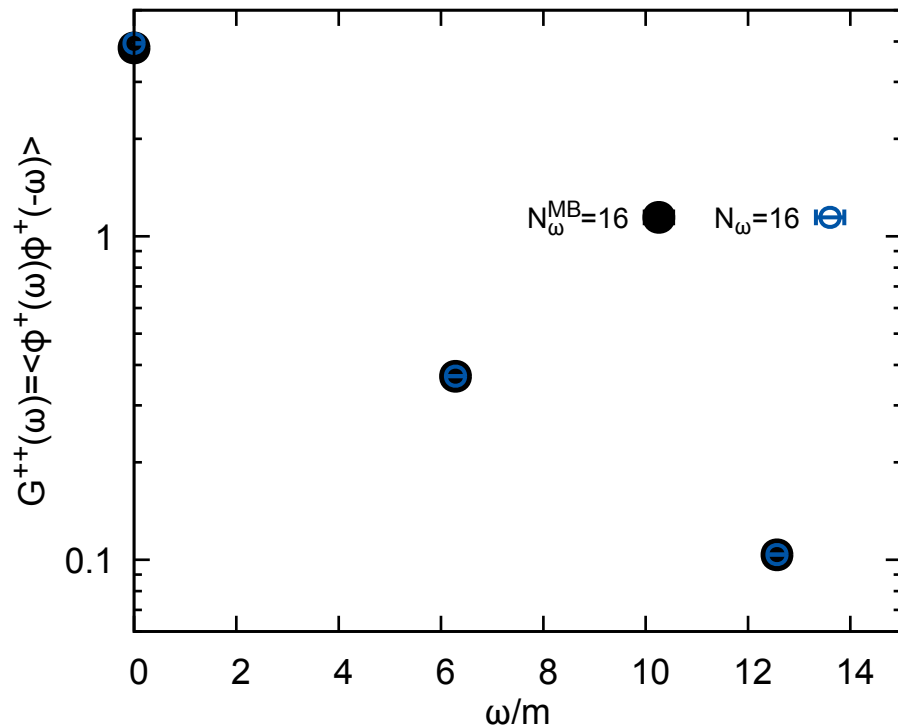
- Motivation
 - Coherent picture of in-medium heavy-quarkonium from the lattice
- In-medium quarkonium from a lattice EFT (NRQCD)
 - Numerical setup and spectral reconstruction
 - Current $T>0$ results from realistic full QCD simulations
- **Towards improved spectral information from thermal fields**
 - Derivation of a novel simulation prescription
 - Current exploratory results from toy models to quenched QCD
- Conclusion

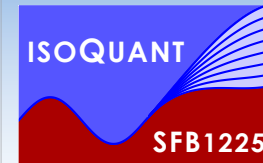


(0+1d) scalar field toy model (II)

- Standard update for φ_E with $N_T=16$ $m=1$ $\lambda=24$ $N_T d\tau=1$ (compare to QM of A.H.O.)
- Mixed update for φ^+ in imaginary frequencies ω and imaginary time τ

$$\partial_{t_5} \varphi^+(\omega_l) = -\frac{\delta S_0}{\delta \varphi^+(\omega_l)} - \frac{\delta S_E^{\text{int}}}{\delta \varphi^+(\tau_j)} \frac{\delta \varphi^+(\tau_j)}{\delta \varphi^+(\omega_l)} + \eta(\omega_l)$$

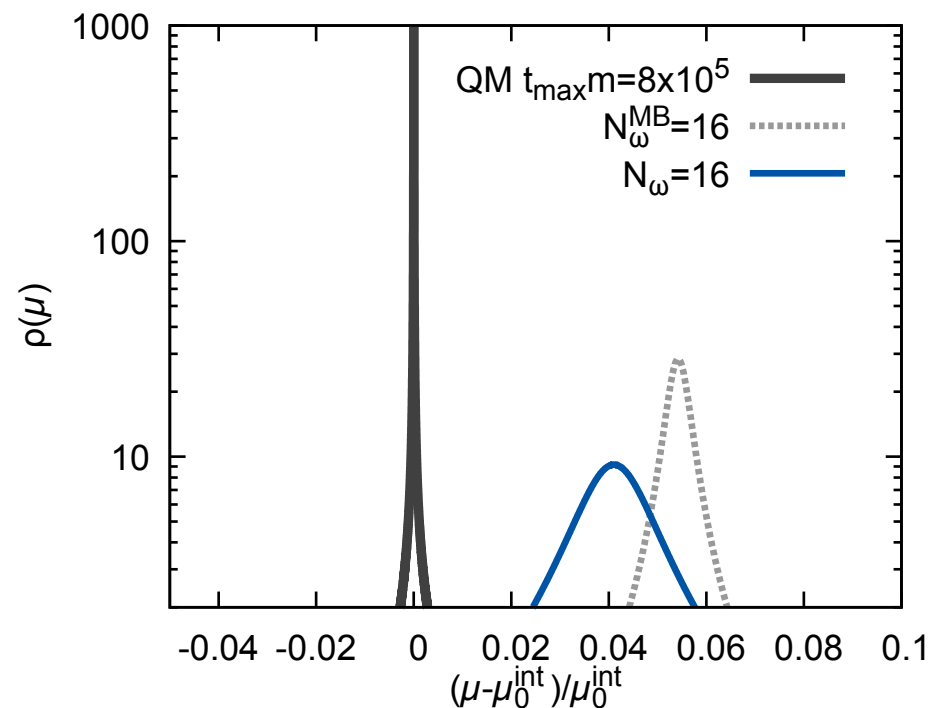
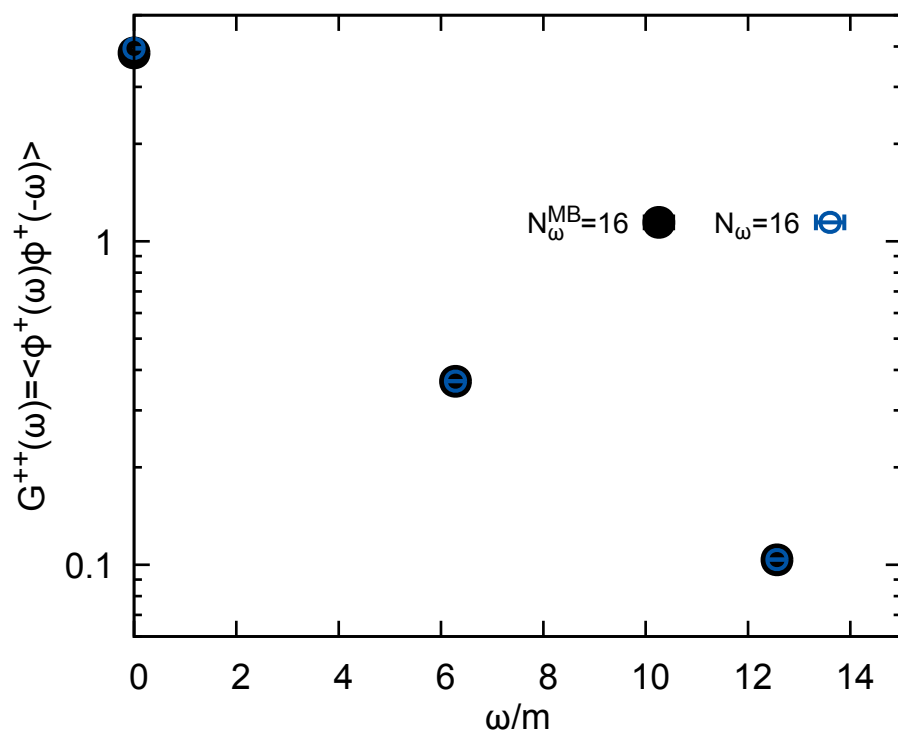


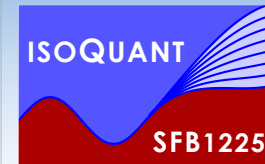


(0+1d) scalar field toy model (II)

- Standard update for φ_E with $N_T=16$ $m=1$ $\lambda=24$ $N_T d\tau=1$ (compare to QM of A.H.O.)
- Mixed update for φ^+ in imaginary frequencies ω and imaginary time τ

$$\partial_{t_5} \varphi^+(\omega_l) = -\frac{\delta S_0}{\delta \varphi^+(\omega_l)} - \frac{\delta S_E^{\text{int}}}{\delta \varphi^+(\tau_j)} \frac{\delta \varphi^+(\tau_j)}{\delta \varphi^+(\omega_l)} + \eta(\omega_l)$$

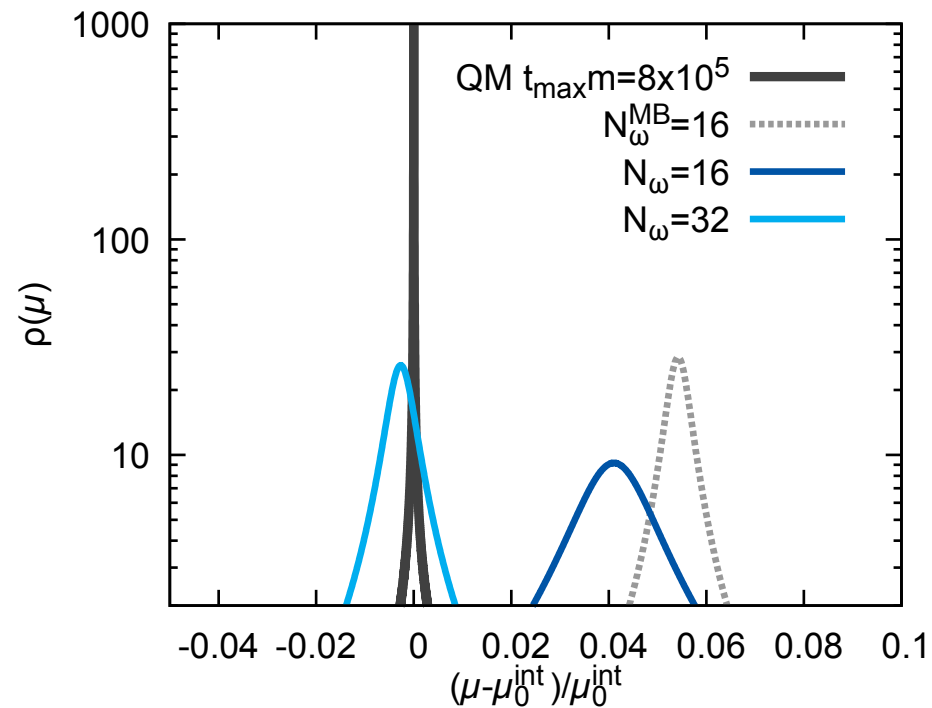
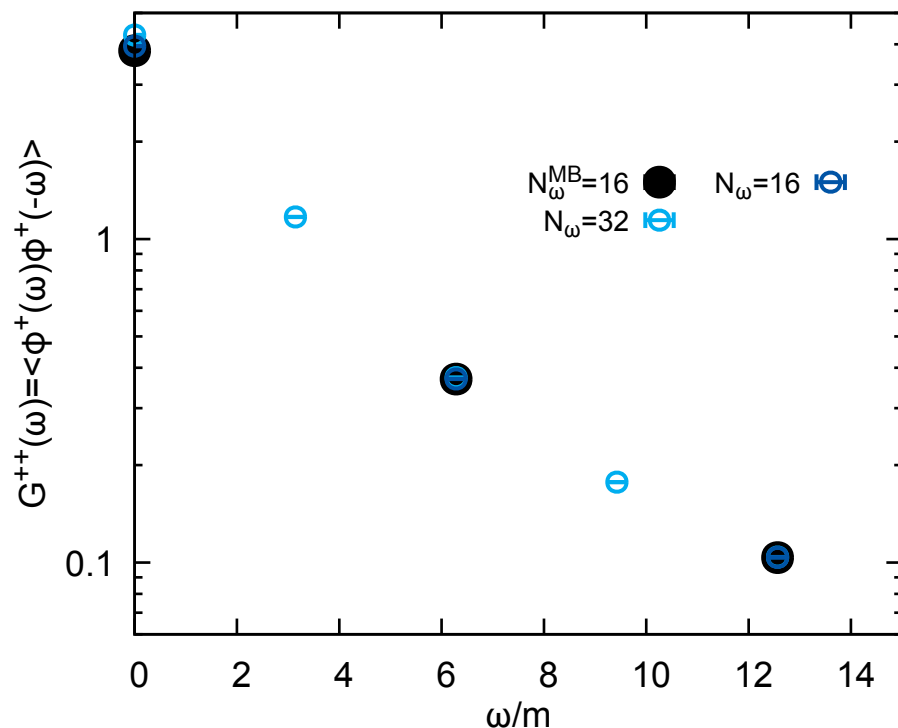


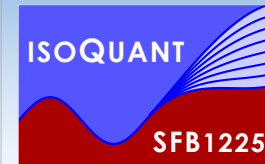


(0+1d) scalar field toy model (II)

- Standard update for φ_E with $N_T=16$ $m=1$ $\lambda=24$ $N_T d\tau=1$ (compare to QM of A.H.O.)
- Mixed update for φ^+ in imaginary frequencies ω and imaginary time τ

$$\partial_{t_5} \varphi^+(\omega_l) = -\frac{\delta S_0}{\delta \varphi^+(\omega_l)} - \frac{\delta S_E^{\text{int}}}{\delta \varphi^+(\tau_j)} \frac{\delta \varphi^+(\tau_j)}{\delta \varphi^+(\omega_l)} + \eta(\omega_l)$$

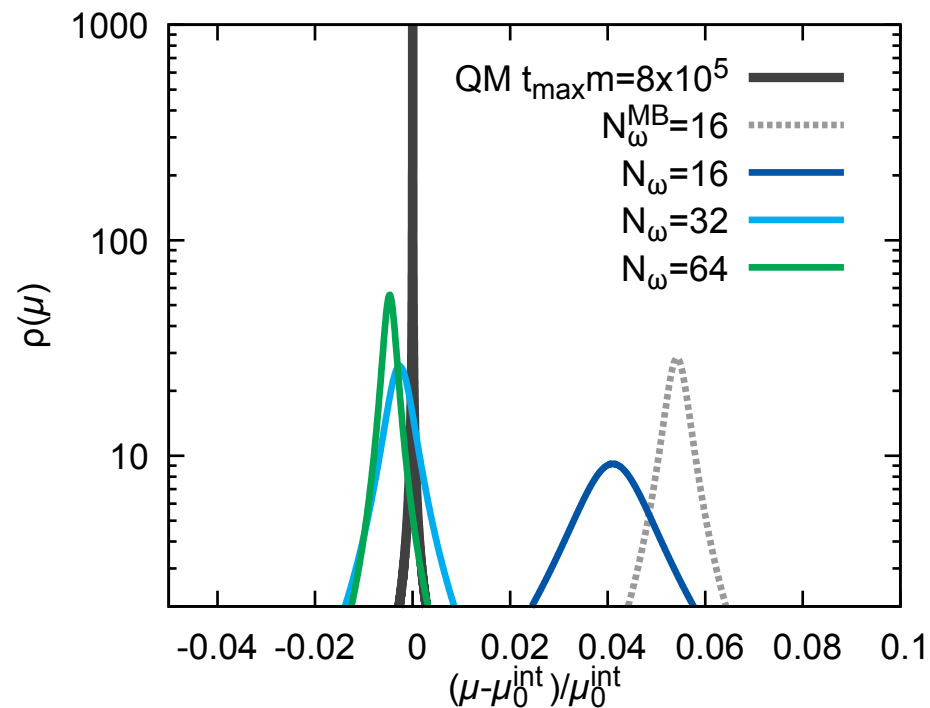
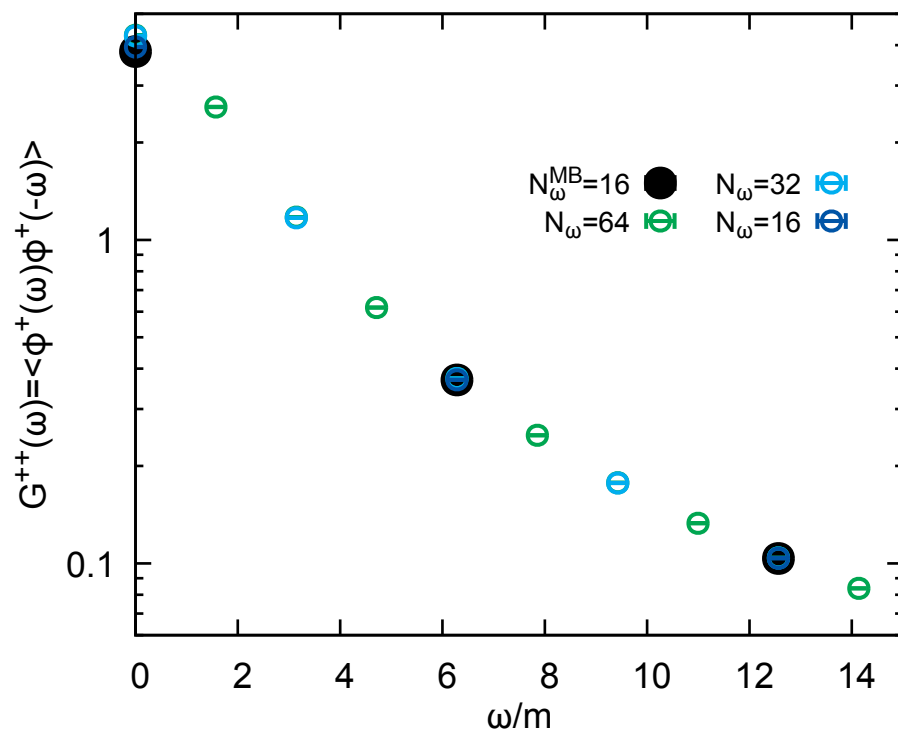


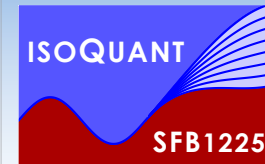


(0+1d) scalar field toy model (II)

- Standard update for φ_E with $N_T=16$ $m=1$ $\lambda=24$ $N_T d\tau=1$ (compare to QM of A.H.O.)
- Mixed update for φ^+ in imaginary frequencies ω and imaginary time τ

$$\partial_{t_5} \varphi^+(\omega_l) = -\frac{\delta S_0}{\delta \varphi^+(\omega_l)} - \frac{\delta S_E^{\text{int}}}{\delta \varphi^+(\tau_j)} \frac{\delta \varphi^+(\tau_j)}{\delta \varphi^+(\omega_l)} + \eta(\omega_l)$$

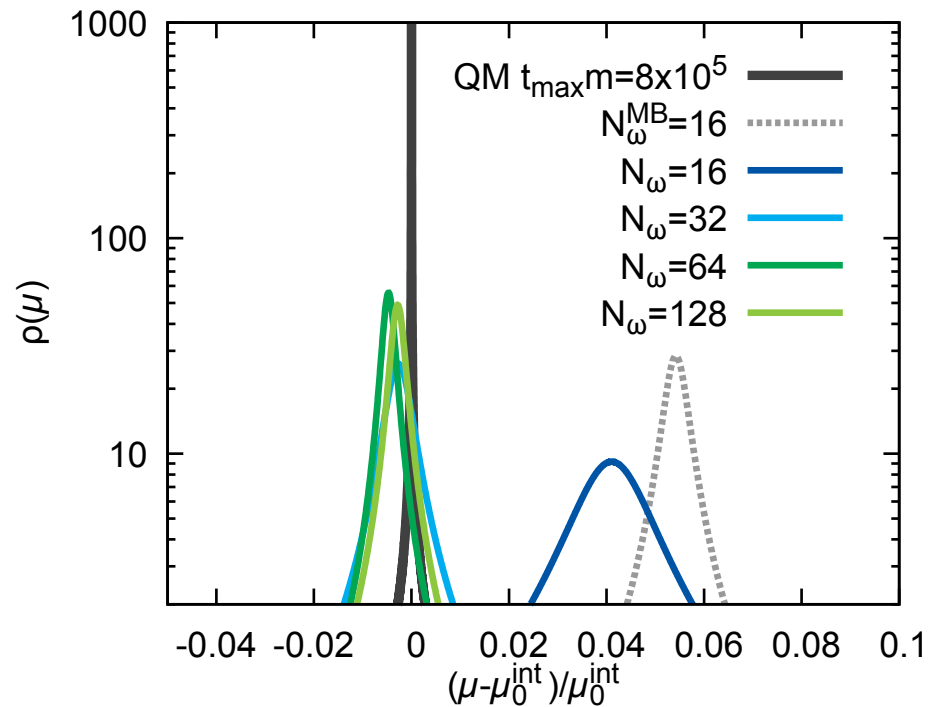
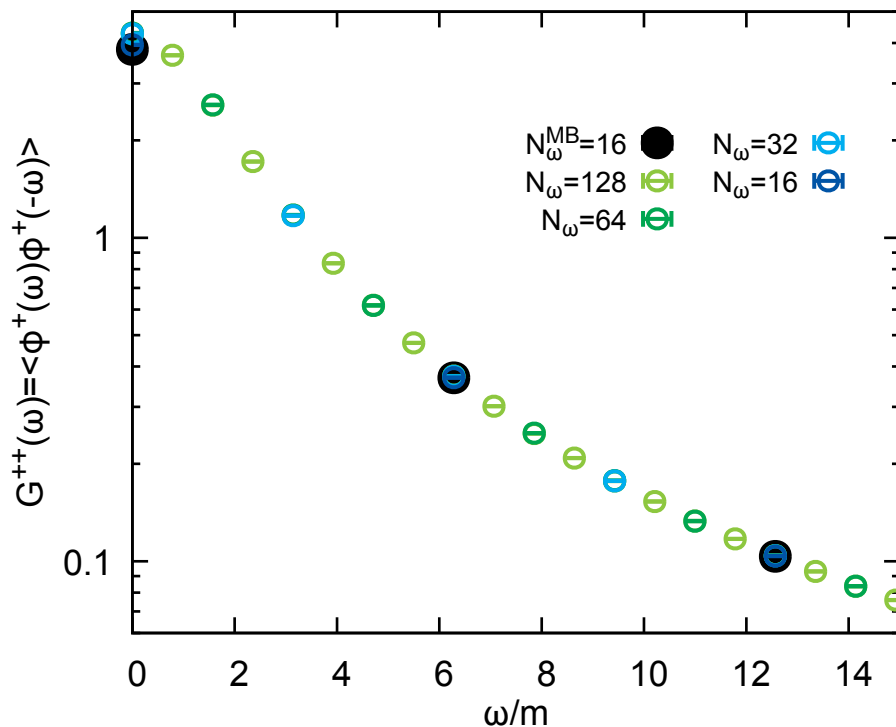


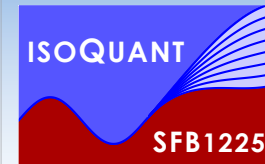


(0+1d) scalar field toy model (II)

- Standard update for φ_E with $N_T=16$ $m=1$ $\lambda=24$ $N_T d\tau=1$ (compare to QM of A.H.O.)
- Mixed update for φ^+ in imaginary frequencies ω and imaginary time τ

$$\partial_{t_5} \varphi^+(\omega_l) = -\frac{\delta S_0}{\delta \varphi^+(\omega_l)} - \frac{\delta S_E^{\text{int}}}{\delta \varphi^+(\tau_j)} \frac{\delta \varphi^+(\tau_j)}{\delta \varphi^+(\omega_l)} + \eta(\omega_l)$$

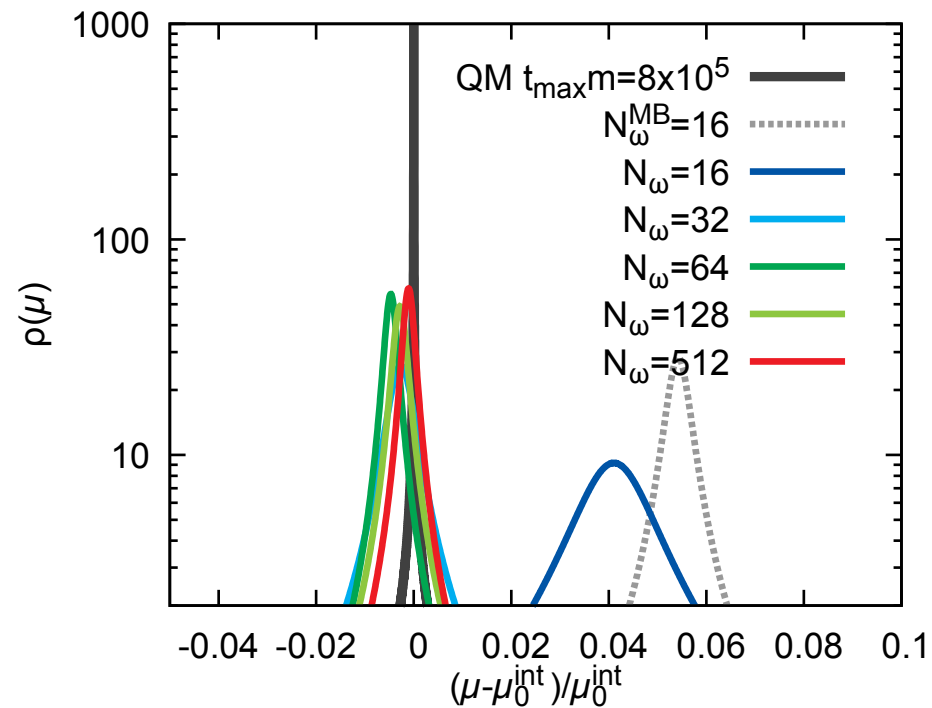
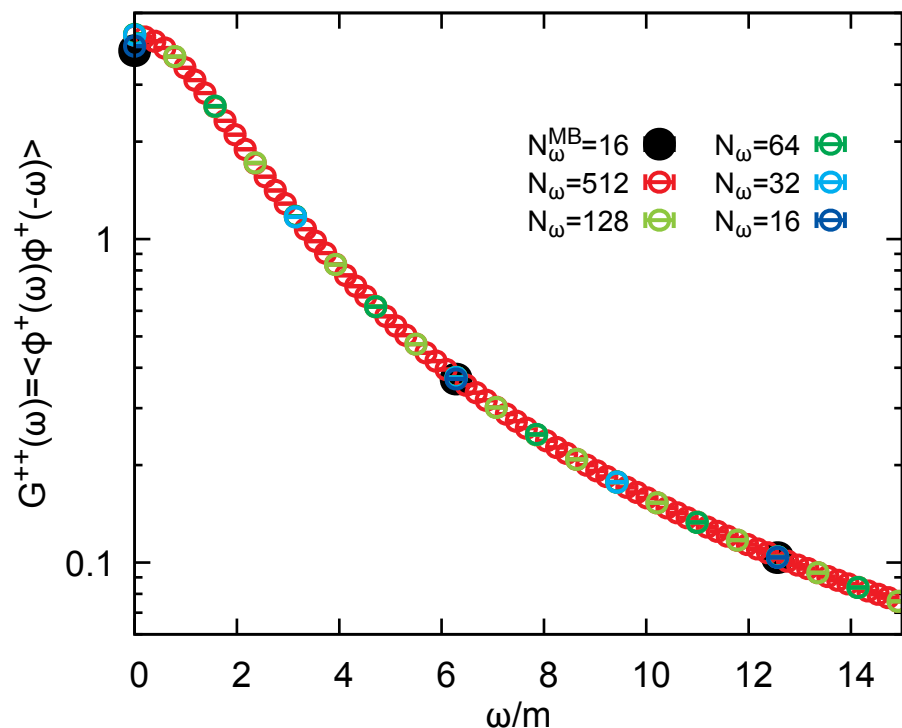


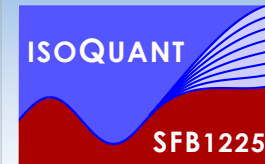


(0+1d) scalar field toy model (II)

- Standard update for φ_E with $N_T=16$ $m=1$ $\lambda=24$ $N_T d\tau=1$ (compare to QM of A.H.O.)
- Mixed update for φ^+ in imaginary frequencies ω and imaginary time τ

$$\partial_{t_5} \varphi^+(\omega_l) = -\frac{\delta S_0}{\delta \varphi^+(\omega_l)} - \frac{\delta S_E^{\text{int}}}{\delta \varphi^+(\tau_j)} \frac{\delta \varphi^+(\tau_j)}{\delta \varphi^+(\omega_l)} + \eta(\omega_l)$$

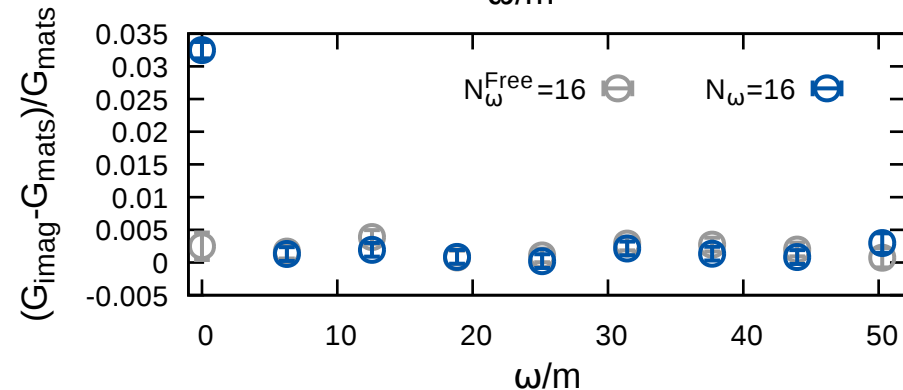
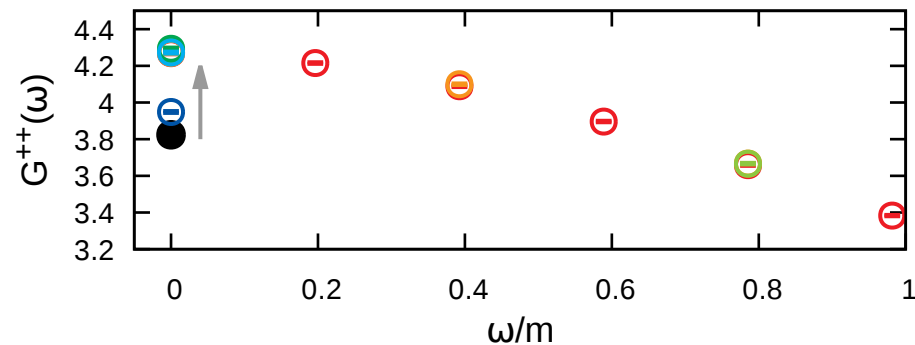
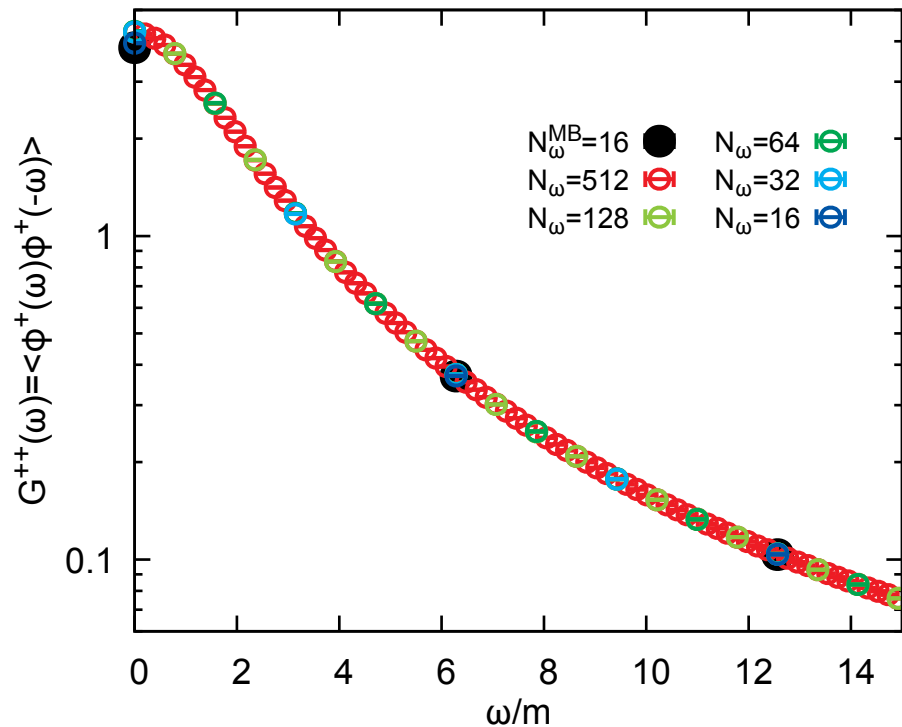


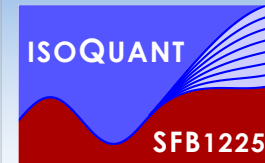


(0+1d) scalar field toy model (II)

- Standard update for φ_E with $N_T=16$ $m=1$ $\lambda=24$ $N_T d\tau=1$ (compare to QM of A.H.O.)
- Mixed update for φ^+ in imaginary frequencies ω and imaginary time τ

$$\partial_{t_5} \varphi^+(\omega_l) = -\frac{\delta S_0}{\delta \varphi^+(\omega_l)} - \frac{\delta S_E^{\text{int}}}{\delta \varphi^+(\tau_j)} \frac{\delta \varphi^+(\tau_j)}{\delta \varphi^+(\omega_l)} + \eta(\omega_l)$$



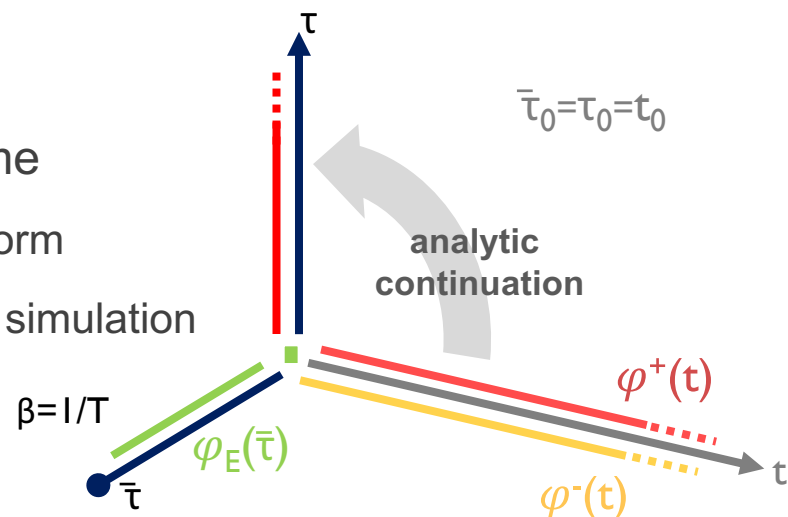


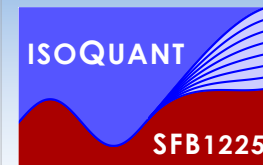
Exploring quenched QCD

- SU(2) Yang-Mills fields in 3+1d $\beta=2/g^2=1.8$ $N_s=4$ $N_\tau=4$ $N_\omega=4 \dots 256$

$$S_E[\mathbf{U}] = \frac{2}{g^2} \sum_x \sum_{\mu < \nu} \text{Re}[\mathbb{1} - U_{\mu\nu}(x)]$$

- Direct simulations in non-compact Euclidean time
 - Fully gauge invariant formulation, no Fourier transform
 - Thermal information via staples at τ_0 from standard simulation



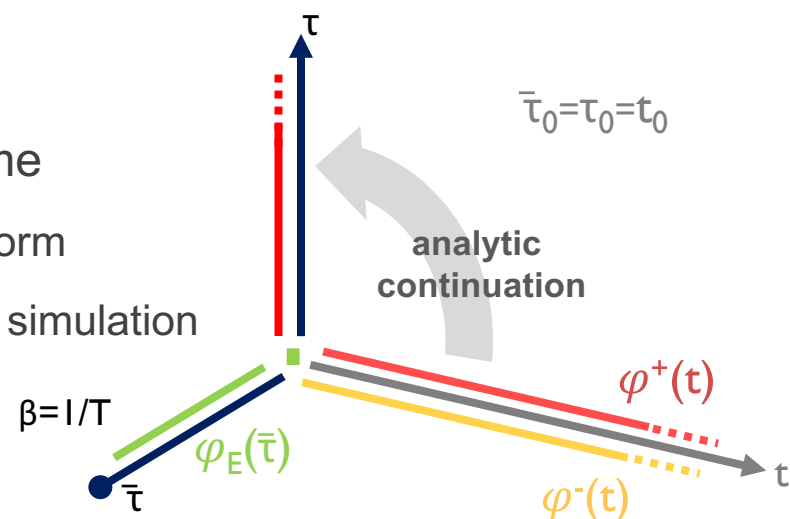
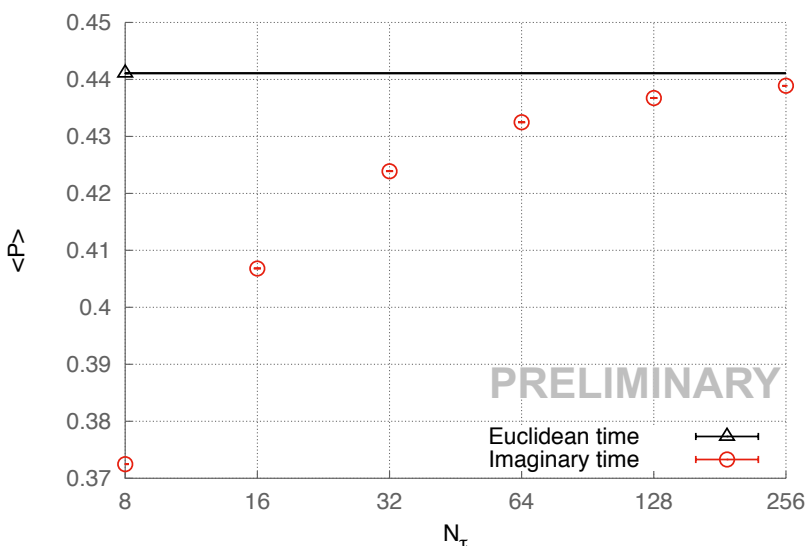


Exploring quenched QCD

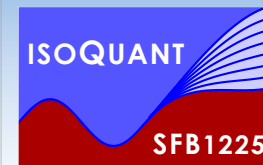
- SU(2) Yang-Mills fields in 3+1d $\beta=2/g^2=1.8$ $N_s=4$ $N_\tau=4$ $N_w=4 \dots 256$

$$S_E[\mathbf{U}] = \frac{2}{g^2} \sum_x \sum_{\mu < \nu} \text{Re}[\mathbb{1} - U_{\mu\nu}(x)]$$

- Direct simulations in non-compact Euclidean time
 - Fully gauge invariant formulation, no Fourier transform
 - Thermal information via staples at τ_0 from standard simulation

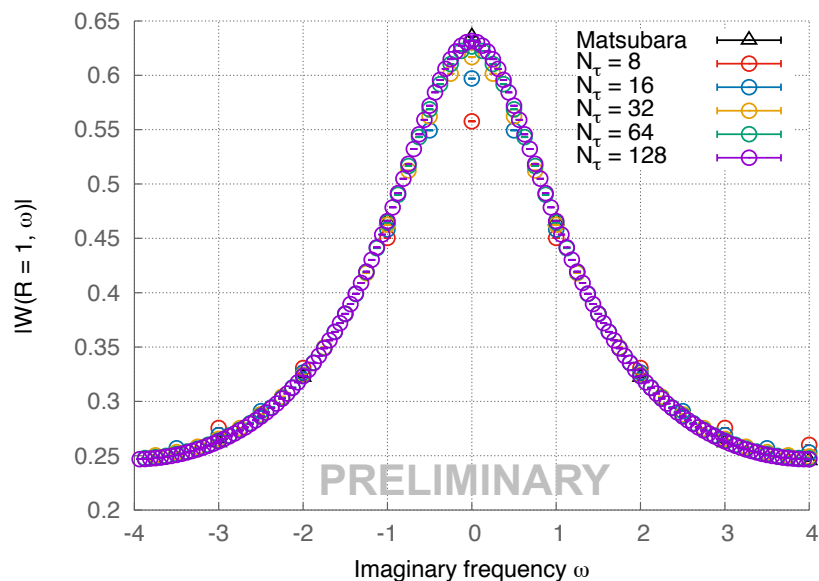


- Naïve approach appears to converge slowly but monotonously to correct results for $N_\tau \rightarrow \infty$



Observables in SU(2)

- Gauge invariant observables of interest: Wilson loop (left) and EMT correlator (right)

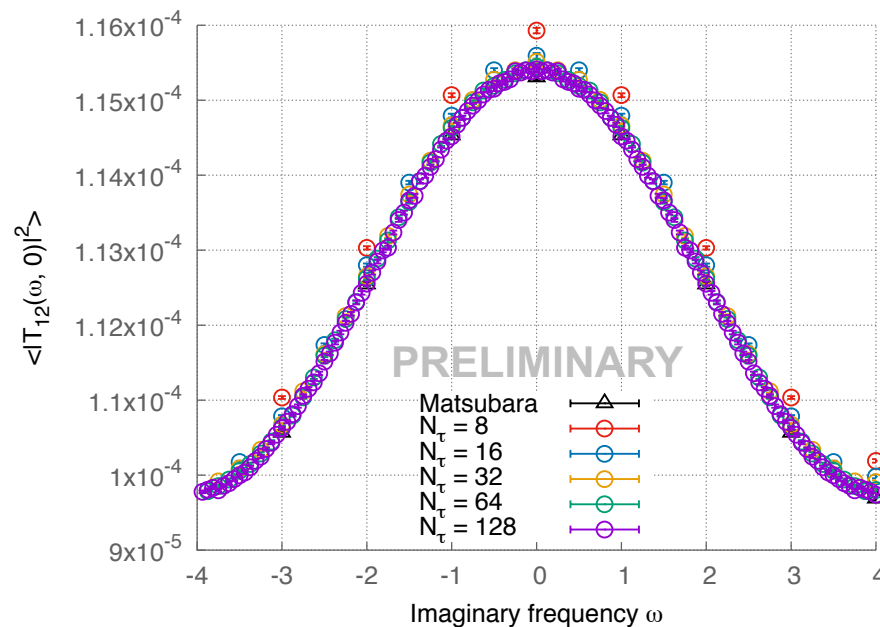
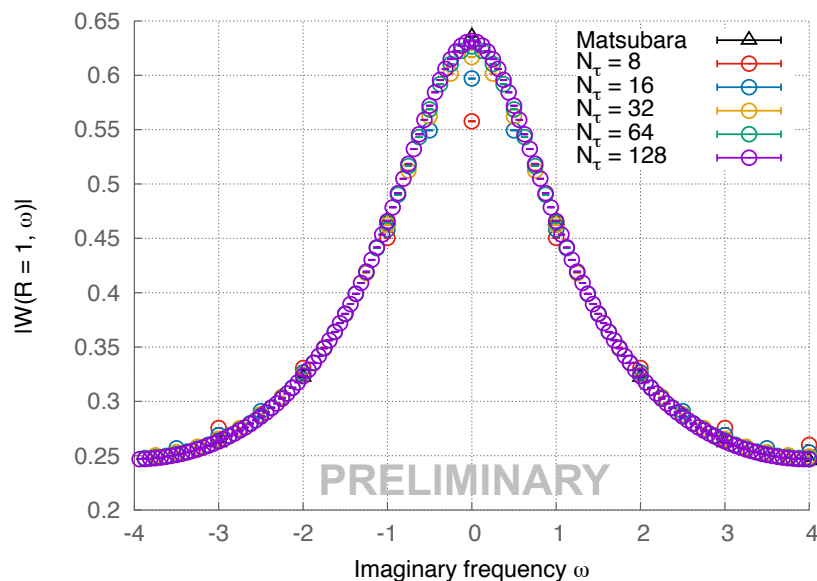


- Wilson loop at $N_t=128$ agrees very well with Matsubara data for $w_n > 0$



Observables in SU(2)

- Gauge invariant observables of interest: Wilson loop (left) and EMT correlator (right)

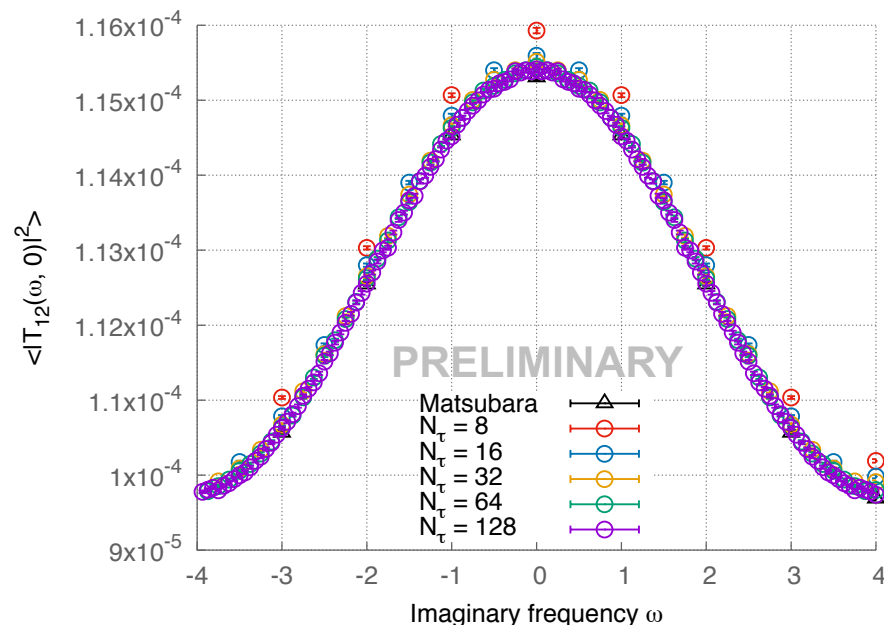
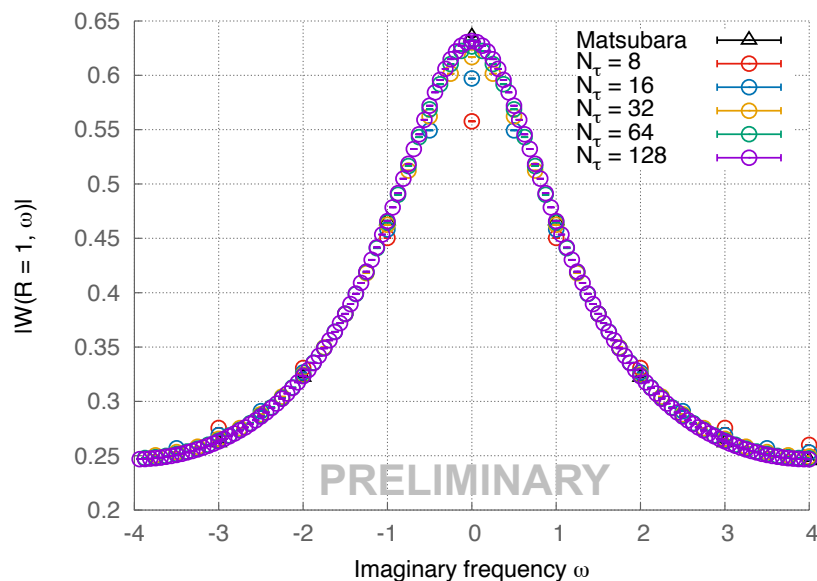


- Wilson loop at $N_\tau=128$ agrees very well with Matsubara data for $\omega_n > 0$
- EMT correlator converges more slowly and requires extremely high statistics

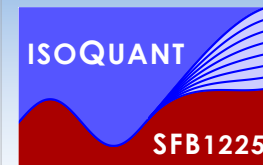


Observables in SU(2)

- Gauge invariant observables of interest: Wilson loop (left) and EMT correlator (right)

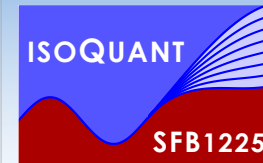


- Wilson loop at $N_\tau=128$ agrees very well with Matsubara data for $\omega_n > 0$
- EMT correlator converges more slowly and requires extremely high statistics
- Stay tuned for more results in the near future...



Conclusion

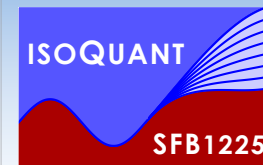
- Consistent theory answer to in-medium quarkonium spectra needed
- Updated results from the EFT NRQCD on realistic $N_f=2+1$ lattices
S.Kim, P. Petreczky, A.R.: Phys.Rev. D91 (2015) 54511, Nucl.Phys. A956 (2016) 713 and work in progress
 - **Tech progress:** New Bayesian spectral reconstruction reduces methods uncertainties
 - First quantitative determination of in-medium **shifts to lower masses**
 - Indications of **sequential** in-medium **modification** according to vacuum E_{bind}
- Towards improved spectral information from thermal fields J. Pawłowski and A.R. arXiv:1610.09531
 - Initial value problem on real-time SK contour continued to **noncompact Euclidean time**
 - Discretization in imaginary frequencies gives access to correlators **between Matsubaras**
 - Promising results in a **toy model (0+1d)** and ongoing work on **(3+1)d SU(2) Yang-Mills**
J. Pawłowski, A.R., F. Ziegler in progress



Conclusion

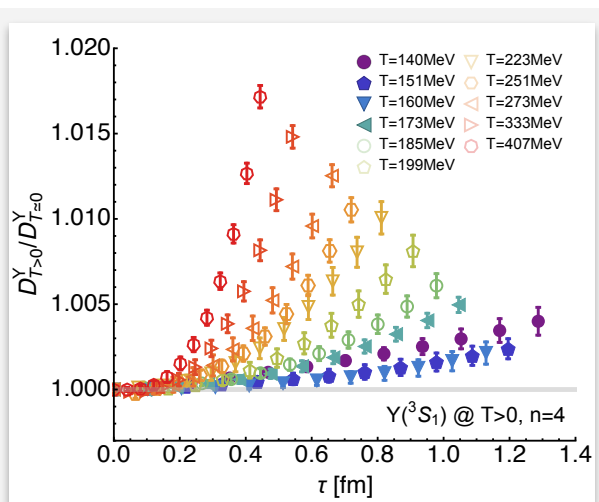
- Consistent theory answer to in-medium quarkonium spectra needed
- Updated results from the EFT NRQCD on realistic $N_f=2+1$ lattices
S.Kim, P. Petreczky, A.R.: Phys.Rev. D91 (2015) 54511, Nucl.Phys. A956 (2016) 713 and work in progress
 - **Tech progress:** New Bayesian spectral reconstruction reduces methods uncertainties
 - First quantitative determination of in-medium **shifts to lower masses**
 - Indications of **sequential** in-medium **modification** according to vacuum E_{bind}
- Towards improved spectral information from thermal fields J. Pawłowski and A.R. arXiv:1610.09531
 - Initial value problem on real-time SK contour continued to **noncompact Euclidean time**
 - Discretization in imaginary frequencies gives access to correlators **between Matsubaras**
 - Promising results in a **toy model (0+1d)** and ongoing work on **(3+1)d SU(2) Yang-Mills**
J. Pawłowski, A.R., F. Ziegler in progress

Thank you for your attention

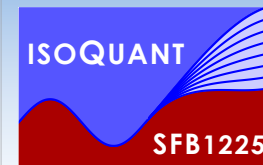


T>0 effects in $Q\bar{Q}$ correlators

$E_{\text{bind}}(T=0) \sim 1.1 \text{ GeV}$

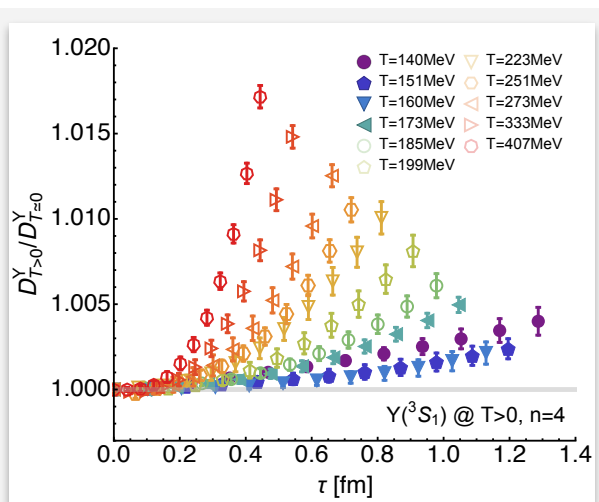


S.Kim, P.Petreczky, A.R. in preparation



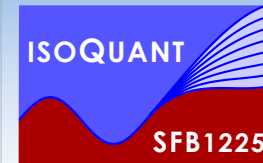
T>0 effects in $Q\bar{Q}$ correlators

$E_{\text{bind}}(T=0) \sim 1.1 \text{ GeV}$



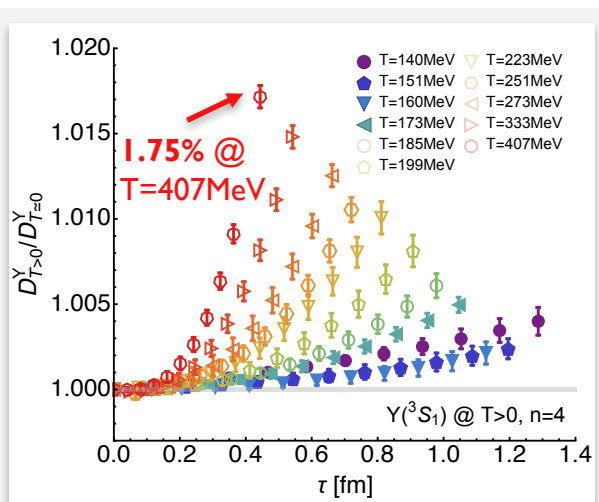
S.Kim, P.Petreczky, A.R. in preparation

- Upsilon shows non-monotonic behavior around $T \sim T_C$
(bb $3S_1$ channel contains most excited states)



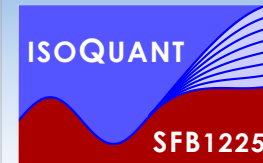
T>0 effects in $Q\bar{Q}$ correlators

$E_{\text{bind}}(T=0) \sim 1.1 \text{ GeV}$



S.Kim, P.Petreczky, A.R. in preparation

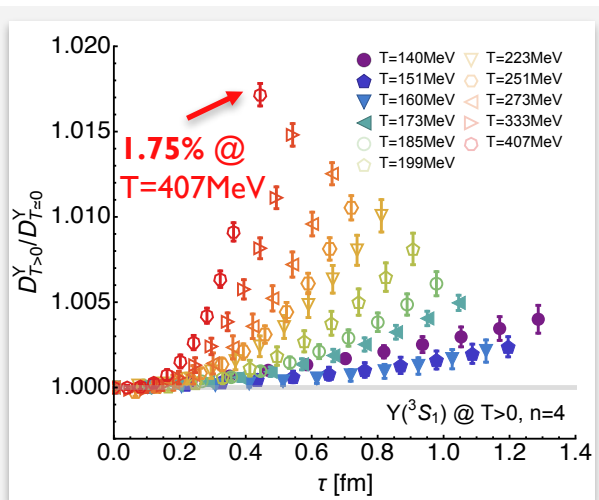
- Upsilon shows non-monotonic behavior around $T \sim T_C$
(bb $3S_1$ channel contains most excited states)



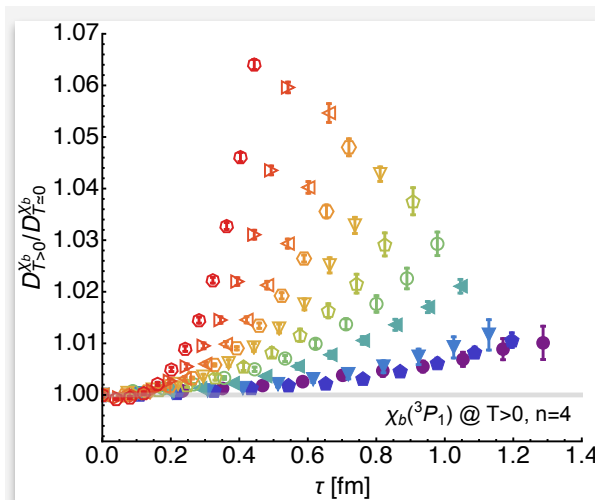
T>0 effects in $Q\bar{Q}$ correlators

$E_{\text{bind}}(T=0) \sim 1.1 \text{ GeV}$

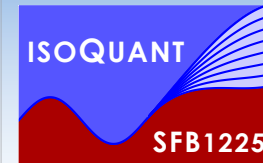
$E_{\text{bind}}(T=0) \sim 640 \text{ MeV}$



S.Kim, P.Petreczky, A.R. in preparation



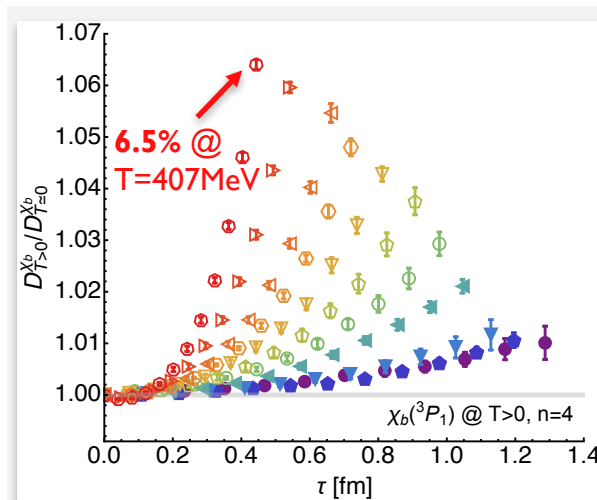
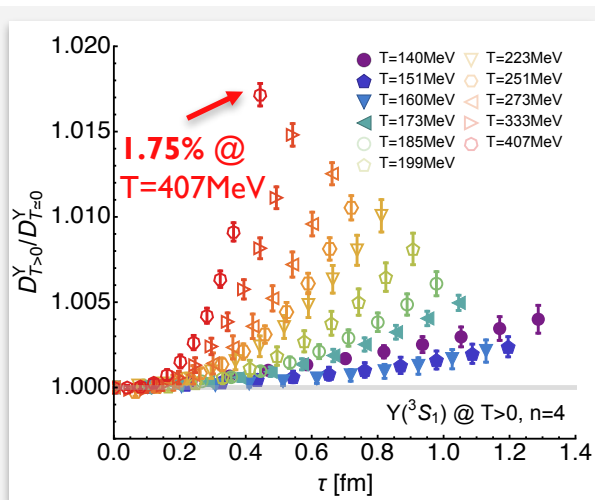
- Upsilon shows non-monotonous behavior around $T \sim T_C$
(bb $3S_1$ channel contains most excited states)



T>0 effects in $Q\bar{Q}$ correlators

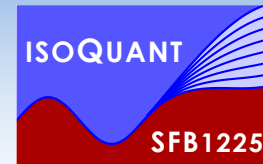
$E_{\text{bind}}(T=0) \sim 1.1 \text{ GeV}$

$E_{\text{bind}}(T=0) \sim 640 \text{ MeV}$



S.Kim, P.Petreczky, A.R. in preparation

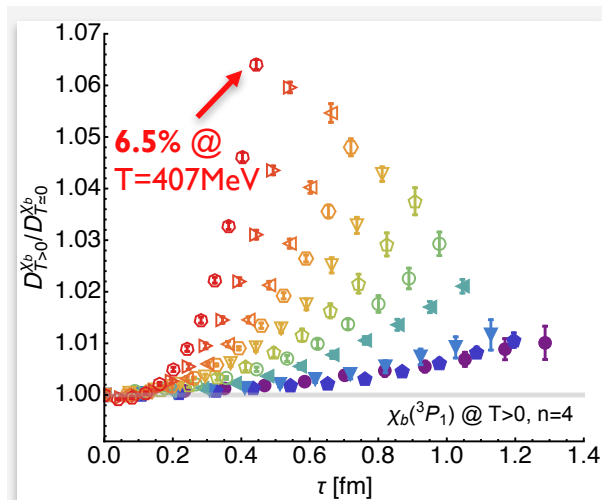
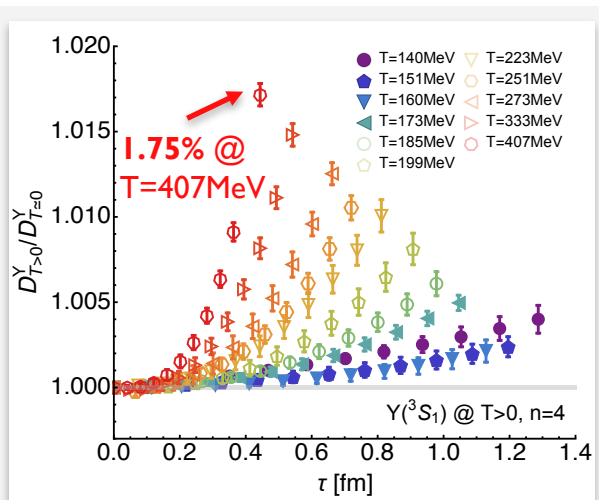
- Upsilon shows non-monotonic behavior around $T \sim T_C$
(bb $3S_1$ channel contains most excited states)



T>0 effects in $Q\bar{Q}$ correlators

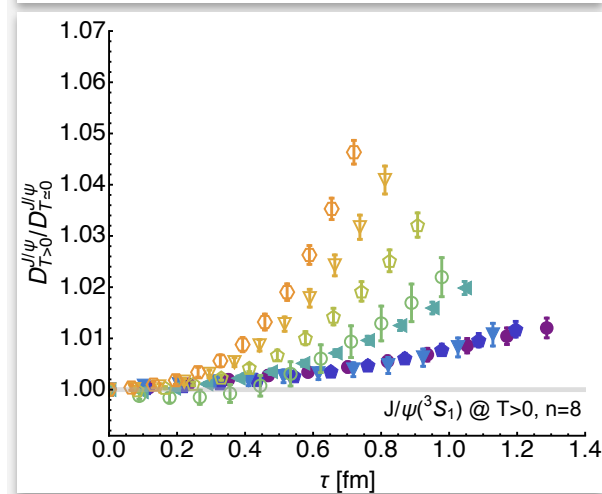
$E_{\text{bind}}(T=0) \sim 1.1 \text{ GeV}$

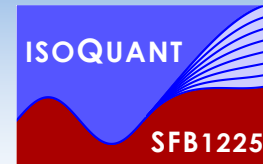
$E_{\text{bind}}(T=0) \sim 640 \text{ MeV}$



S.Kim, P.Petreczky, A.R. in preparation

- Upsilon shows non-monotonous behavior around $T \sim T_C$
(bb $3S_1$ channel contains most excited states)

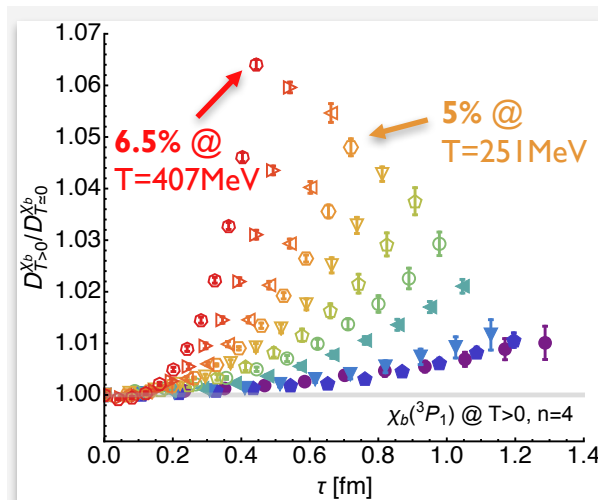
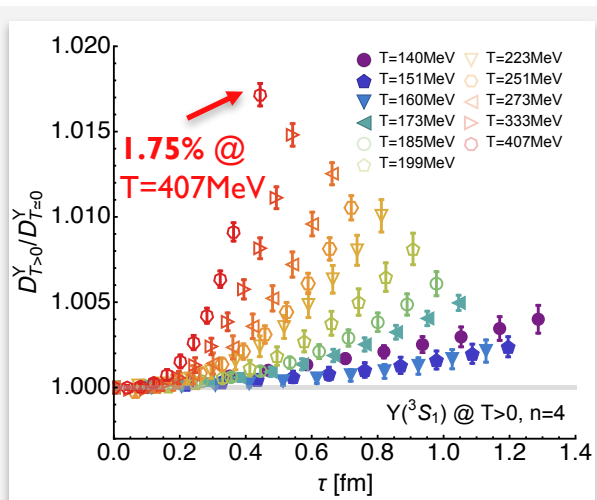




T>0 effects in $Q\bar{Q}$ correlators

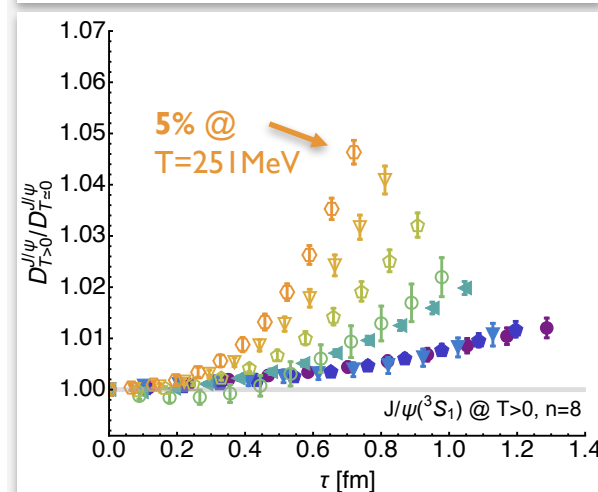
$E_{\text{bind}}(T=0) \sim 1.1 \text{ GeV}$

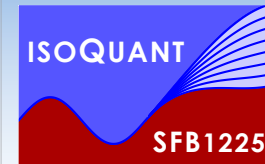
$E_{\text{bind}}(T=0) \sim 640 \text{ MeV}$



S.Kim, P.Petreczky, A.R. in preparation

- Upsilon shows non-monotonous behavior around $T \sim T_C$
(bb $3S_1$ channel contains most excited states)



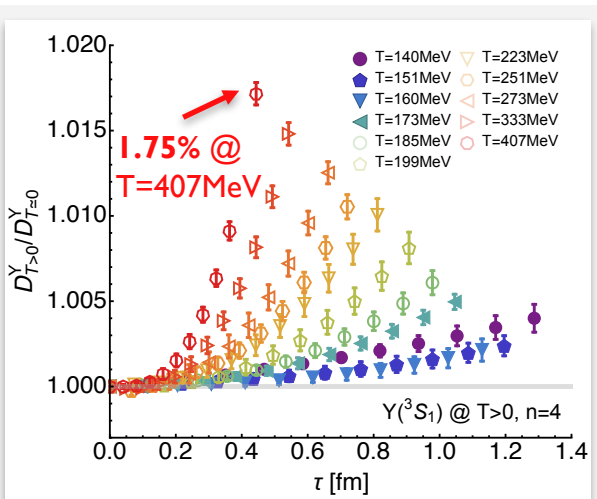


T>0 effects in QQ correlators

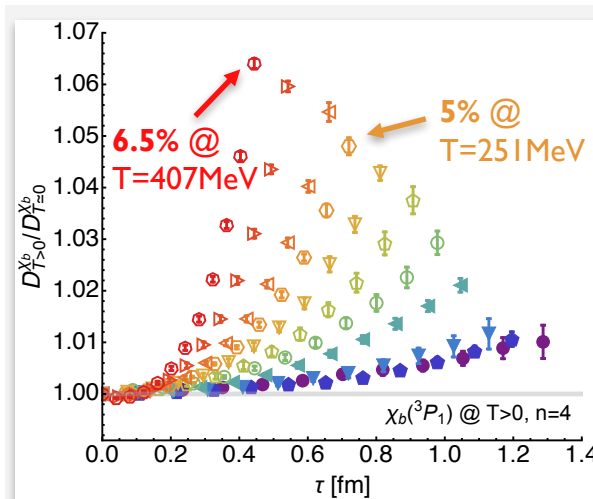
$E_{\text{bind}}(T=0) \sim 1.1 \text{ GeV}$

$E_{\text{bind}}(T=0) \sim 640 \text{ MeV}$

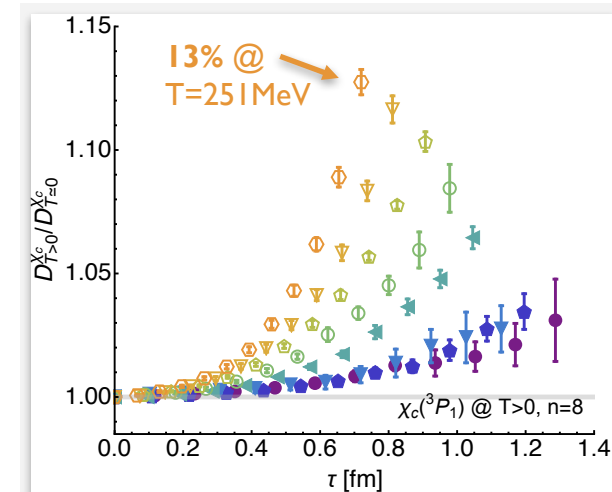
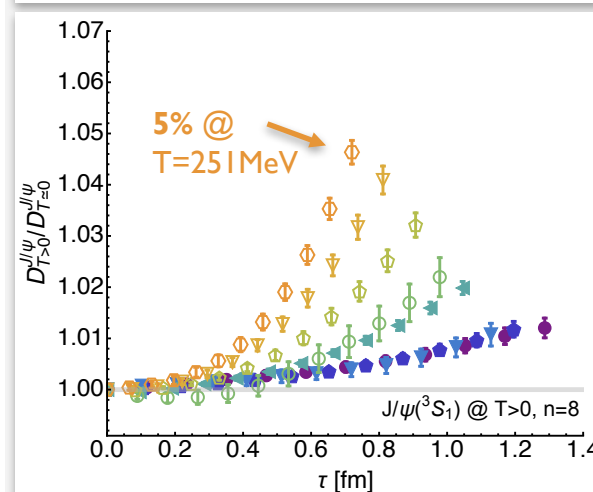
$E_{\text{bind}}(T=0) \sim 200 \text{ MeV}$

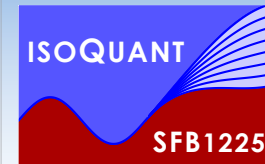


S.Kim, P.Petreczky, A.R. in preparation



- Upsilon shows non-monotonous behavior around $T \sim T_C$
(bb $3S_1$ channel contains most excited states)



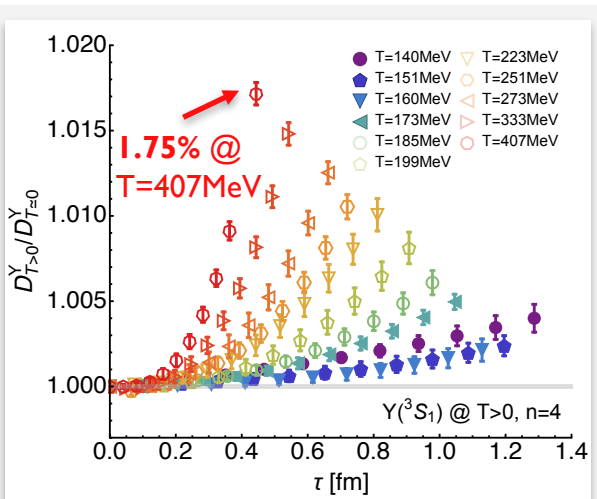


T>0 effects in QQ correlators

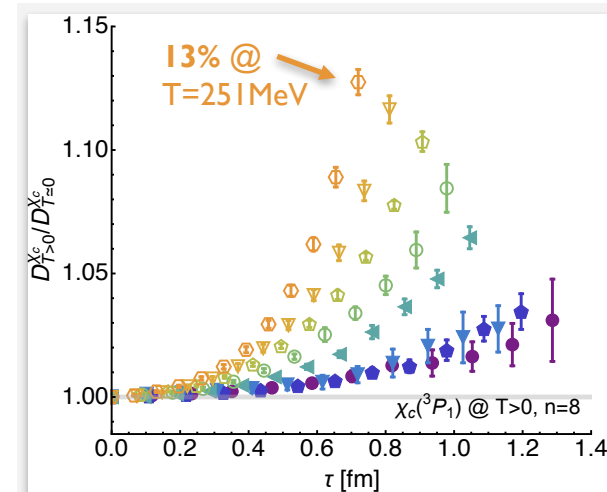
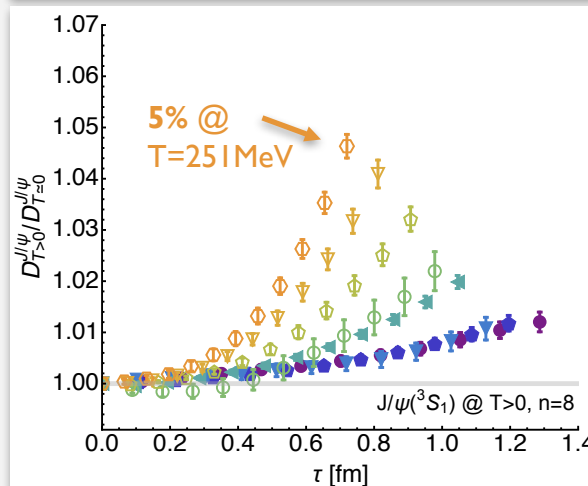
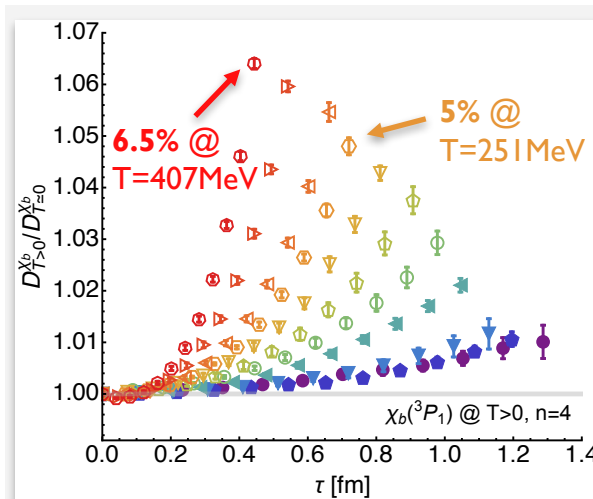
$E_{\text{bind}}(T=0) \sim 1.1 \text{ GeV}$

$E_{\text{bind}}(T=0) \sim 640 \text{ MeV}$

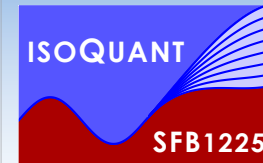
$E_{\text{bind}}(T=0) \sim 200 \text{ MeV}$



S.Kim, P.Petreczky, A.R. in preparation

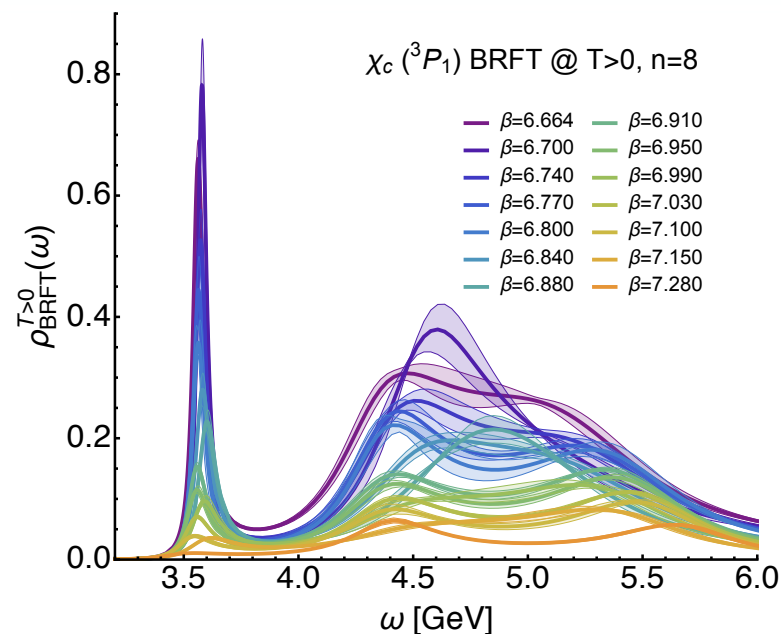
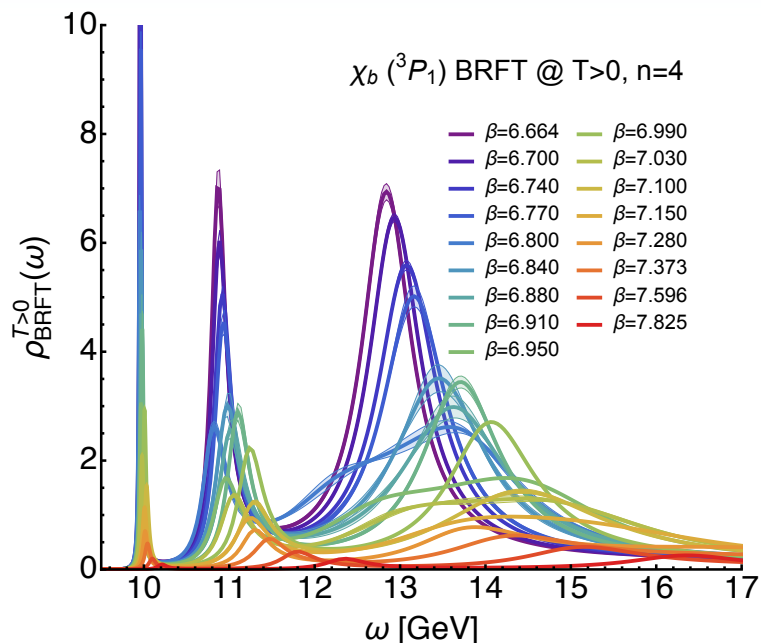


- Upsilon shows non-monotonous behavior around $T \sim T_C$
(bb 3S1 channel contains most excited states)
- Hierarchical T>0 modification w.r.t. vacuum binding energy

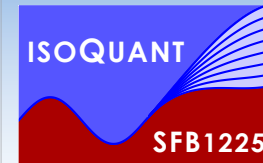


NRQCD P-wave spectra at $T>0$

S.Kim, P.Petreczky, A.R. in preparation

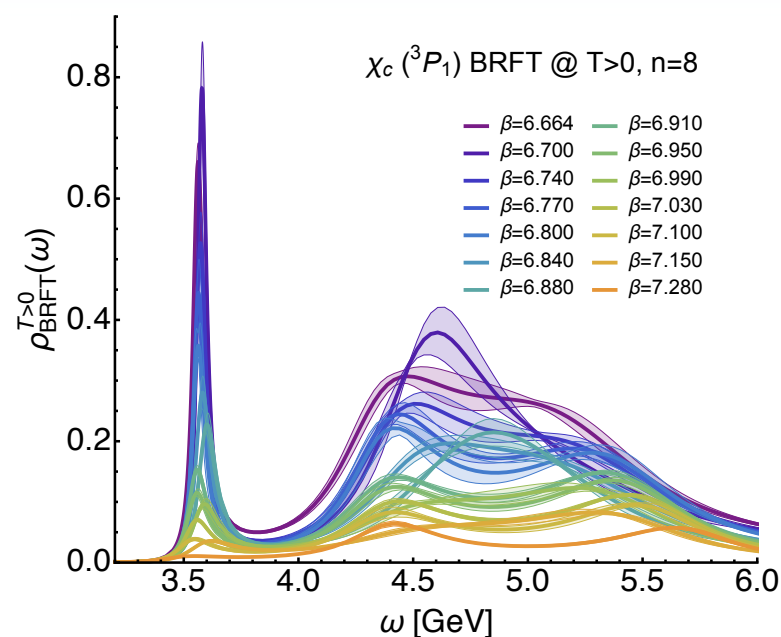
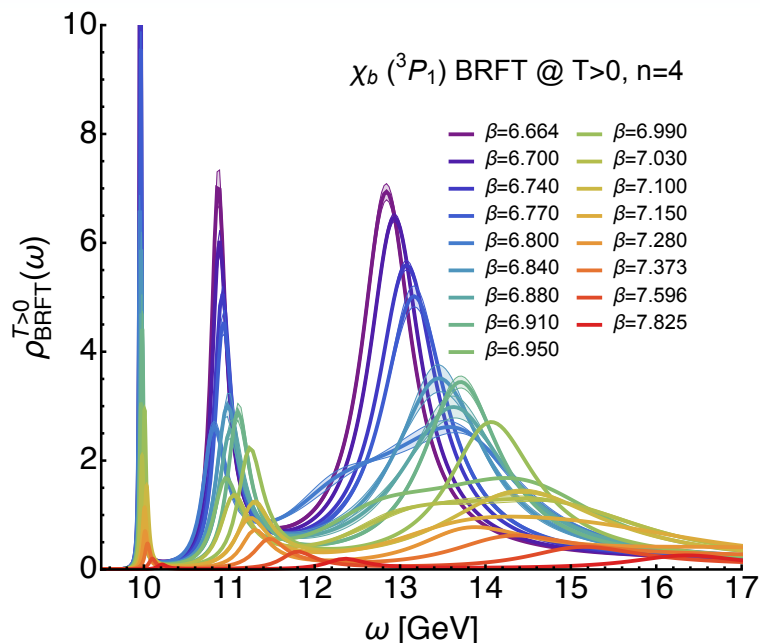


- Lower signal to noise ratio in underlying correlators makes reconstruction less precise

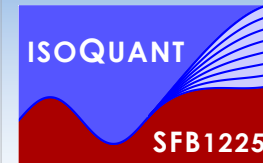


NRQCD P-wave spectra at $T>0$

S.Kim, P.Petreczky, A.R. in preparation

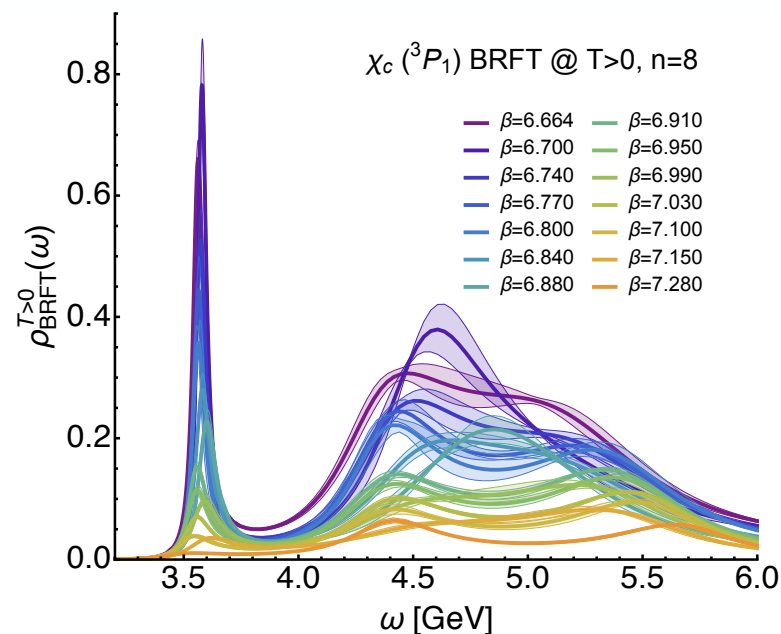
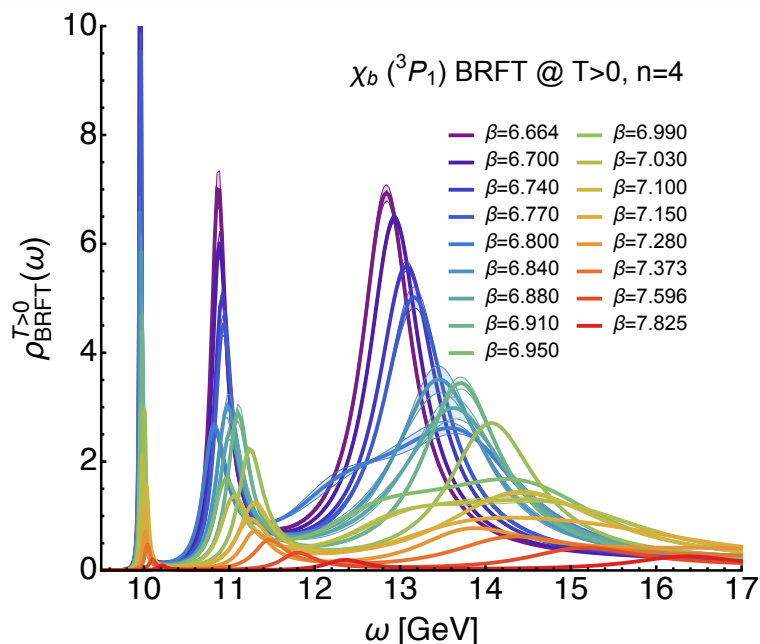


- Lower signal to noise ratio in underlying correlators makes reconstruction less precise
- Ground state well resolved and well separated from higher lying structures

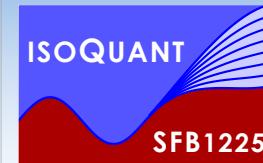


NRQCD P-wave spectra at $T>0$

S.Kim, P.Petreczky, A.R. in preparation

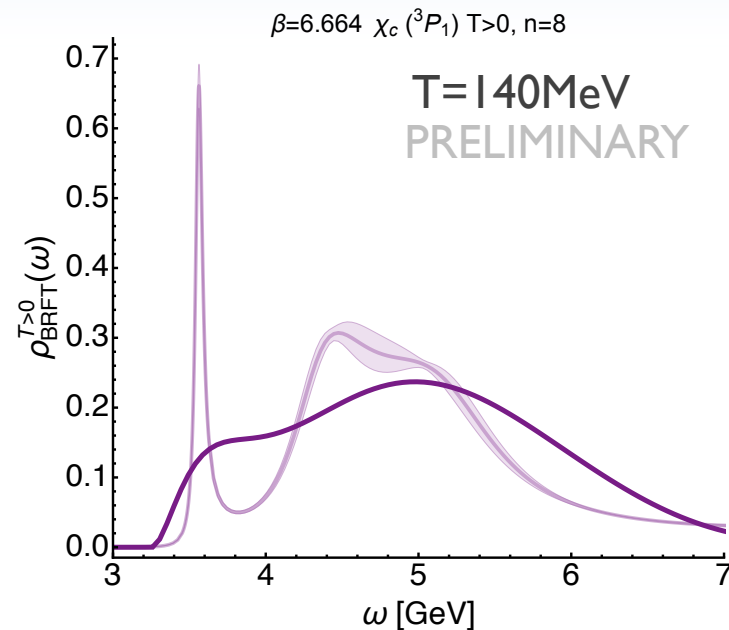
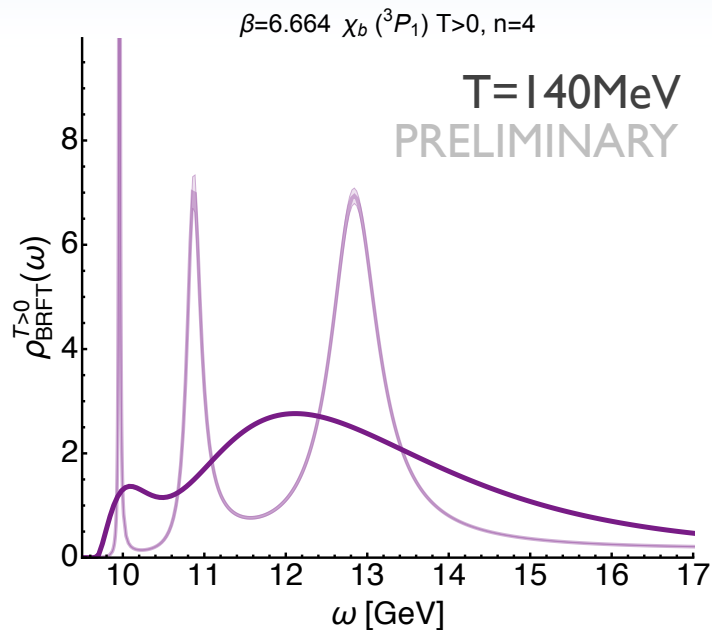


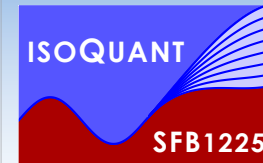
- Lower signal to noise ratio in underlying correlators makes reconstruction less precise
- Ground state well resolved and well separated from higher lying structures
- Gradual broadening and shifting of lowest lying peak visible



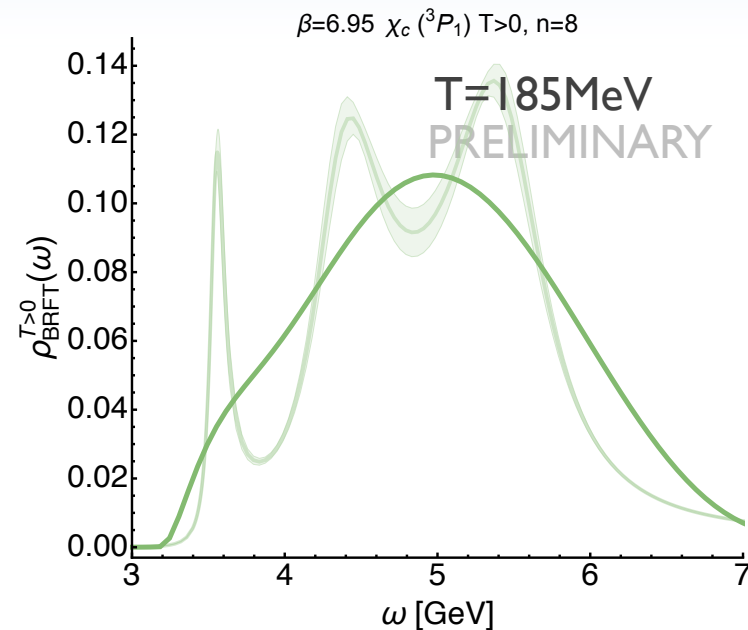
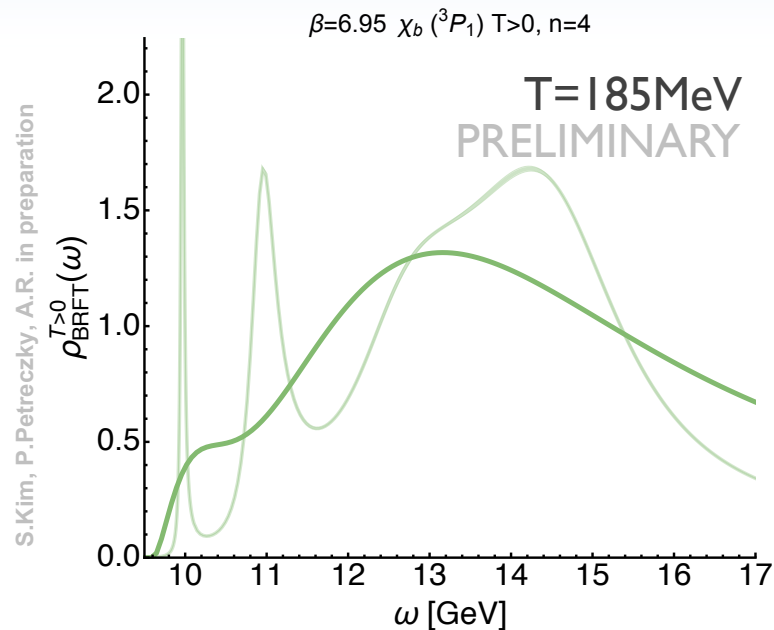
Survival of ground state signals?

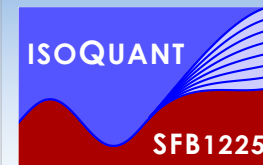
S.Kim, P.Petreczky, A.R. in preparation



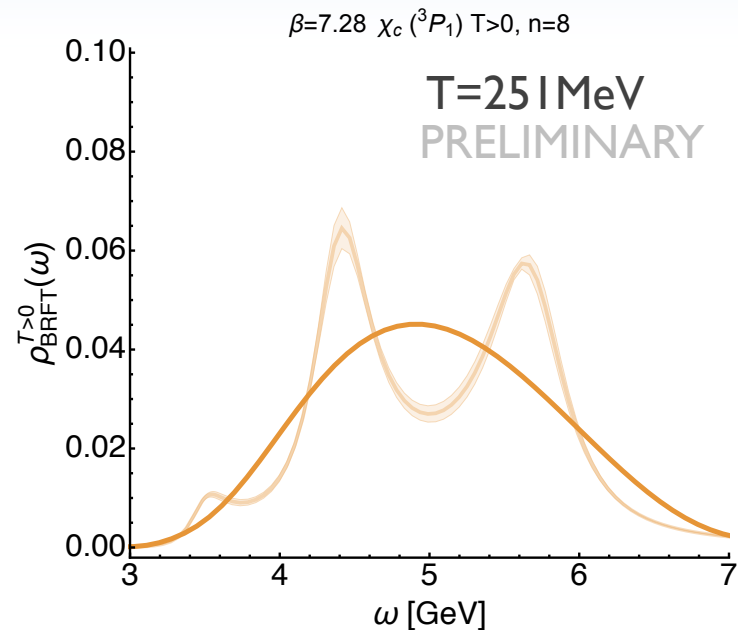
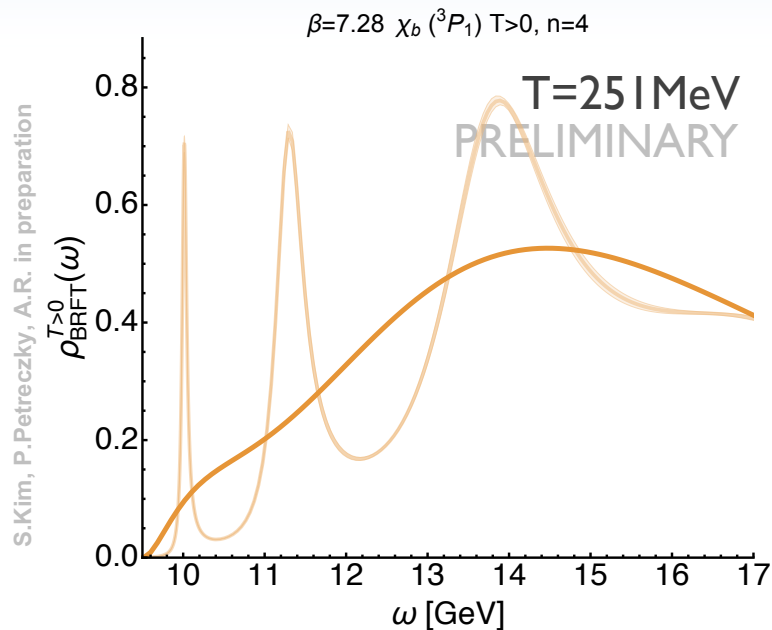


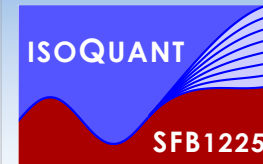
Survival of ground state signals?



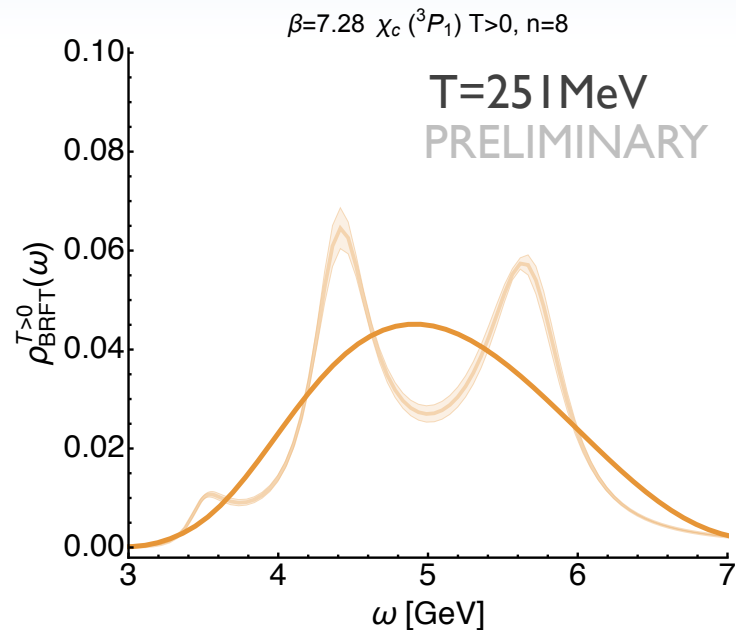
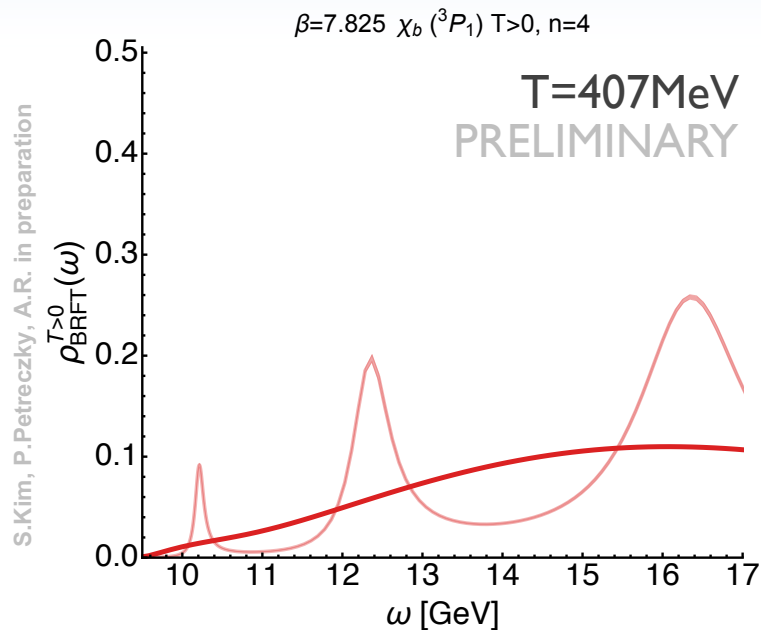


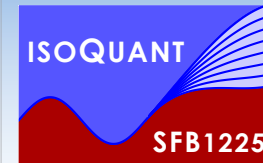
Survival of ground state signals?



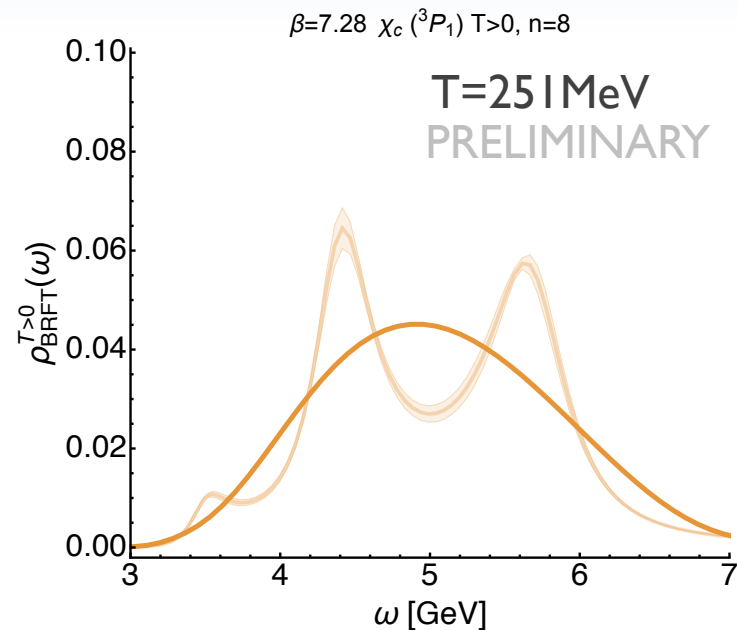
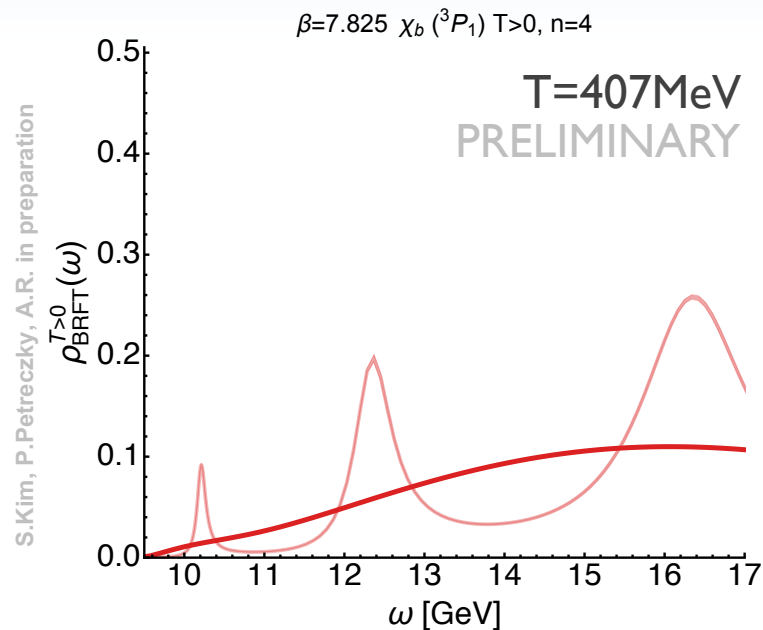


Survival of ground state signals?

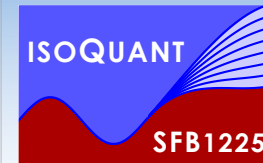




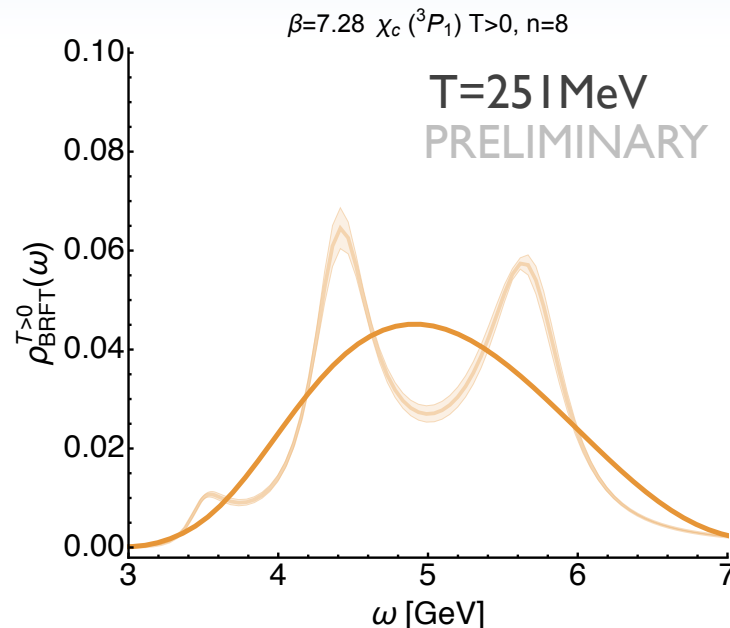
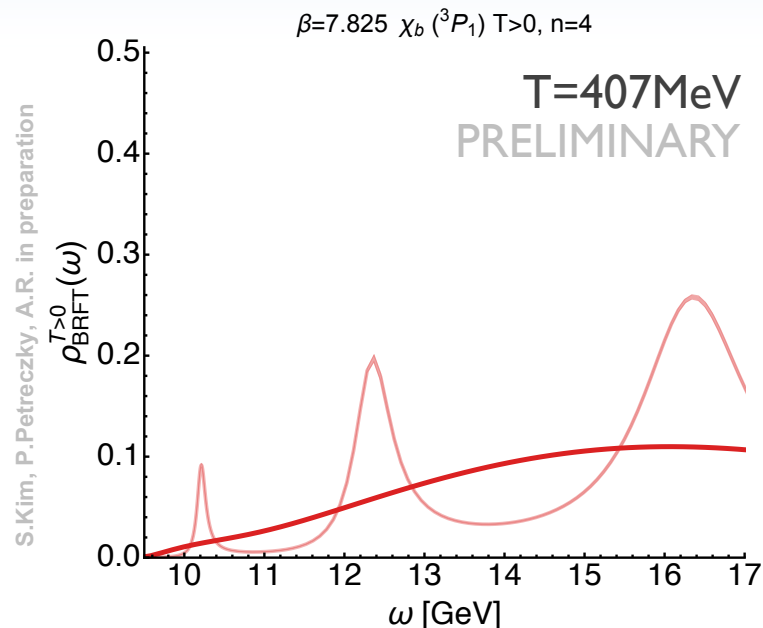
Survival of ground state signals?



- New “low-gain” BR method shows gradual weakening of ground state signal



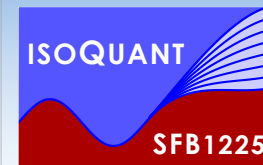
Survival of ground state signals?



- New “low-gain” BR method shows gradual weakening of ground state signal
- Genuine bound state signal lost at intermediate temperatures

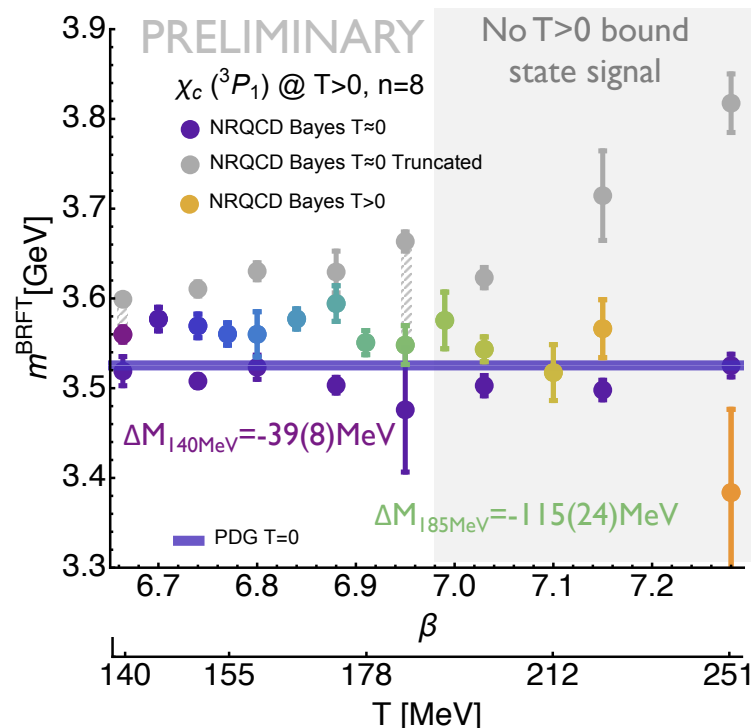
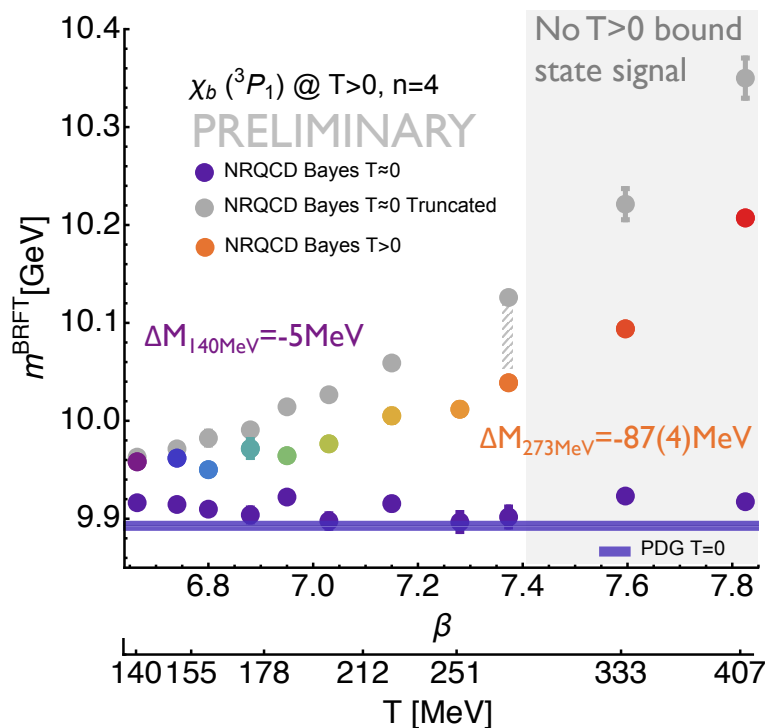
χ_b signal up to $T=273\text{MeV}$

χ_c signal up to $T=185\text{MeV}$

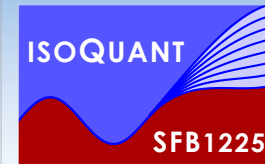


In-medium P-wave mass shifts

S.Kim, P.Petreczky, A.R. in preparation

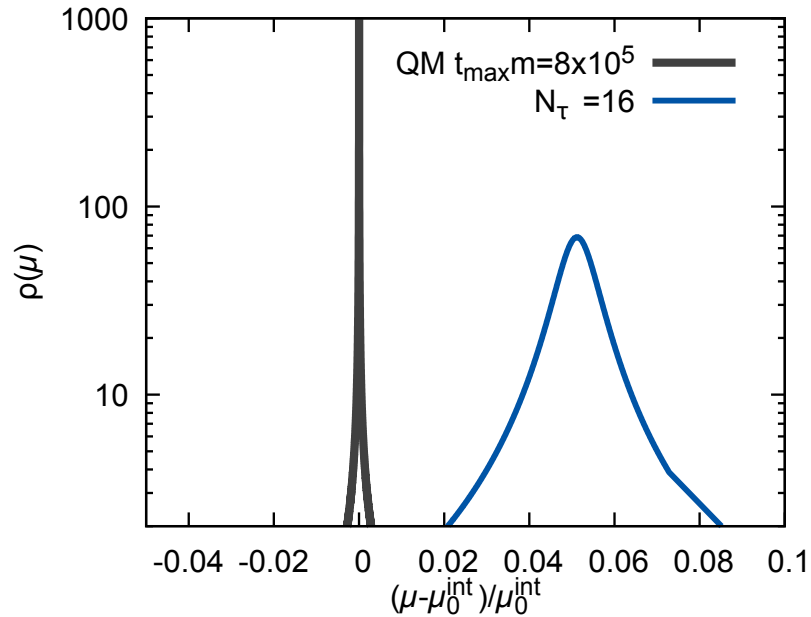
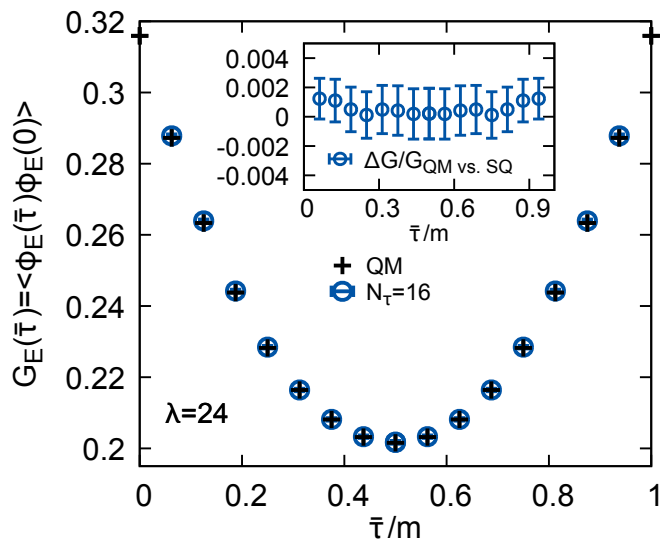


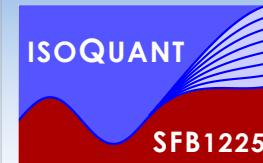
- Naïve inspection of in-medium modification appears to show increasing masses
- BR method systematics: Low number of datapoints introduces shifts to larger masses
- Actual in-medium effect: lowering of bound state mass, consistent with potential studies



(0+1d) scalar field toy model (I)

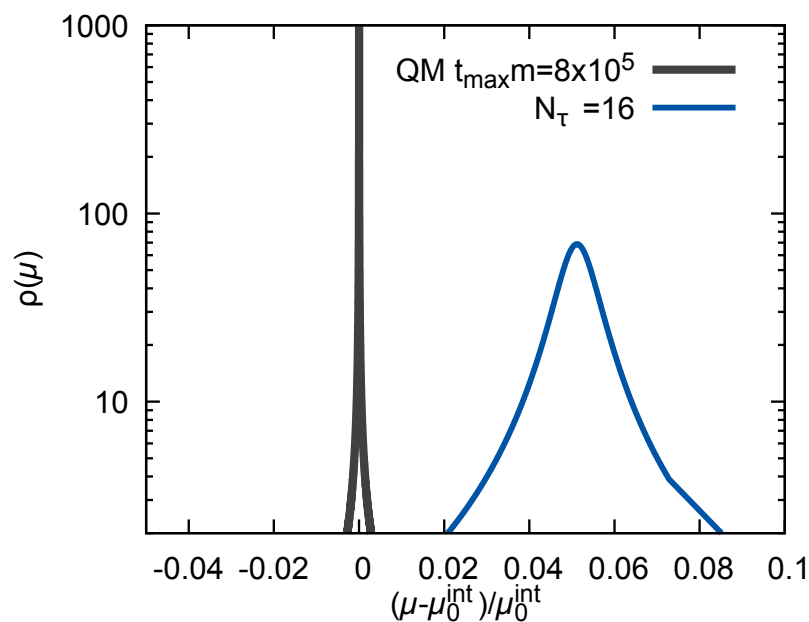
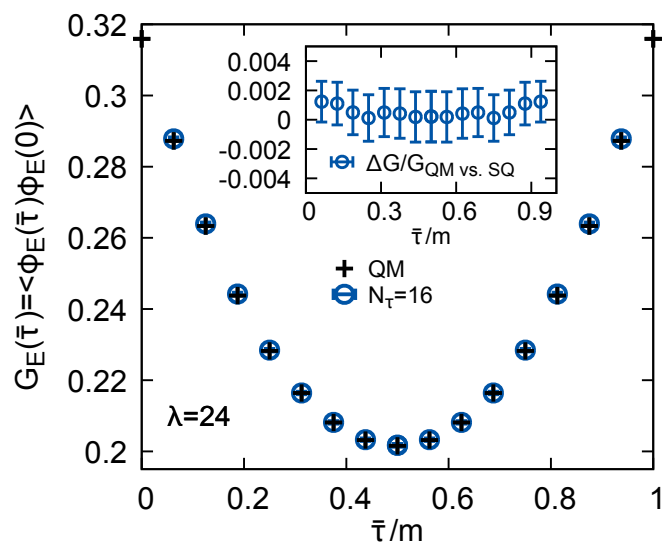
- Standard update for φ_E with $N_\tau=16$ $m=1$ $\lambda=24$ $N_\tau d\tau=1$ (compare to QM of A.H.O.)

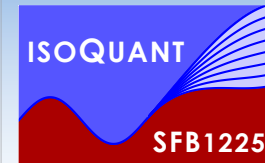




(0+1d) scalar field toy model (I)

- Standard update for φ_E with $N_\tau=16$ $m=1$ $\lambda=24$ $N_\tau d\tau=1$ (compare to QM of A.H.O.)
- Let us check, whether we can improve spectral reconstruction by increasing N_τ
- Decreasing $d\tau$ increases drift in $\partial_{t_5} \varphi_E(\bar{\tau}) = -\frac{\delta S_E[\varphi_E]}{\delta \varphi_E(\bar{\tau})} + \eta(\bar{\tau})$: need to reduce dt_5





(0+1d) scalar field toy model (I)

- Standard update for φ_E with $N_\tau=16$ $m=1$ $\lambda=24$ $N_\tau d\tau=1$ (compare to QM of A.H.O.)
- Let us check, whether we can improve spectral reconstruction by increasing N_τ
- Decreasing $d\tau$ increases drift in $\partial_{t_5} \varphi_E(\bar{\tau}) = -\frac{\delta S_E[\varphi_E]}{\delta \varphi_E(\bar{\tau})} + \eta(\bar{\tau})$: need to reduce dt_5

